EUROPEAN CIVIL
AVIATION CONFERENCE

Tel : +33 1 46 41 85 44

CONFERENCE EUROPEENNE
DE L'AVIATION CIVILE

Fax : +33 1 46 24 18 18

SECRETARIAT
3 bis, Villa Emile Bergaret
9522 Neuilly-sur-Seine Cédex
FRANCE

ECAC.CEAC Doc 29

4th Edition

Report on Standard Method of Computing
Noise Contours around Civil Airports

Volume 2: Technical Guide

As endorsed by DGCA/147 on 7 December 2016

FOREWORD

This is the second of three volumes of updated guidance on aircraft noise contour modelling. The first provides a general and largely non-technical introduction to the topic, as well as practical advice to model users. Those for whom the subject is new might usefully treat **Volume 1** as a primer for **Volume 2**. This second volume recommends a specific methodology for calculating aircraft noise exposure around civil aerodromes; this is described in sufficient detail for computer modelling by competent programmers/analysts.

Since the 3rd Edition was published, a number of noise models have been developed based on the algorithms set out in Volume 2. Through the development of these models, some parts of the guidance were identified that required clarification to ensure consistency in calculation methodology.

The 4th Edition replaces the previous (2007) 3rd edition of ECAC-CEAC Doc 29 which should now be discarded. This Volume 2 gives the clarity needed to improve the harmonisation of noise models across ECAC member states.

The recommended approach to noise modelling is not the only way to produce accurate noise contours; indeed for specific airports different methods can sometimes be more effective. However, it is considered by ECAC, and the international aircraft noise modelling community as a whole, to represent current best practice for general application. Used diligently it can be expected to deliver reasonably accurate noise contours for most airports in Europe and beyond. This does not mean that the guidance cannot be improved upon. Indeed the methodology and the supporting data remain under constant review and development and intermittent updates should be anticipated. Eventually, advances in computer technology and aircraft operations monitoring systems may well make segmentation-based models obsolete.

This new edition contains the first part of an additional two-part **Volume 3** covering the subjects of model verification and validation respectively. It nevertheless remains the responsibility of the model user to assure the quality of modelling outputs. The methodology and the Aircraft Noise and Performance (ANP) data are as accurate as understanding and facilities presently allow but, throughout this guidance, it is stressed that achieving reliable results requires meticulous collection and pre-processing of scenario data (describing airport and aircraft operations). Doing this in a measured and cost-effective way is perhaps the practitioner's greatest challenge. Increasingly noise contour calculations are compared with on-site measurements; discrepancies can point to modelling deficiencies but it must always be remembered that obtaining appropriate, accurate measurements is at least as difficult as modelling itself. However, persistent disagreement might well be symptomatic of model or data deficiencies and this should be reported via the feedback mechanisms of the ANP website.

The recommended methodology can be used to model airport and aircraft operations in minute detail - if that is necessary. But often such detail is inappropriate, for example when the accuracy and reliability of the data, or the resources to do the job, are limited. In this case the scope of the modelling must be tailored accordingly - ensuring that attention is focused on the most noise-significant factors.

TABLE OF CONTENTS

EXPLANATION OF TERMS AND SYMBOLS

Some important *terms* are described here by the general meanings attributed to them in this document. The list is not exhaustive; only expressions and acronyms used frequently are included. Others are described where they first occur. More explanation can be found in **Volume 1**.

The mathematical *symbols* (listed after the terms) are the main ones used in equations in the main text. Other symbols used locally in both the text and the appendices are defined where they are used.

The reader is reminded periodically of the interchangeability of the words *sound* and *noise* in this document (as in **Volume 1**). Although the word *noise* has subjective connotations - it is usually defined by acousticians as 'unwanted sound' - in the field of aircraft noise control it is commonly taken to mean just sound - airborne energy transmitted by acoustic wave motion. The symbol → denotes cross references to other terms included in the list.

Terms

AIP	Aeronautical Information Publication
Aircraft configuration	The positions of slats, flaps and landing gear.
Aircraft movement	An arrival, departure or other aircraft action that affects noise exposure around an aerodrome.
Aircraft noise and performance data	Data describing the acoustic and performance characteristics of different aeroplanes types that are required by the modelling process. They include → *NPD relationships* and information that allows engine thrust/power to be calculated as a function of → *flight configuration*. The data are usually supplied by the aircraft manufacturer although when that is not possible it is sometimes obtained from other sources. When no data are available, it is usual to represent the aircraft concerned by adapting data for a suitably similar aircraft - this is referred to as *substitution*.
Altitude	Height above mean sea level.
ANP database	The international Aircraft Noise and Performance database www.aircraftnoisemodel.org
A-weighted sound level, L_A	Basic sound/noise level scale used for measuring environmental noise including that from aircraft and on which most noise contour metrics are based.
Backbone ground track	A representative or nominal ground track which defines the centre of a swathe of tracks.
Baseline noise event level	The noise event level read from an NPD database.
Brake release	→ *Start of roll*
Corrected net thrust	At a given power setting (e.g. *EPR* or N_1) net thrust falls with air density and thus with increasing aircraft altitude; corrected net thrust is the value at sea level.

Cumulative sound/noise level	A decibel measure of the noise received over a specified period of time, at a point near an airport, from aeroplane traffic using normal operating conditions and flight paths. It is calculated by accumulating in some way the event sound/noise levels occurring at that point.
Decibel sum or average	Sometimes referred to elsewhere as 'energy' or 'logarithmic' (as opposed to arithmetic) values. Used when it is appropriate to sum or average the underlying energy-like quantities; e.g. *decibel sum* $= 10 \cdot \lg \sum 10^{L_i/10}$
Energy fraction, *F*	Ratio of sound energy received from segment to energy received from infinite flight path.
Engine power setting	Value of the → *noise related power parameter* used to determine noise emission from the NPD database.
Equivalent (continuous) sound level, L_{eq}	A measure of long-term sound. The level of a hypothetical steady sound, which over a specified period of time, contains the same total energy as the actual variable sound.
Event sound/noise level	A decibel measure of the finite quantity of sound (or noise) received from a passing aeroplane → *sound exposure level*
Flight configuration	= → *Aircraft configuration* + → *Flight parameters*
Flight parameters	Aircraft power setting, speed, bank angle and weight.
Flight path	The path of an aeroplane through the air, defined in three dimensions, usually with reference to an origin at the start of takeoff roll or at the landing threshold.
Flight path segment	Part of an aircraft flight path represented for noise modelling purposes by a straight line of finite length.
Flight procedure	The sequence of operational steps followed by the aircraft crew or flight management system: expressed as changes of flight configuration as a function of distance along the ground track.
Flight profile	Variation of aeroplane height along the ground track (sometimes includes changes of → *flight configuration* too) - described by a set of → *profile points*
Ground plane	(Or Nominal Ground Plane) Horizontal ground surface through the aerodrome reference point on which the contours are normally calculated.
Ground speed	Aircraft speed relative to a fixed point on the ground.
Ground track	Vertical projection of the flight path onto the ground plane.
Height	Vertical distance between aircraft and → *ground plane*
Integrated sound level	Otherwise termed → *single event sound exposure level*.
ISA	International Standard Atmosphere – defined by ICAO [ref. 1]. Defines variation of air temperature, pressure, and density with height above mean sea level. Used to normalise

	the results of aircraft design calculations and analysis of test data.
Lateral attenuation	Excess attenuation of sound with distance attributable, directly or indirectly, to the presence of the ground surface. Significant at low angles of elevation (of the aircraft above the ground plane).
Maximum noise/sound level	The maximum sound level reached during an event.
Mean Sea Level, *MSL*	The standard earth surface elevation to which the → ISA is referred.
Net thrust	The propulsive force exerted by an engine on the airframe.
Noise	Noise is defined as unwanted sound. But metrics such as *A-weighted sound level* (L_A) and *effective perceived noise level* (*EPNL*) effectively convert sound levels into noise levels (see **Volume 1**). Despite a consequent lack of rigour, the terms sound and noise are sometimes used interchangeably in this document, as elsewhere - especially in conjunction with the word *level*.
Noise contour	A line of constant value of a cumulative aircraft noise level or index around an airport.
Noise impact	The adverse effect(s) of noise on its recipients; importantly it is implied that noise metrics are indicators of noise impact.
Noise index	A measure of long term, or cumulative sound which correlates with (i.e. is considered to be a predictor of) its effects on people. May take some account of factors in addition to the magnitude of sound (especially time of day). An example is day-evening-night level L_{den}.
Noise level	A decibel measure of sound on a scale which indicates its loudness or noisiness. For environmental noise from aircraft, two scales are generally used: A-weighted sound level and Perceived Noise Level. These scales apply different weights to sound of different frequencies - to mimic human perception.
Noise metric	An expression used to describe any measure of quantity of noise at a receiver position whether it be a single event or an accumulation of noise over extended time. There are two commonly used measures of single event noise: the *maximum level* reached during the event, or its *sound exposure level*, a measure of its total sound energy determined by time integration.
Noise-power-distance (NPD) relationships/data	Noise event levels tabulated as a function of distance below an aeroplane in steady level flight at a reference speed in a reference atmosphere, for each of a number of → *engine power settings*. The data account for the effects of sound attenuation due to spherical wave spreading (inverse-square

	law) and atmospheric absorption. The distance is defined perpendicular to the aeroplane flight path and the aircraft wing-axis (i.e. vertically below the aircraft in non-banked flight).
Noise-related power parameter	Parameter that describes or indicates the propulsive effort generated by an aircraft engine to which acoustic power emission can logically be related; usually taken to be → *corrected net thrust.* Loosely termed "power" or "power setting" throughout the text.
Noise significance	The contribution from a flight path segment is 'noise significant' if it affects the event noise level to an appreciable extent. Disregarding segments that are not noise-significant yields massive savings in computer processing.
Observer	→ *Receiver*
Procedural steps	Prescription for flying a profile - steps include changes of speed and/or altitude.
Profile point	Height of flight path segment end point - in a vertical plane above the ground track.
Receiver	A recipient of noise that arrives from a source; principally at a point on or near the ground surface.
Reference atmosphere	A tabulation of sound absorption rates used to standardise NPD data (see **Appendix D**).
Reference day	A set of atmospheric conditions on which ANP data are standardised.
Reference duration	A nominal time interval used to standardise single event sound exposure level measurements; equal to 1 second in the case of → *SEL*.
Reference speed	Aeroplane groundspeed to which *NPD* → *SEL* data are normalised.
SEL	→ *Sound Exposure Level*
Single event sound exposure level	The sound level an event would have if all its sound energy were compressed uniformly into a standard time interval known as the → *reference duration.*
Soft ground	A ground surface that is acoustically 'soft', typically grassy, that surrounds most aerodromes. Acoustically hard, i.e. highly reflective, ground surfaces includes concrete and water. The noise contour methodology described herein applies to soft ground conditions.
Sound	Energy transmitted through air by (longitudinal) wave motion which is sensed by the ear.
Sound attenuation	The decrease in sound intensity with distance along a propagation path. For aircraft noise its causes include

	spherical wave spreading, atmospheric absorption and → *lateral attenuation.*
Sound exposure	A measure of total sound energy immission over a period of time.
Sound Exposure Level, L_{AE}	(Acronym *SEL*) A metric standardised in ISO 1996-1 [ref. 2] or ISO 3891 [ref. 3] = A-weighted single event sound exposure level referenced to 1 second.
Sound intensity	The strength of sound immission at a point - related to acoustical energy (and indicated by measured sound levels).
Sound level	A measure of sound energy expressed in decibel units. Received sound is measured with or without 'frequency weighting'; levels measured with a weighting are often termed → *noise levels.*
Stage/trip length	Distance to first destination of departing aircraft; taken to be an indicator of aircraft weight.
Start of Roll, *SOR*	The point on the runway from which a departing aircraft commences its takeoff. Also termed 'brake release'.
True airspeed	Actual speed of aircraft relative to air (= groundspeed in still air during level flight).
Weighted equivalent sound level, $L_{eq,W}$	A modified version of L_{eq} in which different weights are assigned to noise occurring during different period of the day (usually day, evening and night).

Symbols

c	Speed of sound
d	Shortest distance from an observation point to a flight path segment
d_p	Perpendicular distance from an observation point to the flight path (slant distance or slant range)
d_λ	Scaled distance
F_n	Actual net thrust per engine
F_n/δ	Corrected net thrust per engine
h	Aircraft altitude (above MSL)
L	Event noise level (scale undefined)
$L(t)$	Sound level at time t (scale undefined)
L_A, $L_A(t)$	A-weighted sound pressure level (at time t) - measured on the *slow* sound level meter scale
L_{AE}	(SEL) Sound Exposure Level [refs. 2,3]
L_{Amax}	Maximum value of $L_A(t)$ during an event
L_E	Single event sound exposure level

$L_{E\infty}$	Single event sound exposure level determined from NPD database
L_{EPN}	Effective Perceived Noise Level
L_{eq}	Equivalent (continuous) sound level
L_{max}	Maximum value of $L(t)$ during an event
$L_{max,seg}$	Maximum level generated by a segment
ℓ	Perpendicular distance from an observation point to the ground track
lg	Logarithm to base 10
N	Number of segments or sub-segments
NAT	Number Above Threshold, i.e. number of events with L_{max} exceeding a specified threshold
P	Power parameter in NPD variable $L(P,d)$
P_{seg}	Power parameter relevant to a particular segment
q	Distance from start of segment to closest point of approach
R	Radius of turn
S	Standard deviation
s	Distance along ground track
s_{RWY}	Runway length
t	Time
t_e	Effective duration of single sound event
t_0	Reference time for integrated sound level
V	Groundspeed
V_{seg}	Equivalent segment groundspeed
V_{ref}	Reference groundspeed for which NPD data are defined
x,y,z	Local coordinates
x',y',z'	Aircraft coordinates
X_{ARP},Y_{ARP},Z_{ARP}	Position of aerodrome reference point in geographical coordinates
z	Height of aircraft above ground plane / aerodrome reference point
z'	Set of values of height of aircraft for sub-segmentation
α	Parameter used for calculation of the finite segment correction Δ_F
β	Elevation angle of aircraft relative to ground plane
ε	Aircraft bank angle
γ	Climb/descent angle
φ	Depression angle (lateral directivity parameter)
λ	Total segment length
ψ	Angle between direction of aircraft movement and direction to observer

ρ	Air density
ξ	Aircraft heading, measured clockwise from magnetic north
$\Lambda(\beta,\ell)$	Air-to-ground lateral attenuation
$\Lambda(\beta)$	Long range air-to-ground lateral attenuation
$\Gamma(\ell)$	Lateral attenuation distance factor
Δ	Change in value of a quantity, or a correction (as indicated in the text)
Δ_F	Finite segment correction
$\Delta'_{F,a}$	Finite segment correction, reduced form for arrivals
$\Delta'_{F,d}$	Finite segment correction, reduced form for departures
Δ_I	Engine installation correction
Δ_i	Weighting for *i*-th time of day period
Δ_{rev}	Reverse thrust
Δ_{SOR}	Start of roll correction
Δ_V	Duration (speed) correction

Subscripts

1, 2	Subscripts denoting start and end values of an interval or segment
E	Exposure
i	Aircraft type/category summation index, or aircraft height index
j	Ground track/subtrack summation index
k	Segment summation index
max	Maximum
ref	Reference value
seg	Segment specific value
SOR	Related to start of roll
TO	Takeoff

1 INTRODUCTION

1.1 AIM AND SCOPE OF DOCUMENT

Contour maps are used to indicate the extent and magnitude of aircraft noise impact around airports, that impact being indicated by values of a specified noise metric or index. A contour is a line along which the index value is constant. The index value aggregates in some way all the individual aircraft noise events that occur during some specified period of time, normally measured in days or months (see **Volume 1** [ref. 4] for a review).

The noise at points on the ground from aircraft flying into and out of a nearby aerodrome depends on many factors. Principal among these are the types of aeroplane and their powerplant; the power, flap and airspeed management procedures used on the aeroplanes themselves; the distances from the points concerned to the various flight paths; and local topography and weather. Airport operations generally include different types of aeroplanes, various flight procedures and a range of operational weights.

Volume 1 of this ECAC guidance on aircraft noise contour modelling, an Applications Guide, is aimed primarily at noise model users who do not necessarily need a comprehensive understanding of the modelling process, but who need a good understanding of the principles, the problems involved, and the requirements for getting results that adequately meet the objectives of particular noise impact assessments.

This second volume, a Technical Guide, is written for modellers themselves, those who develop and maintain the computer models and their databases. It fully describes a specific noise contour modelling system which is considered by ECAC to represent current best practice. It does not prescribe a computer program but rather the equations and logic that need to be programmed to construct a physical 'working model'. Any physical model that complies fully with the methodology described can be expected to generate contours of aircraft noise exposure around civil airports with reasonable accuracy. *The methodology applies only to long-term average noise exposure; it cannot be relied upon to predict with any accuracy the absolute level of noise from a single aircraft movement and should not be used for that purpose.*

Contours are generated by calculating surfaces of local noise index values mathematically. This document explains in detail how to calculate, at one observer point, the individual aircraft noise event levels, each for a specific aircraft flight or type of flight, that are subsequently averaged in some way, or *accumulated*, to yield index values at that point. The required surface of index values is generated merely by repeating the calculations as necessary for different aircraft movements – taking care to maximise efficiency by excluding events that are not 'noise-significant' (i.e. which do not contribute significantly to the total).

Volume 2, builds on, but replaces, ECAC.CEAC Document 29, the third edition of which was published in 2007 [ref. 5] and which should now be discarded. Many essential features of the previously recommended process have been retained; only parts that have subsequently proved to be inadequate or inappropriate have been improved or replaced. The document is not a programming manual; it does not provided detailed step-by-step instructions for constructing a computer code. Such details are left to the modeller/programmer who therefore has the flexibility to adapt the model to project needs. An important reference document is Aerospace Information Report No 1845 [ref. 6] published by the A-21 Aircraft Noise Subcommittee of the Society of Automotive Engineers. That body of aviation industry specialists has long been engaged in the development of aircraft noise standards and recommended practices.

A linked international aircraft noise and performance (ANP) database is available on-line and the recommended methodology is designed to make full use of that comprehensive ECAC-endorsed data source. It includes aircraft and engine performance data and noise-power-distance (NPD) tables for the civil aircraft types that dominate the noise at most of the world's busy airports.

There are a number of noise-generating activities on operational airports which are excluded from the 'air noise' calculation procedures given here. These include taxiing, engine testing and use of auxiliary power-units, and their noise generally comes under the heading of ground noise. In practice, the effects of these activities are unlikely to affect the noise contours in regions beyond the airport boundary. This does not necessarily mean that their impact is insignificant; however assessments of ground noise are usually undertaken independently of air noise analyses.

Aircraft engine testing (sometimes referred to as 'engine run-ups') at airports is usually carried out for engineering purposes to check engine performance, and aircraft are safely positioned away from buildings, other aircraft, vehicular and/or personnel movements to avoid jet-blast related damage. However, for additional safety and noise control reasons, airports, particularly those with maintenance facilities that can lead to frequent engine tests, can install so-called 'noise pens', which are three-sided baffled enclosures specially designed to deflect and dissipate jet blast and noise. Investigating the ground noise impact of such facilities, which can be further attenuated and reduced by the use of additional earth bunds or substantial noise barrier fencing, can be accomplished by treating the noise pen as a source of industrial noise and using an appropriate noise and sound propagation model.

1.2 OUTLINE OF THE DOCUMENT

It is assumed that users are familiar with basic noise modelling principles that are described in **Volume 1** - which may be regarded as a primer for **Volume 2**. That document stresses the fact that having a *best practice modelling methodology* is only one of three requirements for valid noise contour modelling. The others are *an accurate aircraft noise and performance database* and a detailed understanding and description of *the aircraft operations* that are the source of the subject noise. All three elements are covered in this volume.

The noise contour generation process is illustrated in **Figure 1-1**. General guidance on the acquisition and pre-processing of the input data is given in **Volume 1**. Contours are produced for various purposes and these tend to control the requirements for sources and pre-processing of input data. Contours that depict historical noise impact might be generated from actual records of aircraft operations – of movements, weights, radar-measured flight paths, etc. Contours used for future planning purposes of necessity rely more on forecasts – of traffic and flight tracks and the performance and noise characteristics of future aircraft.

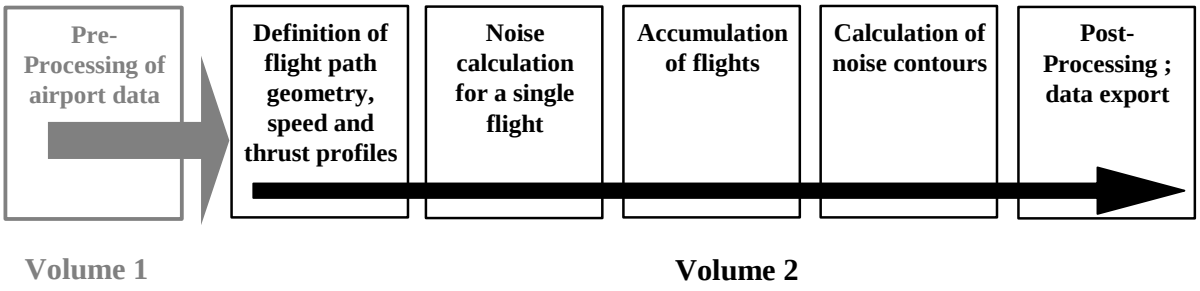

Figure 1-1: The noise contour generation process

Whatever the source of flight data, each different aircraft movement, arrival or departure, is defined in terms of its flight path geometry and the noise emission from the aircraft as it follows that path (movements that are essentially the same in noise and flight path terms are included by simple multiplication). The noise emission depends on the characteristics of the aircraft - mainly on the power generated by its engines. The recommended methodology involves dividing the flight path into segments. **Chapter 2** outlines the elements of the methodology and explains the principle of segmentation on which it is based; that the observed event noise level is an aggregation of contributions from all 'noise-significant' segments of the flight path, each of which can be calculated independently of the others. **Chapter 2** also outlines the input data requirements for producing a set of noise contours. Detailed specifications for the operational data needed are set out in **Appendix A**.

How the flight path segments are calculated from pre-processed input data is described in **Chapter 3**. This involves applications of aircraft flight performance analysis, equations for which are detailed in **Appendix B**, using data from the international Aircraft Noise and Performance (ANP) database. Flight paths are subject to significant variability - aircraft following any route are dispersed across a swathe due to the effects of differences in atmospheric conditions, aircraft weights and operating procedures, air traffic control constraints, etc. This is taken into account by describing each flight path statistically – as a central or 'backbone' path which is accompanied by a set of dispersed paths. This too is explained in **Chapter 3** with reference to additional information in **Appendix C**.

Chapter 4 sets out the steps to be followed in calculating the noise level of one single event – the noise generated at a point on the ground by one aircraft movement. Data in the international (ANP) database apply to specific reference conditions. **Appendix D** deals with the re-calculation of NPD-data for non-reference conditions. It presents two methods, the first, SAE-ARP-5534 provides an updated methodology (2013) to calculate atmospheric absorption which is consistent with current scientific information, and is the recommended method. However, the flexibility is given for transition purposes to model non-standard atmospheric conditions with the legacy SAE-ARP-866A method (1975). **Appendix E** explains the acoustic dipole source used in the model to define sound radiation from flight path segments of finite length. **Appendix F** gives additional guidance for the case when the event level metric is L_{max} rather than L_E.

Applications of the modelling relationships described in Chapters 3 and 4 require, apart from the relevant flight paths, appropriate noise and performance data for the aircraft in question. The source of that information, the ECAC-endorsed international ANP database website, and how data can be obtained from it, is described in **Appendix G**.

Determining the event level for a single aircraft movement at a single observer point is the core calculation. It has to be repeated for all aircraft movements at each of a prescribed array of points covering the expected extent of the required noise contours. At each point the event levels are aggregated or averaged in some way to arrive at a 'cumulative level' or noise index value. This part of the process is described in **Chapter 5**.

Chapter 6 summarises the options and requirement for fitting noise contours to arrays of noise index values. It provides guidance on contour generation and post-processing.

Some existing aircraft noise contour models are based on previous ECAC guidance published in Doc 29 3rd Edition. For the benefit of users of that previous guidance **Appendix H** lists and explains the changes that have now been made; this should allow existing models to be amended to incorporate this updated methodology. Finally, **Appendix I** lists conversions between the SI and US units that are used frequently throughout.

2 SUMMARY AND APPLICABILITY OF THE METHOD

Volume 1 describes three different ways in which most practical noise models calculate aircraft noise single event levels. In order of increasing elaboration these are (1) *closest point of approach* (CPA), (2) *segmentation* and (3) *simulation* methods. Each has its strengths and weaknesses but it is considered that, on balance, segmentation (otherwise known as 'integrated') models represent current best practice. This situation may change at some point in the future: 'simulation' models have greater potential and it is only a shortage of the comprehensive data they require, and their higher demands on computing capacity, that presently restrict them to special applications (including research).

A crucial factor underpinning the ascendancy of segmentation modelling, and a principal reason why the recommended practice is based upon it, is that it is supported by a comprehensive aircraft noise and performance database of unparalleled depth and scope. This has been assembled over many years by the aircraft manufacturing industry in collaboration with the noise certificating authorities. This international aircraft noise and performance (ANP) database is now accessible on the Internet; the ANP website is a primary source of data for the methodology recommended in this guidance.

A computer model that implements the recommended methodology and the ANP database together comprise the contour modelling system. To apply it to a particular airport scenario, the user has to supply a substantial quantity of data that describes, principally, the airport and the air traffic using it - in terms of the aircraft types, numbers, routeings and operating procedures.

These basic elements of the noise contour generation process are summarised in this chapter by way of introduction to the more detailed descriptions that comprise the rest of this document.

2.1 THE CONCEPT OF SEGMENTATION

For any specific aircraft, the database contains baseline Noise-Power-Distance (NPD) relationships. These define, for steady straight flight at a *reference speed* in specified *reference atmospheric conditions* and in a specified flight configuration, the received sound event levels, both maximum and time integrated, directly beneath the aircraft[1] as a function of distance. For noise modelling purposes, the all-important propulsive power is represented by a *noise-related power parameter*; the parameter generally used is *corrected net thrust*. Baseline event levels determined from the database are adjusted to account for, firstly, differences between actual (i.e. modelled) and reference atmospheric conditions and (in the case of sound exposure levels) aircraft speed and, secondly, for receiver points that are not directly beneath the aircraft, differences between downwards and laterally radiated noise. This latter difference is due to *lateral directivity* (engine installation effects) and *lateral attenuation*. But the event levels so adjusted still apply only to the total noise from the aircraft in steady level flight.

Segmentation is the process by which the recommended noise contour model adapts the infinite path NPD and lateral data to calculate the noise reaching a receiver from a non-uniform flight path, i.e. one along which the aircraft flight configuration varies. For the purposes of calculating the event sound level of an aircraft movement, the flight path is represented by a set of contiguous straight-line segments, each of which can be regarded as a

[1] Actually beneath the aircraft perpendicular to the wing axis and direction of flight; taken to be vertically below the aircraft when in non-turning (i.e. non-banked) flight.

finite part of an infinite path for which an NPD and the lateral adjustments are known. The maximum level of the event is simply the greatest of the individual segment values. The time integrated level of the whole noise event is calculated by summing the noise received from a sufficient number of segments, i.e. those which make a significant contribution to the total event noise.

The method for estimating how much noise one finite segment contributes to the integrated event level is a purely empirical one. The *energy fraction F* – the segment noise expressed as a proportion of the total infinite path noise – is described by a relatively simple expression which allows for the longitudinal directivity of aircraft noise and the receiver's 'view' of the segment. One reason why a simple empirical method is generally adequate is that, as a rule, most of the noise comes from the nearest, usually, adjacent segment – for which the *closest point of approach* (CPA) to the receiver lies within the segment (not at one of its ends). This means that estimates of the noise from non-adjacent segments can be increasingly approximate as they get further away from the receiver without compromising the accuracy significantly.

2.2 FLIGHT PATHS: TRACKS AND PROFILES

In the modelling context, a *flight path* (or trajectory) is a full description of the motion of the aircraft in space and time[2]. Together with the propulsive thrust (or other noise related power parameter) this is the information required to calculate the noise generated. The gro*und track* is the vertical projection of the flight path on level ground. This is combined with the vertical *flight profile* to construct the 3-D flight path. Segmentation modelling requires that the flight path of every different aircraft movement is described by a series of contiguous straight segments. The manner in which the segmentation is performed is dictated by a need to balance accuracy and efficiency – it is necessary to approximate the real curved flight path sufficiently closely while minimising the computational burden and data requirements. Each segment has to be defined by the geometrical coordinates of its end points and the associated speed and engine power parameters of the aircraft (on which sound emission depends). Flight paths and engine power may be determined in various ways, the main ones involving (a) synthesis from a series of procedural steps and (b) analysis of measured flight profile data.

Synthesis of the flight path (a) requires knowledge of (or assumptions for) ground tracks and their lateral dispersions, aircraft weight, speed, flap and thrust-management procedures, airport elevation, and wind and air temperature. Equations for calculating the flight profile from the required propulsion and aerodynamic parameters are given in **Appendix B**. Each equation contains coefficients (and/or constants) which are based on empirical data for each specific aircraft type. The aerodynamic-performance equations in **Appendix B** permit the consideration of any reasonable combination of aircraft operational weight and flight procedure, including operations at different takeoff gross weights.

Analysis of measured data (b), e.g. from flight data recorders, radar or other aircraft tracking equipment, involves 'reverse engineering', effectively a reversal of the synthesis process (a). Instead of estimating the aircraft and powerplant states at the ends of the flight segments by integrating the effects of the thrust and aerodynamic forces acting on the airframe, the forces are estimated by differentiating the changes of height and speed of the airframe. Procedures for processing the flight path information are described in **Section 3.5**.

[2] Time is accounted for via the aircraft speed.

In an ultimate noise modelling application, each individual flight could, theoretically, be represented independently; this would guarantee accurate accounting for the spatial dispersion of flight paths - which can be very significant. But to keep data preparation and computer time within reasonable bounds it is normal practice to represent flight path swathes by a small number of laterally displaced 'subtracks'. (Vertical dispersion is usually represented satisfactorily by accounting for the effects of varying aircraft weights on the vertical profiles.)

2.3 AIRCRAFT NOISE AND PERFORMANCE

To support this methodology, ECAC recommends use of data from the on-line international Aircraft Noise and Performance (ANP) database (www.aircraftnoisemodel.org) which is fully described in **Appendix G**.

The ANP database contains aircraft and engine performance coefficients and NPD relationships for a substantial proportion of civil aircraft operating from airports in ECAC states. In particular, data on additional aircraft types, old and new, will be added as soon as they have been supplied to, and verified by, the database managers.

All new inputs are supplied or endorsed by the aircraft manufacturers and generated according to SAE specifications [ref. 6] that are approved by ECAC. For aircraft that are common to both, the data are identical to those in the US INM database [ref. 7]. For aircraft types or variants for which data are not currently listed, **Volume 1** provides guidance on how they can best be represented by data for other, normally similar, aircraft that are listed.

The ANP database includes default 'procedural steps' to enable the construction of flight profiles for at least one common noise abatement departure procedure. More recent database entries cover two different noise abatement departure procedures. However it should be noted that these carry the caveat:

> *"Users should examine the applicability of ANP database default 'procedural steps' to the airport under consideration. These data are generic and in some cases may not realistically represent flight operations at your airport."*

Although the manufacturers and database managers strive to ensure that the data are generated in strict accordance with the standard specifications, ultimate validation of the ANP data lies effectively within the province of the user; at present there is no practicable way in which the accuracy of the data entries can be systematically and independently checked. Inconsistencies or deficiencies are most likely to be discovered by users who compare model predictions with measured data. Evidence of inconsistencies is fed back to the data suppliers through the database managers. The suppliers then decide on the action required; only they can amend or approve database entries. To this end it must be recognised that acquiring reliable measured data is a very demanding task and it is necessary for data users to demonstrate that the evidence they provide meets acceptable quality criteria. It is anticipated that a future Volume 3 of this guidance will specify appropriate procedures for comparing measured and modelled noise levels. These will be designed to provide assurance that the supporting information can be relied upon.

Access to the database is subject to terms and conditions designed to prevent misuse. User registration and password protection are overseen by the database managers.

2.4 AIRPORT AND AIRCRAFT OPERATIONS

Case-specific data from which to calculate the noise contours for a particular airport scenario includes the following:

2.4.1 GENERAL AIRPORT DATA

- The aerodrome reference point (simply to locate the aerodrome in appropriate geographic co-ordinates). The reference point is set as the origin of the local Cartesian co-ordinate system used by the calculation procedure.
- The aerodrome reference altitude (= altitude of aerodrome reference point). This is the altitude of the nominal ground plane on which, in the absence of topography corrections, the noise contours are defined.
- Average meteorological parameters at or close to the aerodrome reference point (temperature, relative humidity, average windspeed and wind direction).

Example datasheets for the presentation of airport data can be found in **Appendix A1**.

2.4.2 RUNWAY DATA

For each runway:

- Runway designation
- Runway reference point (centre of runway expressed in local co-ordinates)
- Runway length, direction and mean gradient
- Location of start-of-roll and landing threshold[3]. Datasheets for runway data representation are shown in **Appendix A2**.

2.4.3 GROUND TRACK DATA

Aircraft ground tracks have to be described by a series of coordinates in the (horizontal) ground-plane. The source of ground track data depends on whether relevant radar data are available or not. If they are, a reliable backbone track and suitable associated (dispersed) sub-tracks can be established by statistical analysis of the data. If not, backbone tracks are usually constructed from appropriate procedural information, e.g. using standard instrument departure procedures from Aeronautical Information Publications. This conventional description includes the following information:

- Designation of the runway the track originates from
- Description of the track origin (start of roll, landing threshold)
- Length of segments (for turns, radius and change of direction)

This information is the minimum necessary to define the core (backbone) track. But average noise levels calculated on the assumption that aircraft follow the nominal routes exactly can be liable to localized errors of several decibels. Thus lateral dispersion should be represented, and the following additional information is necessary:

- Width of the swathe (or other dispersion statistic) at each segment end
- Number of subtracks

[3] Displaced thresholds can be taken into account by defining additional runways.

- Distribution of movements perpendicular to the backbone track

Example datasheets for ground track representation can be found in **Appendix A3**.

2.4.4 AIR TRAFFIC DATA

Air traffic data normally comprise the following information:

- the time period covered by the data and
- the number of movements (arrivals or departures) of each aircraft type on each flight track, subdivided by (1) time of day as appropriate for specified noise descriptors, (2) for departures, operating weights or stage lengths, and (3), if necessary, operating procedures.

Most noise descriptors require that events (i.e. aircraft movements) are defined as average daily values during specified periods of the day (e.g. day, evening and night) - see **Chapter 5**.

Air traffic example datasheets can be found in **Appendix A4**.

2.4.5 TOPOGRAPHICAL DATA

The terrain around most airports is relatively flat. However this is not always the case and there may sometimes be a need to account for variations in terrain elevation relative to the airport reference elevation. The effect of terrain elevation can be especially important in the vicinity of approach tracks, where the aircraft is operating at relatively low altitudes.

Terrain elevation data are usually provided as a set of (x,y,z) co-ordinates for a rectangular grid of a certain mesh-size. But the parameters of the elevation grid are likely to be different from those of the grid used for the noise computation. If so, linear interpolation may be used to estimate the appropriate z-co-ordinates in the latter.

Comprehensive analysis of the effects of markedly non-level ground on sound propagation is complex and beyond the scope of this guidance. Moderate unevenness can be accounted for by assuming 'pseudo-level' ground; i.e. simply raising or lowering the level ground plane to the local ground elevation (relative to the reference ground plane) at each receiver point (see **Section 3.3.4**).

2.5 REFERENCE CONDITIONS

The international aircraft noise and performance (ANP) data are normalised to standard reference conditions that are widely used for airport noise studies (see **Appendices D** and **G**).

Reference conditions for NPD data

1) Atmospheric pressure: 101.325 kPa (1013.25 mb)
2) Atmospheric absorption: Attenuation rates listed in **Table D-1** of **Appendix D**
3) Precipitation: None
4) Windspeed: Less than 8 m/s (15 knots)
5) Groundspeed: 160 knots
6) Local terrain: Flat, soft ground free of large structures or other reflecting objects within several kilometres of aircraft ground tracks.

Standardised aircraft sound measurements are made 1.2m above the ground surface. However no special account of this is necessary as, for modelling purposes, it may be assumed that event levels are relatively insensitive to receiver height[4].

Comparisons of estimated and measured airport noise levels indicate that the NPD data can be assumed applicable when the near surface average conditions lie within the following envelope:

- Air temperature less than 30 °C
- Product of air temperature (°C) and relative humidity (percent) greater than 500
- Wind speed less than 8 m/s (15 knots)

This envelope is believed to encompass conditions encountered at most of the world's major airports. **Appendix D** provides a method for converting NPD data to average local conditions which fall outside it, but in extreme cases, it is suggested that the relevant aeroplane manufacturers be consulted.

Reference conditions for aeroplane aerodynamic and engine data

1) Runway elevation: Mean sea level
2) Air temperature: 15 °C
3) Takeoff gross weight: As defined as a function of stage length in the ANP database (see **Appendix G3.5**)
4) Landing gross weight: 90 percent of maximum landing gross weight
5) Engines supplying thrust: All

Although ANP aerodynamic and engine data are based on these conditions, they can be used as tabulated for non-reference runway elevations and average air temperatures in ECAC states without significantly affecting the accuracy of the calculated contours of cumulative average sound level (see **Appendix B**).

The ANP database tabulates aerodynamic data for the takeoff and landing gross weights noted in items 3 and 4 above. Although, for cumulative noise calculations, the aerodynamic data themselves need not be adjusted for other gross weights, calculation of the takeoff and climbout flight profiles, using the procedures described in **Appendix B**, should be based on the appropriate operational takeoff gross weights.

[4] Calculated levels at 4 m or higher are sometimes requested. Comparison of measurements at 1.2 m and 10 m and theoretical calculation of ground effects show that variations of the A-weighted sound exposure level are relatively insensitive to receiver height. The variations are in general smaller than one decibel, except if the maximum angle of sound incidence is below 10° and if the A-weighted spectrum at the receiver has its maximum in the range of 200 to 500 Hz. Such low frequency dominated spectra may occur e.g. at long distances for low-bypass ratio engines and for propeller engines with discrete low frequency tones.

3 DESCRIPTION OF THE FLIGHT PATH

The noise model requires that each different aircraft movement is described by its three-dimensional flight path and the varying engine power and speed along it. As a rule, one modelled movement represents a subset of the total airport traffic, e.g. a number of (assumed) identical movements, with the same aircraft type, weight and operating procedure, on a single ground track. That track may itself be one of several dispersed 'sub-tracks' used to model what is really a swathe of tracks following one designated route. The ground track swathes, the vertical profiles and the aircraft operational parameters are all determined from the input scenario data - in conjunction with aircraft data from the ANP database.

The noise-power-distance data (in the ANP database) define noise from aircraft traversing idealised horizontal flight paths of infinite length at constant speed and power. To adapt this data to terminal area flight paths that are characterised by frequent changes of power and velocity, every path is broken into finite straight-line segments; the noise contributions from each of these are subsequently summed at the observer position.

3.1 RELATIONSHIPS BETWEEN FLIGHT PATH AND FLIGHT CONFIGURATION

The three-dimensional flight path of an aircraft movement determines the geometrical aspects of sound radiation and propagation between aircraft and observer. At a particular aircraft weight and in particular atmospheric conditions, the flight path is governed entirely by the sequence of power, flap and attitude changes that are applied by the pilot (or automatic flight management system) in order to follow routes and maintain heights and speeds specified by ATC - in accordance with the aircraft operator's standard operating procedures. These instructions and actions divide the flight path into distinct phases which form natural segments. In the horizontal plane they involve straight legs, specified as a distance to the next turn, and turns, defined by radius and change of heading. In the vertical plane, segments are defined by the time and/or distance taken to achieve required changes of forward speed and/or height at specified power and flap settings. The corresponding vertical coordinates are often referred to as *profile points*.

For noise modelling, flight path information is generated either by *synthesis* from a set of procedural steps (i.e. those followed by the pilot) or by *analysis* of radar data - physical measurements of actual flight paths flown. Whatever method is used, both horizontal and vertical shapes of the flight path, are reduced to segmented forms. Its horizontal shape (i.e. its 2-D projection on the ground) is the *ground track* defined by the inbound or outbound routeing. Its vertical shape, given by the profile points, and the associated flight parameters speed, bank angle and power setting, together define the *flight profile* which depends on the *flight procedure* that is normally prescribed by the aircraft manufacturer and/or the operator. The flight path is constructed by merging the 2-D flight profile with the 2-D ground track to form a sequence of 3-D flight path segments.

It should be remembered that, for a given set of procedural steps, the profile depends on the ground track; e.g. at the same thrust and speed the aircraft climb rate is less in turns than in straight flight. Although this guidance explains how to take this dependency into account, it has to be acknowledged that doing so would normally involve a very large computing overhead and users may prefer to assume that, for noise modelling purposes, the flight profile and ground track can be treated as independent entities; i.e. that the climb profile is unaffected by any turns. However, it is important to determine changes of bank angle that turns require as this has an important bearing on the directionality of sound emission.

The noise received from a flight path segment depends on the geometry of the segment in relation to the observer and the aircraft flight configuration. But these are interrelated - a change in one causes a change in the other and it is necessary to ensure that, at all points on the path, the configuration of the aircraft is consistent with its motion along the path.

In a flight path synthesis, i.e. when constructing a flight path from a set of 'procedural steps' that describe the pilot's selections of engine power, flap angle, and acceleration/vertical speed, it is the motion that has to be calculated. In a flight path analysis, the reverse is the case: the engine power settings have to be estimated from the observed motion of the aeroplane - as determined from radar data, or sometimes, in special studies, from aircraft flight recorder data (although in the latter case engine power is usually part of the data). In either case, the coordinates and flight parameters at all segment end points have to be fed into the noise calculation.

The operational steps followed by arriving and departing aircraft are explained in **Chapter 4** of **Volume 1**. **Appendix B** presents the equations that relate the forces acting on an aircraft and its motion and explains how they are solved to define the properties of the segments that make up the flight paths. The different kinds of segments (and the sections of **Appendix B** that cover them) are *takeoff ground roll* (B5), *climb at constant speed* (B6), *power cutback* (B7), *accelerating climb and flap retraction* (B8), *accelerating climb after flap retraction* (B9), *descent and deceleration* (B10) and *final landing approach* (B11).

Inevitably, practical modelling involves varying degrees of simplification - the requirement for this depends on the nature of the application, the significance of the results and the resources available (see **Volume 1**). A general simplifying assumption, even in the most elaborate applications, is that when accounting for flight track dispersion, the flight profiles and configurations on all the sub-tracks are the same as those on the backbone track. As at least 6 subtracks are recommended (see **Section 3.4**) this reduces computations massively for an extremely small penalty in fidelity.

3.2 SOURCES OF FLIGHT PATH DATA

3.2.1 RADAR DATA

Although aircraft flight data recorders can yield very high quality data, this is difficult to obtain for noise modelling purposes and radar data must be regarded as the most readily accessible source of information on actual flight paths flown at airports[5]. As it is usually available from airport noise and flight path monitoring systems, it is now used increasingly for noise modelling purposes. However the analysis of radar data is a complex task for which methods are still under development [ref. 8]. Thus it is not possible at present to recommend a specific methodology. Only general guidance can be offered; it is for users to take stock of specific circumstances when deciding on an appropriate approach.

Secondary surveillance radar presents the flight path of an aircraft as a sequence of positional coordinates at intervals equal to the period of rotation of the radar scanner, typically about 4 seconds. The position of the aircraft over the ground is determined in polar coordinates - range and azimuth - from the reflected radar return (although the monitoring system normally

[5] Aircraft flight data recorders provide comprehensive operational data. However this is not readily accessible and is costly to provide; thus its use for noise modelling purposes is normally restricted to special projects and model development studies.

transforms these to Cartesian coordinates); its height[6] is measured by the aeroplane's own altimeter and transmitted to the ATC computer by a radar-triggered transponder. But inherent positional errors due to radio interference and limited data resolution are significant (although of no consequence for the intended air traffic control purposes). Thus, if the flight path of a specific aircraft movement is required, it is necessary to smooth the data using an appropriate curve-fitting technique [e.g. refs. 9,10]. However, for noise modelling purposes the usual requirement is for a statistical description of a swathe of flight paths; e.g. for all movements on a route or for just those of a specific aircraft type. Here the measurement errors associated with the relevant statistics can be reduced to insignificance by the averaging processes.

3.2.2 PROCEDURAL STEPS

In many cases is not possible to model flight paths on the basis of radar data - because the necessary resources are not available or because the scenario is a future one for which there are no relevant radar data.

In the absence of radar data, or when its use is inappropriate, it is necessary to estimate the flight paths on the basis of operational guidance material, for example instructions given to flight crews via AIPs and aircraft operating manuals - referred to here as *procedural steps*. Advice on interpreting this material should be sought from air traffic control authorities and the aircraft operators where necessary.

3.3 CO-ORDINATE SYSTEMS

3.3.1 THE LOCAL CO-ORDINATE SYSTEM

The local co-ordinate system (x,y,z) is a Cartesian one and has its origin (0,0,0) at the aerodrome reference point (X_{ARP},Y_{ARP},Z_{ARP}), where Z_{ARP} is the airport reference altitude and $z = 0$ defines the nominal ground plane on which contours are usually calculated. The aircraft heading ξ in the xy-plane is measured clockwise from magnetic north (see **Figure 3-1**). All observer locations, the basic calculation grid and the noise contour points are expressed in local co-ordinates[7].

[6] Usually measured as altitude above MSL (i.e. relative to 1013 mb) and corrected to airport elevation by the airport monitoring system.

[7] Usually the axes of the local co-ordinate are parallel to the axis of the map that contours are drawn on. However it is sometimes useful to choose the x-axis parallel to a runway in order to get symmetrical contours without using a fine computational grid (see **Chapter 6**).

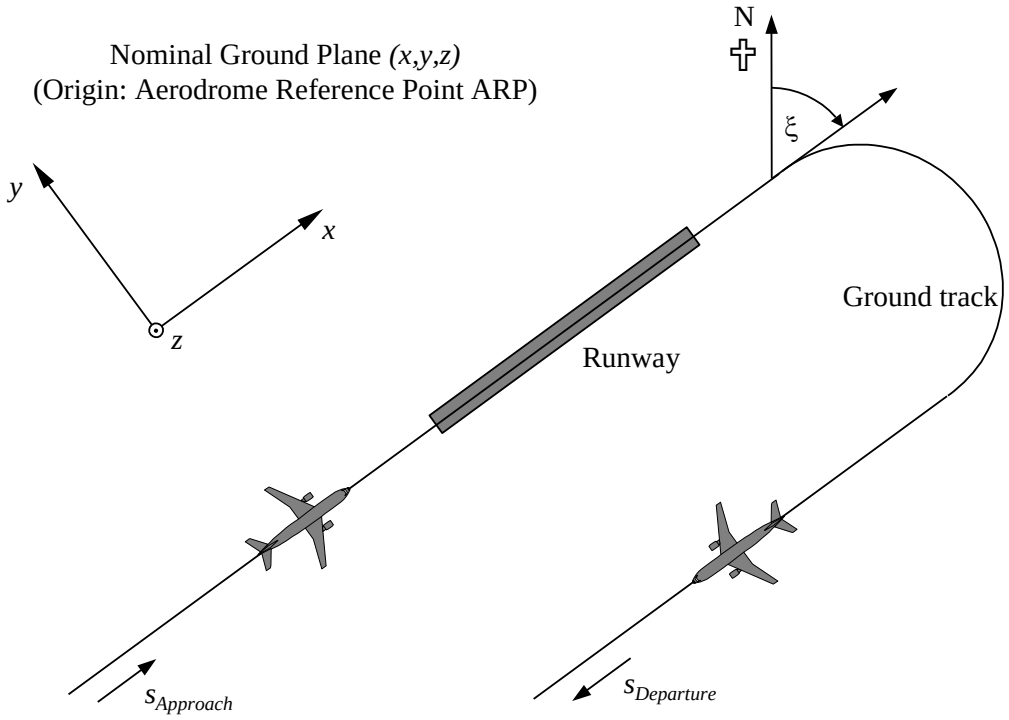

Figure 3-1: Local co-ordinate system (*x,y,z*) and ground-track fixed co-ordinates

3.3.2 THE GROUND-TRACK FIXED CO-ORDINATE SYSTEM

This co-ordinate is specific for each ground track and represents distance *s* measured along the track in the flight direction. For departure tracks *s* is measured from the start of roll, for approach tracks from the landing threshold. Thus *s* becomes negative in areas

- behind the start of roll for departures and
- before crossing the runway landing threshold for approaches.

Flight operational parameters such as height, speed and power setting are expressed as functions of *s*.

3.3.3 THE AIRCRAFT CO-ORDINATE SYSTEM

The aircraft-fixed Cartesian co-ordinate system (*x′,y′,z′*) has its origin at the actual aircraft location. The axis-system is defined by the climb-angle γ, the flight direction ξ and the bank-angle ε (see **Figure 3-2**).

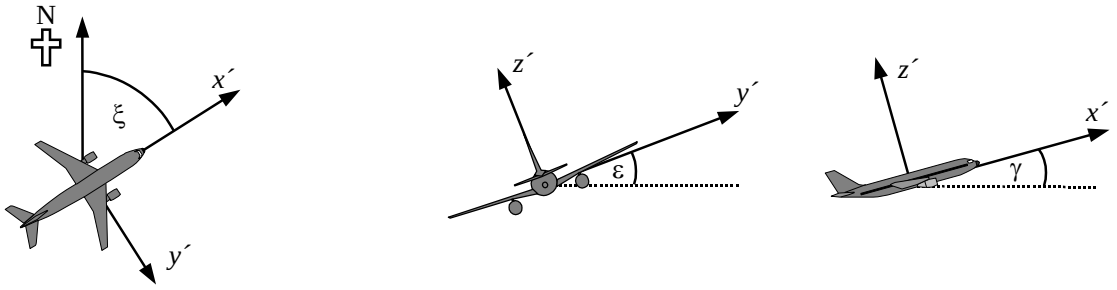

Figure 3-2: Aircraft fixed co-ordinate system (*x',y',z'*)

3.3.4 ACCOUNTING FOR TOPOGRAPHY

In cases where topography has to be taken into account (see **Section 2.4.5**), the aircraft height coordinate z has to be replaced by $z' = z - z_o$ (where z_o is the z co-ordinate of the observer location O) when estimating the propagation distance d. The geometry between aircraft and observer is shown in **Figure 3-3**. For the definitions of d and ℓ see **Chapter 4** [8].

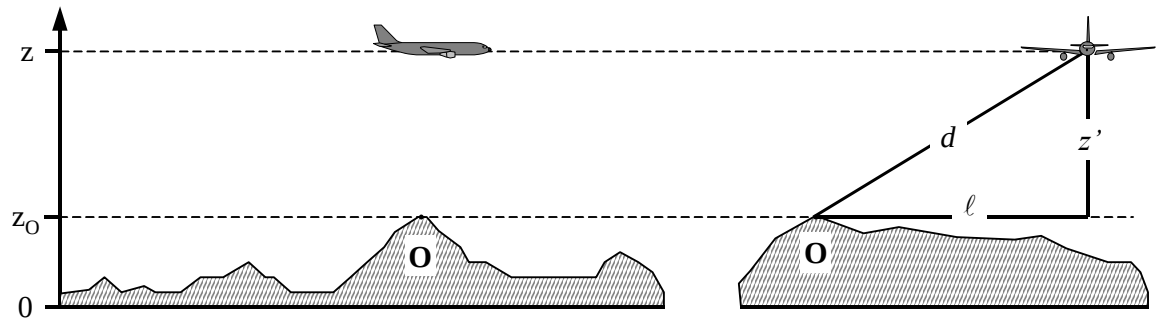

Figure 3-3: Ground elevation along (left) and lateral (right) to ground track. The nominal ground plane z = 0 passes through the aerodrome reference point. O is the observer location.

3.4 GROUND TRACKS

3.4.1 BACKBONE TRACKS

The backbone track defines the centre of the swathe of tracks followed by aircraft using a particular routeing. For the purposes of aircraft noise modelling it is defined either (i) by prescriptive operational data such as the instructions given to pilots in AIPs, or (ii) by statistical analysis of radar data as explained in **Section 3.2.1** - when this is available and appropriate to the needs of the modelling study. Constructing the track from operational instructions is normally quite straightforward as these prescribe a sequence of legs which are either straight - defined by length and heading, or circular arcs defined by turn rate and change of heading; see **Figure 3-4** for an illustration.

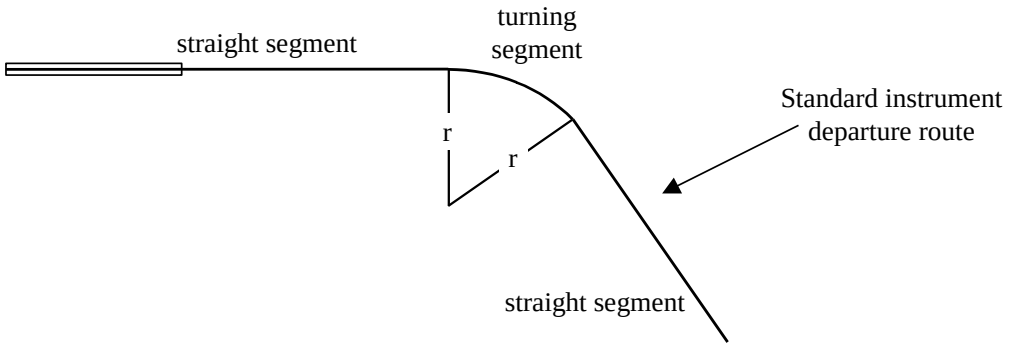

Figure 3-4: Ground track geometry in terms of turns and straight segments

[8] For non-level ground it is possible for the observer to be above the aircraft in which case, for calculating sound propagation, z' (and the corresponding elevation angle β - see Chapter 4) is put equal to zero.

Fitting a backbone track to radar data is more complex, firstly because actual turns are made at a varying rate and secondly because its line is obscured by the scatter of the data. As explained, formalised procedures have not yet been developed and it is common practice to match segments, straight and curved, to the average positions calculated from cross-sections of radar tracks at intervals along the route. Computer algorithms to perform this task are likely to be developed in future but, for the present, it is for the modeller to decide how to use available data to best advantage. A major factor is that the aircraft speed and turn radius dictate the angle of bank and, as will be seen in **Section 4.5**, non-symmetries of sound radiation around the flight path govern noise on the ground, as well as the position of the flight path itself.

Theoretically, seamless transition from straight flight to fixed radius turn would require an instantaneous application of bank angle ε, which is physically impossible. In reality it takes a finite time for the bank angle to reach the value required to maintain a specified speed and turn radius *r*, during which the turn radius tightens from infinity to *r*. For modelling purposes the radius transition can be disregarded and the bank angle assumed to increase steadily from zero (or other initial value) to ε at the start of the turn and to the next value of ε at the end of the turn[9].

3.4.2 LATERAL TRACK DISPERSION

Where possible, definitions of lateral dispersion and representative sub-tracks should be based on relevant past experience from the study airport; normally via an analysis of radar data samples. The first step is to group the data by route. Departure tracks are characterised by substantial lateral dispersion which, for accurate modelling, has to be taken into account. Arrival routes normally coalesce into a very narrow swathe about the final approach path and it is usually sufficient to represent all arrivals by a single track. But if the approach swathes are wide within the region of the noise contours they might need to be represented by sub-tracks in the same way as departure routes.

It is common practice to treat the data for a single route as a sample from a single population; i.e. to be represented by one backbone track and one set of dispersed subtracks. However, if inspection indicates that the data for different categories of aircraft or operations differ significantly (e.g. should large and small aircraft have substantially different turn radii), further subdivision of the data into different swathes may be desirable. For each swathe, the lateral track dispersions are determined as a function of distance from the origin; movements then being apportioned between a backbone track and a suitable number of dispersed sub-tracks on the basis of the distribution statistics.

As it is normally unwise to disregard the effects of track dispersion, in the absence of measured swathe data a nominal lateral spread across and perpendicular to the backbone track should be defined by a conventional distribution function. Calculated values of noise indices are not particularly sensitive to the precise shape of the lateral distribution: the Normal (Gaussian) Distribution provides an adequate description of many radar-measured swathes.

Typically a 7-point discrete approximation is used (i.e. representing the lateral dispersion by 6 subtracks equally spaced around the backbone track). The spacing of the subtracks depends on the standard deviation of the lateral dispersion function.

---

[9] How best to implement this is left to the user as this will depend on the way in which turn radii are defined. When the starting point is a sequence of straight or circular legs, a relatively simple option is to insert bank angle transition segments at the start of the turn and at its end in which the aircraft rolls at a constant rate (e.g. expressed in °/m or °/s).

For normally distributed tracks with a standard deviation *S*, 98.8% of the tracks are located within a corridor with boundaries located at ±2.5·*S*. **Table 3-1** gives the spacing of the six subtracks and the percentage of the total movements assigned to each. **Appendix C** gives values for other numbers of subtracks.

Table 3-1: **Percentages of movements for a normal distribution function with standard deviation *S* for 7 subtracks (backbone track is subtrack 1).**

Subtrack number	Location of subtrack	Percentage of movements on subtrack
7	–2.14·*S*	3 %
5	–1.43·*S*	11 %
3	–0.71·*S*	22 %
1	0	28 %
2	0.71·*S*	22 %
4	1.43·*S*	11 %
6	2.14·*S*	3 %

The standard deviation *S* is a function of the co-ordinate *s* along the backbone-track. It can be specified – together with the description of the backbone-track – in the flight track data sheet shown in **Appendix A3**. In the absence of any indicators of the standard deviation – e.g. from radar data describing comparable flight tracks – the following values are recommended:

For tracks involving turns of less than 45 degrees:

$$\begin{aligned} S(s) &= 0.055 \cdot s - 150 \quad \text{for} \quad 2700\,\text{m} \le s \le 30000\,\text{m} \\ S(s) &= 1500\,\text{m} \quad \text{for} \quad s > 30000\,\text{m} \end{aligned} \tag{3-1a}$$

For tracks involving turns of more than 45 degrees:

$$\begin{aligned} S(s) &= 0.128 \cdot s - 420 \quad \text{for} \quad 3300\,\text{m} \le s \le 15000\,\text{m} \\ S(s) &= 1500\,\text{m} \quad \text{for} \quad s > 15000\,\text{m} \end{aligned} \tag{3-1b}$$

For practical reasons, *S(s)* is assumed to be zero between the start of roll and s = 2700 m or s = 3300 m depending on the amount of turn. Routes involving more than one turn should be treated as per equation 3-1b. For arrivals, lateral dispersion can be neglected within 6000 m of touchdown.

3.5 FLIGHT PROFILES

The flight profile is a description of the aircraft motion in the vertical plane above the ground track, in terms of its position, speed, bank angle and engine power setting. One of the most important tasks facing the model user is that of defining aircraft flight profiles that adequately meet the requirements of the modelling application - efficiently, without consuming excessive time and resources. Naturally, to achieve high accuracy, the profiles have to reflect closely the aircraft operations they are intended to represent. This requires reliable information on the

atmospheric conditions, aircraft types and variants, operating weights and the operating procedures – the variations of thrust and flap settings and the trade-offs between changes of height and speed – all appropriately averaged over the time period(s) of interest. Often such detailed information are not available but this is not necessarily an obstacle; even if they are, the modeller has to exercise judgement to balance the accuracy and detail of the input information with the needs for, and uses of, the contour outputs.

The synthesis of flight profiles from 'procedural steps' obtained from the ANP database or from aircraft operators is described in **Section 3.6** and **Appendix B**. That process, usually the only recourse open to the modeller when no radar data are available, yields both the flight path geometry and the associated speed and thrust variations. It would normally be assumed that all (alike) aircraft in a swathe, whether assigned to the backbone or the dispersed subtracks, follow the backbone track profile.

Beyond the ANP database, which provides default information on procedural steps, the aircraft operators are the best source of reliable information, i.e. the procedures they use and the typical weights flown. For individual flights, the 'gold standard' source is the aircraft flight data recorder (FDR) from which all relevant information can be obtained. But even if such data are available, the pre-processing task is formidable. Thus, and in keeping with the necessary modelling economies, the normal practical solution is to make educated assumptions about mean weights and operating procedures.

Caution must be exercised before adopting *default* procedural steps provided in the ANP database (customarily assumed when actual procedures are not known). These are standardised procedures that are widely followed but which may or may not be used by operators in particular cases. A major factor is the definition of takeoff (and sometimes climb) engine thrust that can depend to an extent on prevailing circumstances. In particular, it is common practice to reduce thrust levels during departure (from maximum available) in order to extend engine life. **Appendix B** gives guidance on representing typical practice; this will generally produce more realistic contours than a full thrust assumption. However, if, for example, runways are short and/or average air temperatures are high, full thrust is likely to be a more realistic assumption.

When modelling actual scenarios, improved accuracy can be achieved by using radar data to supplement or replace this nominal information. Flight profiles can be determined from radar data in a similar way to the lateral backbone tracks - but only after segregating the traffic by aircraft type and variant and sometimes by weight or stage length (but not by dispersion) - to yield for each sub-group a mean profile of height and speed against ground distance travelled. Again, when merging with the ground tracks subsequently, this single profile is normally assigned to the backbone and sub-tracks alike.

Knowing the aircraft weight, the variation of speed and propulsive thrust can be calculated via step-by-step solution of the equations of motion. Before doing so it is helpful to pre-process the data to minimise the effects of radar errors which can make acceleration estimates unreliable. The first step in each case is to redefine the profile by fitting straight line segments to represent the relevant stages of flight; with each segment being appropriately classified; i.e. as a ground roll, constant speed climb or descent, thrust cutback, or acceleration/deceleration with or without flap change. The aircraft weight and atmospheric state are also required inputs.

An aircraft noise source should be entered at a minimum height of 1.0 m (3.3 ft) above the aerodrome level, or above the terrain elevation levels of the runway, as relevant.

Section 3.4 makes it clear that special provision has to be made to account for the lateral dispersion of flight tracks about the nominal or backbone routeings. Radar data samples are characterised by similar dispersions of flight paths in the vertical plane. However it is not usual practice to model vertical dispersion as an independent variable; it arises mainly due to differences in aircraft weights and operating procedures that are taken into account when pre-processing traffic input data.

3.6 CONSTRUCTION OF FLIGHT PATH SEGMENTS

Each flight path has to be defined by a set of segment co-ordinates (nodes) and flight parameters. The flight profile is calculated, remembering that for a given set of procedural steps, the profile depends on the ground track; e.g. at the same thrust and speed the aircraft climb rate is less in turns than in straight flight (**Section 3.6.1**). Sub-segmentation is then undertaken for the aircraft on the runway (takeoff or landing ground roll, **Sections 3.6.2** and **3.6.3** respectively), and for the aircraft near to the runway (initial climb or final approach, **Section 3.6.4**). Airborne segments with significantly different speeds at their start and end points should then be sub-segmented (**Section 3.6.5**). The two-dimensional co-ordinates of the ground track segments are determined and merged with the two-dimensional flight profile to construct the three-dimensional flight path segments (**Section 3.6.6**). Finally, any flight path points that are too close together are removed (**Section 3.6.7**).

3.6.1 FLIGHT PROFILE

The parameters describing each flight profile segment at the start (suffix 1) and end (suffix 2) of the segment are:

s_1, s_2	distance along the ground track,
z_1, z_2	aeroplane height,
V_1, V_2	groundspeed,
P_1, P_2	noise-related power parameter (matching that for which the NPD curves are defined), and
ε_1, ε_2	bank angle.

To build a flight profile from a set of procedural steps (*flight path synthesis*), segments are constructed in sequence to achieve required conditions at the end points. The end-point parameters for each segment become the start-point parameters for the next segment. In any segment calculation the parameters are known at the start; required conditions at the end are specified by the procedural step. The steps themselves are defined either by the ANP defaults or by the user (e.g. from aircraft flight manuals). The end conditions are usually height and speed; the profile building task is to determine the track distance covered in reaching those conditions. The undefined parameters are determined via flight performance calculations described in **Appendix B**.

If the ground track is straight, the profile points and associated flight parameters can be determined independently of the ground track (bank angle is always zero). However ground tracks are rarely straight; they usually incorporate turns and, to achieve best results, these have to be accounted for when determining the 2-D flight profile, where necessary splitting profile segments at ground track nodes to inject changes of bank angle. As a rule the length of the next segment is unknown at the outset and it is calculated provisionally assuming no change of bank angle. If the provisional segment is then found to span one or more ground track nodes, the first being at s, i.e. $s_1 < s < s_2$, the segment is truncated at s, calculating the parameters there by interpolation (see below). These become the end-point parameters of the

current segment and the start-point parameters of a new segment - which still has the same target end conditions. If there is no intervening ground track node the provisional segment is confirmed.

If the effects of turns on the flight profile are to be disregarded, the straight flight, single segment solution is adopted although the bank angle information is retained for subsequent use.

Whether or not turn effects are fully modelled, each 3-D flight path is generated by merging its 2-D flight profile with its 2-D ground track. The result is a sequence of co-ordinate sets (*x*,*y*,*z*), each being either a node of the segmented ground track, a node of the flight profile or both, the profile points being accompanied by the corresponding values of height *z*, ground speed *V*, bank angle ε and engine power *P*. For a track point (*x*,*y*) which lies between the end points of a flight profile segment, the flight parameters are interpolated as follows:

$$z = z_1 + f \cdot (z_2 - z_1) \tag{3-2a}$$

$$V = \sqrt{V_1^2 + f \cdot \left(V_2^2 - V_1^2\right)} \tag{3-2b}$$

$$\varepsilon = \varepsilon_1 + f \cdot (\varepsilon_2 - \varepsilon_1) \tag{3-2c}$$

$$P = \sqrt{P_1^2 + f \cdot \left(P_2^2 - P_1^2\right)} \tag{3-2d}$$

where

$$f = (s - s_1)/(s_2 - s_1) \tag{3-2e}$$

Note that whilst *z* and ε are assumed to vary linearly with distance, *V* and *P* are assumed to vary linearly with time (i.e. constant acceleration[10]).

When matching flight profile segments to radar data (*flight path analysis*), all end-point distances, heights, speeds and bank angles are determined directly from the data; only the power settings have to be calculated using the performance equations. As the ground track and flight profile co-ordinates can also be matched appropriately, this is usually quite straightforward.

3.6.2 TAKEOFF GROUND ROLL

When taking off, as an aircraft accelerates between the point of brake release (alternatively termed Start-of-Roll *SOR*) and the point of lift-off, speed changes dramatically over a distance of 1500 to 2500 m, from zero to between around 80 and 100 m/s.

The takeoff roll is thus divided into segments with variable lengths over each of which the aircraft speed changes by specific increment ΔV of no more than 10 m/s (about 20 kt). Although it actually varies during the takeoff roll, an assumption of constant acceleration is adequate for this purpose. For equivalent takeoff distance s_{TO} (see **Appendix B**) and takeoff speed V_{TO}, the number n_{TO} of segments for the ground roll is:

$$n_{TO} = \text{int}(1 + V_{TO}/10) \tag{3-3a}$$

[10] Even if engine power settings remain constant along a segment, propulsive force and acceleration can change due to variation of air density with height. However, for the purposes of noise modelling these changes are normally negligible.

and hence the change of velocity along a segment is

$$\Delta V = V_{TO} / n_{TO} \tag{3-3b}$$

and the time Δt on each segment is (constant acceleration assumed)

$$\Delta t = \frac{2 \cdot s_{TO}}{V_{TO} \cdot n_{TO}} \tag{3-3c}$$

The length $s_{TO,k}$ of segment k ($1 \le k \le n_{TO}$) of the takeoff roll is then:

$$s_{TO,k} = (k - 0.5) \cdot \Delta V \cdot \Delta t = \frac{(2k-1) \cdot s_{TO}}{n_{TO}^{\,2}} \tag{3-3d}$$

Example: For a takeoff distance s_{TO} = 1600 m and V_{TO} = 75 m/s, this yields n_{TO} = 8 segments with lengths ranging from 25 to 375 m (see **Figure 3-5**):

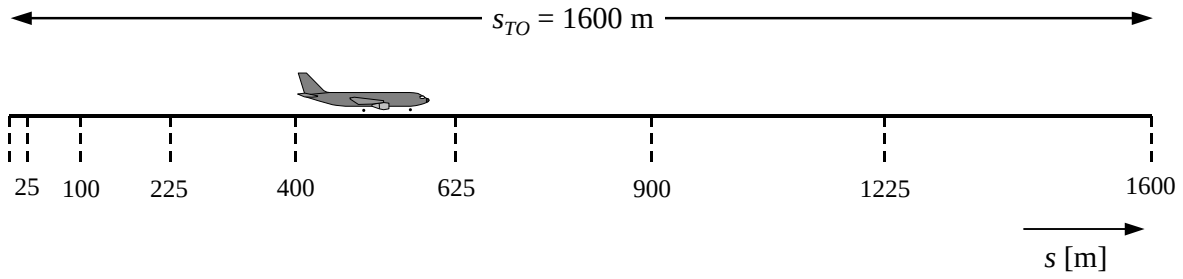

Figure 3-5: Segmentation of a takeoff roll (example for 8 segments)

Similar to the speed changes, the aircraft thrust changes over each segment by a constant increment Δ*P*, calculated as:

$$\Delta P = \left(P_{TO} - P_{init}\right) / n_{TO} \tag{3-3e}$$

where P_{TO} and P_{init} respectively designate the aircraft thrust at the point of lift-off and the aircraft thrust at the start of takeoff roll.

The use of this constant thrust increment (instead of using the quadratic form equation 3-2d) aims at being consistent with the linear relationship between thrust and speed in the case of jet-engine aircraft (Eq. B-1).

Important note: The above equations and example implicitly assume that the initial speed of the aircraft at the start of the takeoff phase is zero. This corresponds to the common situation where the aircraft starts to roll and accelerate from the brake release point. However, there are also situations where the aircraft may start to accelerate from its taxiing speed, without stopping at the runway threshold. In that case of non-zero initial speed V_{init}, the following 'generalised' equations should be used in replacement of Eq. 3-3a, 3-3b, 3-3c and 3-3d.

$$n = \text{int}(1 + |V_2 - V_1| / 10) \tag{3-3f}$$

$$\Delta V = \left(V_2 - V_1\right) / n \tag{3-3g}$$

$$\Delta t = \frac{2 \cdot s}{\left(V_2 + V_1\right) \cdot n} \tag{3-3h}$$

$$s_k = \left(V_1 + \Delta V \cdot \left(k - 0.5\right)\right) \cdot \frac{2 \cdot s}{\left(V_2 + V_1\right) \cdot n} \qquad \text{(3-3i)}$$

In this case, for the takeoff phase, V_1 is initial speed V_{init}, V_2 is the takeoff speed V_{TO}, n is the number of takeoff segment n_{TO}, s is the equivalent takeoff distance s_{TO} and s_k is the length $s_{TO,k}$ of segment k ($1 \le k \le n$).

3.6.3 LANDING GROUND ROLL

Although the landing ground roll is essentially a reversal of the takeoff ground roll, special account has to be taken of:

- *reverse thrust* which is sometimes applied to decelerate the aircraft and
- aeroplanes leaving the runway after deceleration (aircraft that leave the runway no longer contribute to air noise as noise from taxiing is disregarded).

In contrast to the takeoff roll distance, which is derived from aircraft performance parameters, the stop distance s_{stop} (i.e. the distance from touchdown to the point where the aircraft leaves the runway) is not purely aircraft specific. Although a minimum stop distance can be estimated from aircraft mass and performance (and available reverse thrust), the actual stop distance depends also on the location of the taxiways, on the traffic situation, and on airport-specific regulations on the use of reverse thrust.

The use of reverse thrust is not a standard procedure - it is only applied if the needed deceleration cannot be achieved by the use of the wheel brakes. (Reverse thrust can be exceptionally disturbing as a rapid change of engine power from idle to reverse settings produces a sudden burst of noise.)

However, most runways are used for departures as well as for landings so that reverse thrust has a very small effect on the noise contours since the total sound energy in the vicinity of the runway is dominated by the noise produced from takeoff operations. Reverse thrust contributions to contours may only be significant when runway use is limited to landing operations.

Physically, reverse thrust noise is a very complex process but because of its relatively minor significance to air noise contours it can be modelled simplistically - the rapid change in engine power being taken into account by suitable segmentation.

It is clear that modelling the landing ground roll is less straightforward than for takeoff roll noise. The following simplified modelling assumptions are recommended for general use, when no detailed information is available (see **Figure 3-6**).

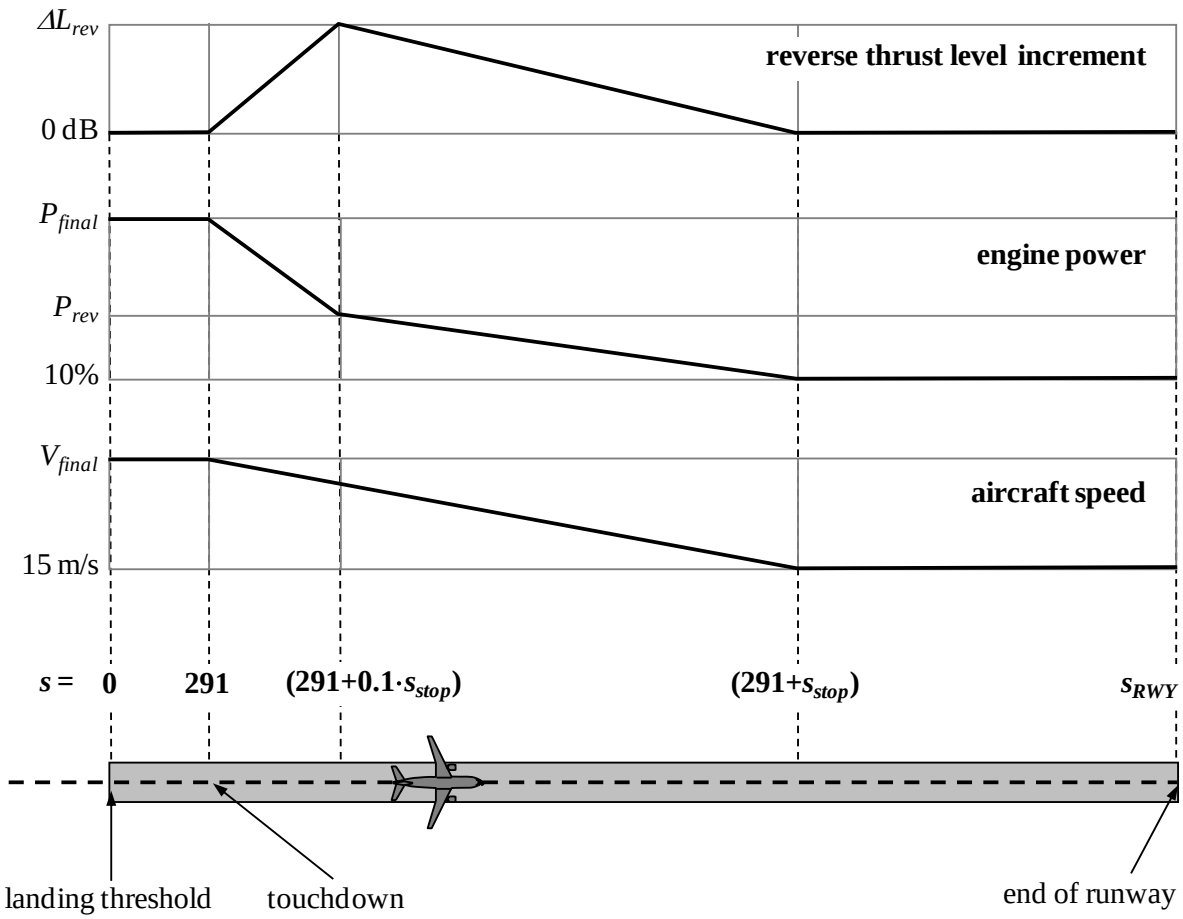

Figure 3-6: Modelling of landing ground roll

The aircraft crosses the landing threshold (which has the co-ordinate s = 0 along the approach ground track) at an altitude of 50 feet, and then continues to descend on its glideslope until it touches down on the runway. For a 3° glideslope, the touch-down point is 291 m beyond the landing threshold (as illustrated in Figure 3-6). The aircraft is then decelerated over a stop-distance s_{stop} - aircraft specific values of which are given in the ANP database - from final approach speed V_{final} to 15 m/s. Because of the rapid changes in speed during this segment it should be sub-segmented in the same manner as for the takeoff ground roll (or airborne segments with rapid speed changes), using the generalised equations 3-3f to 3-3i (as taxi-in speed is not equal to zero).

The engine power changes from final approach power at touchdown to a reverse thrust power setting P_{rev} over a distance $0.1 \cdot s_{stop}$, then decreases to 10 % of the maximum available power over the remaining 90 percent of the stop distance. Up to the end of the runway (at $s = s_{RWY}$) aircraft speed remains constant.

NPD curves for reverse thrust are not at present included in the ANP database, and it is therefore necessary to rely on the conventional curves for modelling this effect. Typically the reverse thrust power P_{rev} is around 20% of the full power setting and this is recommended when no operational information is available. However, at a given power setting, reverse thrust tends to generate significantly more noise than forward thrust and an increment ΔL should be applied to the NPD-derived event level, increasing from zero to a value ΔL_{rev} (5 dB

is recommended provisionally[11]) along $0.1 \cdot s_{stop}$ and then falling linearly to zero along the remainder of the stop distance.

3.6.4 SEGMENTATION OF THE INITIAL CLIMB AND FINAL APPROACH SEGMENTS

The segment-to-receiver geometry changes rapidly along the initial climb and final approach airborne segments, particularly with respect to observer locations to the side of the flight track, where the elevation angle (*beta angle*) also changes rapidly as the aircraft climbs or descends through these initial/final segments. Comparisons with very small segment calculations show that using a single (or a limited number of) climb or approach airborne segment(s) below a certain height (relative to the runway) results in a poor approximation of noise to the side of the flight track for integrated metrics. This is due to the application of a single lateral attenuation adjustment (see **Section 4.5.4**) on each segment, corresponding to a single segment-specific value of the elevation angle, whereas the rapid change of this parameter results in significant variations of the lateral attenuation effect along each segment. Calculation accuracy is improved by sub-segmenting the initial climb and last approach airborne segments. The number of sub-segments and the length of each determine the lateral attenuation change 'granularity' which will be accounted for. Noting the expression of total lateral attenuation for aircraft with fuselage-mounted engines (**Section 4.5.4**), it can be shown that for a limiting change in lateral attenuation of 1.5 dB per sub-segment, the climb and approach airborne segments located below a height of 1289.6 m (4231 ft) above the runway should be sub-segmented based on the following set of height values:

$$z' = \{18.9, 41.5, 68.3, 102.1, 147.5, 214.9, 334.9, 609.6, 1289.6\} \text{ metres, or}$$

$$z' = \{62, 136, 224, 335, 484, 705, 1099, 2000, 4231\} \text{ feet}$$

For each original segment below 1289.6 m (4231 ft), the above heights are implemented by identifying which height in the set above is closest to the original endpoint height (for a climb segment) or start-point height (for an approach segment). The actual sub-segment heights, z_i, would then be calculated using:

$$z_i = z_e \, [z'_i / z'_N] \; (i = k..N) \qquad (3\text{-}4)$$

where:

z_e	is the original segment endpoint height (climb) or start-point height (approach)
z'_i	is the i^{th} member of the set of height values listed above
z'_N	is the closest height from the set of height values listed above to height z_e
k	denotes the index of the first member of the set of height values for which the calculated z_k is strictly greater than the endpoint height of the previous original climb segment or the start-point height of the next original approach segment to be sub-segmented. In the specific case of an initial climb segment or last approach segment, $k = 1$, but in the more general case of airborne segments not connected to the runway, k will be greater than 1.

[11] This was recommended in the previous edition of ECAC Doc 29 but is still considered provisional pending the acquisition of further corroborative experimental data.

This height scaling method ensures that the original segment endpoint heights (for climb) or start point heights (for approach) are preserved.

If the original endpoint height of a climb segment or start point height of an approach segment is greater than 1289.6 m (4231 ft), equation 3-4 should be applied using z_e = 1289.6 m.

This process results in a granularity of the lateral attenuation change across each sub-segment which does not exceed 1.5 dB, hence producing more accurate contours, but without the expense of using a large number of very short segments.

The speed and engine power values on the inserted points are interpolated using equations 3-2b and 3-2d respectively.

Example for an initial climb segment:

If the original segment endpoint height is z_e = 304.8 m, then from the set of height values, 214.9 m < z_e < 334.9 m and the closest height from the set to z_e is z'_7 = 334.9 m. The sub-segment endpoint heights are then computed by:

$$z_i = 304.8\ [z'_i / 334.9] \text{ for } i = 1 \text{ to } 7$$

(noting that $k = 1$ in that case, as this is an initial climb segment)

Thus z_1 would be 17.2 m and z_2 would be 37.8 m, etc.

3.6.5 SEGMENTATION OF AIRBORNE SEGMENTS

For airborne segments where there is a speed change along a segment of greater than 20 knots, this segment should be subdivided as for the ground roll, i.e.

$$n_{seg} = int\left(1 + |V_2 - V_1| / 10\right) \tag{3-5}$$

where V_1 and V_2 are the segment start and end speeds respectively. The corresponding sub-segment parameters are calculated in a similar manner as for the takeoff ground roll, using the generalised equations 3-3f to 3-3i.

3.6.6 GROUND TRACK

A ground track, whether a backbone track or a dispersed sub-track, is defined by a series of (x,y) co-ordinates in the ground plane (e.g. from radar information) or by a sequence of vectoring commands describing straight segments and circular arcs (turns of defined radius r and change of heading $\Delta\xi$).

For segmentation modelling, an arc is represented by a sequence of straight segments fitted to sub-arcs. Although they do not appear explicitly in the ground-track segments, the banking of aircraft during turns influences their definition. **Appendix B4** explains how to calculate bank angles during a steady turn but of course these are not actually applied or removed instantaneously. How to handle the transitions between straight and turning flight, or between one turn and an immediately sequential one, is not prescribed. As a rule, the details, which are left to the user (see **Section 3.4.1**), are likely to have a negligible effect on the final contours; the requirement is mainly to avoid sharp discontinuities at the ends of the turn and this can be achieved simply, for example, by inserting short transition segments over which the bank angle changes linearly with distance. Only in the special case that a particular turn is likely to have a dominating effect on the final contours would it be necessary to model the dynamics of

the transition more realistically, to relate bank angle to particular aircraft types and to adopt appropriate roll rates. Here it is sufficient to state that the end sub-arcs $\Delta\xi_{trans}$ in any turn are dictated by bank angle change requirements. The remainder of the arc with change of heading $\Delta\xi$ - $2\cdot\Delta\xi_{trans}$ degrees is divided into n_{sub} sub-arcs according to the equation:

$$n_{sub} = \text{int}(1 + (\Delta\xi - 2\cdot\Delta\xi_{trans})/10) \tag{3-6a}$$

where int(x) is a function that returns the integer part of x. Then the change of heading $\Delta\xi_{sub}$ of each sub-arc is computed as

$$\Delta\xi_{sub} = (\Delta\xi - 2\cdot\Delta\xi_{trans})/n_{sub} \tag{3-6b}$$

where n_{sub} needs to be large enough to ensure that $\Delta\xi_{sub} \leq 30$ degrees, with a recommended implementation of $\Delta\xi_{sub} \leq 10$ degrees (equation 3-6a calculates n_{sub} for the latter). The segmentation of an arc (excluding the terminating transition sub-segments) is illustrated in **Figure 3-7**[12].

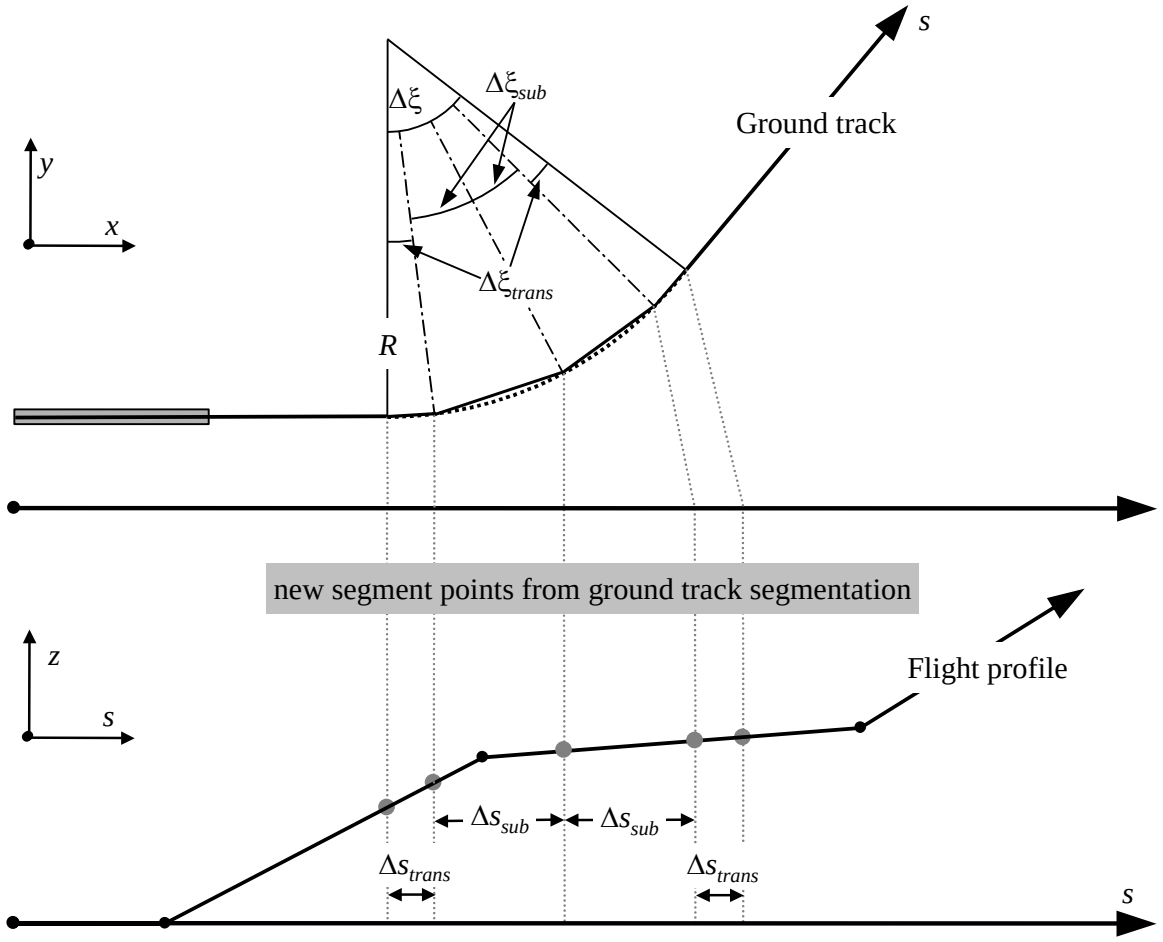

Figure 3-7: Construction of flight path segments dividing turn into segments of length Δs (upper view in horizontal plane, lower view in vertical plane)

[12] Defined in this simple way, the total length of the segmented path is slightly less than that of the circular path. However the consequent contour error is negligible if the angular increments are below 30°.

Once the ground track segments have been established in the x-y plane, the flight profile segments (in the s-z plane) are overlaid to produce the three-dimensional (x, y, z) track segments.

The ground track should always extend from the runway to beyond the extent of the calculation grid (see **Section 6**). This can be achieved, if necessary, by adding a straight segment of suitable length to the last segment of the ground track.

The total length of the flight profile, once merged with the ground track, must also extend from the runway to beyond the extent of the calculation grid. This can be achieved, if necessary, by adding an extra profile point:

- to the end of a departure profile with speed and thrust values equal to those of the last departure profile point, and height extrapolated linearly from the last and penultimate profile points; or
- to the beginning of an arrival profile with speed and thrust value equal to those of the first arrival profile point, and height extrapolated linearly back from the first and second profile points.

3.6.7 SEGMENTATION ADJUSTMENTS OF AIRBORNE SEGMENTS

After the 3-D flight path segments have been derived according to the procedure described in **Sections 3.6.1** to **3.6.6** above, further segmentation adjustments may be necessary to remove flight path points which are too close together.

When adjacent points are within 10 metres of each other, and when the associated speeds and thrusts are the same, one of the points should be eliminated.

4 NOISE CALCULATION FOR A SINGLE EVENT

The core of the modelling process, described here in full, is the calculation of the event noise level from the flight path information described in **Chapter 3**.

4.1 SINGLE EVENT METRICS

The sound generated by an aircraft movement at the observer location is expressed as a 'single event sound (or noise) level', a quantity which is an indicator of its impact on people. The received sound is measured in noise terms using a basic decibel scale *L(t)* which applies a frequency weighting (or filter) to mimic a characteristic of human hearing. The scale of most importance in aircraft noise contour modelling is the A-weighted sound level, L_A [refs. 2,3].

The metrics most commonly used to encapsulate entire events are 'single event sound (or noise) exposure levels', L_E, which account for all (or most of) the sound energy in the events. Making provisions for the time integration that this involves gives rise to the main complexities of segmentation (or simulation) modelling. Simpler to model is an alternative metric L_{max} which is the maximum instantaneous level occurring during the event; however it is L_E which is the basic building block of most modern aircraft noise indices and practical models can in future be expected to embody both L_{max} and L_E. Either metric can be measured on different scales of noise; in this document only A-weighted sound level is considered. Symbolically, the scale is usually indicated by extending the metric suffix, i.e. L_{AE}, L_{Amax}. **Section 3.2** of **Volume 1** provides a fuller description of noise metrics.

The single event sound (or noise) exposure level is expressed exactly as:

$$L_E = 10 \cdot \log\left(\frac{1}{t_0} \int_{t_1}^{t_2} 10^{L(t)/10} dt \right) \tag{4-1}$$

where t_0 denotes a reference time. The integration interval $[t_1,t_2]$ is chosen to ensure that (nearly) all significant sound in the event is encompassed. Very often, the limits t_1 and t_2 are chosen to span the period for which the level *L(t)* is within 10 dB of L_{max}. This period is known as the "10 dB-down" time. Sound (noise) exposure levels tabulated in the ANP database are 10 dB-down values[13].

For aircraft noise contour modelling, the main application of equation 4-1 is the standard metric *Sound Exposure Level* L_{AE} (acronym SEL) [refs. 2,3]:

$$L_{AE} = 10 \cdot \log\left(\frac{1}{t_0} \int_{t_1}^{t_2} 10^{L_A(t)/10} dt \right) \text{ with } t_0 = 1\,\text{second} \tag{4-2}$$

The exposure level equations above can be used to determine event levels when the entire time history of *L(t)* is known. Within the recommended noise modelling methodology such time histories are not defined; event exposure levels are calculated by summing segment values, partial event levels each of which defines the contribution from a single, finite segment of the flight path.

[13] 10dB-down L_E may be up to 0.5 dB lower than L_E evaluated over a longer duration. However, except at short slant distances where event levels are high, extraneous ambient noise often makes longer measurement intervals impractical and 10 dB-down values are the norm. As studies of the effects of noise (used to 'calibrate' the noise contours) also tend to rely on 10 dB-down values, the ANP tabulations are considered to be entirely appropriate.

4.2 DETERMINATION OF EVENT LEVELS FROM NPD DATA

The principal source of aircraft noise data is the international Aircraft Noise and Performance (ANP) database which is described in **Appendix G**. This tabulates L_{max} and L_E as functions of propagation distance d for specific aircraft types, variants, flight configurations (approach, departure, flap settings), and power settings P. They relate to steady flight at specific reference speeds V_{ref} along a notionally infinite, straight flight path[14].

How values of the independent variables P and d are specified is described later. In a single look-up, with input values P and d, the output values required are the *baseline levels* $L_{max}(P,d)$ and/or $L_{E\infty}(P,d)$ (applicable to an infinite flight path). Unless values happen to be tabulated for P and/or d exactly, it will generally be necessary to estimate the required event noise level(s) by interpolation. A linear interpolation is used between tabulated power settings, whereas a logarithmic interpolation is used between tabulated distances (see **Figure 4-1**).

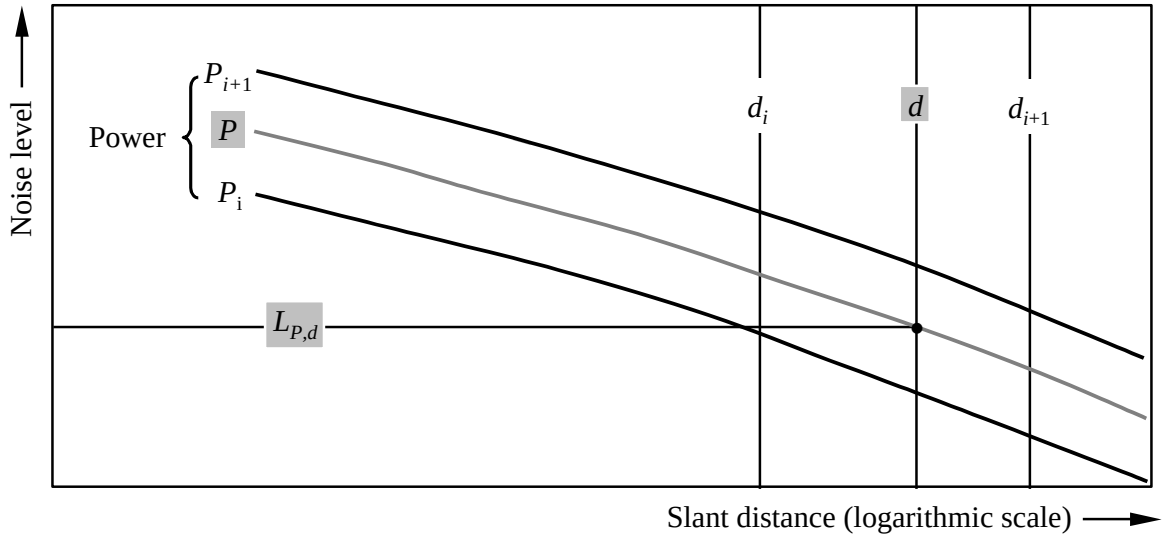

Figure 4-1: Interpolation in noise-power-distance curves

If P_i and P_{i+1} are engine power values for which noise level versus distance data are tabulated, the noise level $L(P)$ at a given distance for intermediate power P, between P_i and P_{i+1}, is given by:

$$L(P) = L(P_i) + \frac{L(P_{i+1}) - L(P_i)}{P_{i+1} - P_i} \cdot (P - P_i) \qquad (4\text{-}3)$$

If, at any power setting, d_i and d_{i+1} are distances for which noise data are tabulated, the noise level $L(d)$ for an intermediate distance d, between d_i and d_{i+1} is given by

[14] Although the notion of an infinitely long flight path is important to the definition of event sound exposure level L_E, it has less relevance in the case of event maximum level L_{max} which is governed by the noise emitted by the aircraft when at a particular position at or near its closest point of approach to the observer. For modelling purposes the NPD distance parameter is taken to be the minimum distance between the observer and segment.

$$L(d) = L(d_i) + \frac{L(d_{i+1}) - L(d_i)}{\log d_{i+1} - \log d_i} \cdot (\log d - \log d_i) \quad (4\text{-}4)$$

By using equations 4-3 and 4-4, a noise level *L(P,d)* can be obtained for any power setting *P* and any distance *d* that is within the envelope of the NPD database.

For distances *d* that lie outside the NPD envelope, equation 4-4 is used to extrapolate from the last two values, i.e. inwards from $L(d_1)$ and $L(d_2)$ or outwards from $L(d_{I-1})$ and $L(d_I)$ where *I* is the total number of NPD points on the curve. Thus

Inwards: $$L(d) = L(d_2) + \frac{L(d_1) - L(d_2)}{\log d_2 - \log d_1} \cdot (\log d_2 - \log d) \quad (4\text{-}5a)$$

Outwards: $$L(d) = L(d_{I-1}) - \frac{L(d_{I-1}) - L(d_I)}{\log d_I - \log d_{I-1}} \cdot (\log d - \log d_{I-1}) \quad (4\text{-}5b)$$

As, at short distances *d*, noise levels increase very rapidly with decreasing propagation distance, it is recommended that a lower limit of 30 m be imposed on *d*, i.e. $d = \max(d, 30\text{ m})$.

4.2.1 IMPEDANCE ADJUSTMENT OF STANDARD NPD DATA

The NPD data provided in the ANP database are normalized to reference day atmospheric conditions. Before applying the interpolation/extrapolation method previously described, an acoustic impedance adjustment shall be applied to these standard NPD data.

Acoustic impedance is related to the propagation of sound waves in an acoustic medium, and is defined as the product of the density of air and the speed of sound. For a given sound intensity (power per unit area) perceived at a specific distance from the source, the associated sound pressure (used to define SEL and L_{Amax} metrics) depends on the acoustic impedance of the air at the measurement location. It is a function of temperature, atmospheric pressure (and indirectly altitude). There is therefore a need to adjust the standard NPD data of the ANP database to account for the actual temperature and pressure conditions at the receiver point, which are generally different from the normalized conditions of the ANP data. To avoid excessive computational demands, the adjustment should be made to actual temperature and pressure conditions at the aerodrome and applied to calculations at all receiver points.

The impedance adjustment to be applied to the standard NPD levels is expressed as follows:

$$\Delta_{impedance} = 10 \cdot \log\left(\frac{\rho \cdot c}{409.81}\right) \quad (4\text{-}6)$$

where:

$\Delta_{impedance}$	Impedance adjustment for the actual atmospheric conditions at the aerodrome (dB)
$\rho \cdot c$	Acoustic impedance (in units of Newton-seconds per cubic metre) of the air at the aerodrome (409.81 Ns/m^3 being the air impedance associated with the reference atmospheric conditions of the NPD data in the ANP database).

Impedance $\rho \cdot c$ is calculated as follows:

$$\rho \cdot c = 416.86 \cdot \left[\frac{\delta}{\theta^{1/2}} \right] \tag{4-7}$$

δ p/p_O, the ratio of the ambient air pressure at the observer altitude to the standard air pressure at mean sea level: p_O = 101.325 kPa (or 1013.25 millibars)

θ $(T + 273.15)/(T_0 + 273.15)$ the ratio of the air temperature at the observer altitude to the air temperature constant: T_0 = 15.0 °C

The acoustic impedance adjustment is usually less than a few tenths of one dB. In particular, it should be noted that under the standard atmospheric conditions (p_O = 101.325 kPa and T_0 = 15.0 °C), the impedance adjustment is less than 0.1 dB (0.074 dB). However, when there is a significant variation in temperature and atmospheric pressure relative to the reference atmospheric conditions of the NPD data, the adjustment can be more substantial.

4.3 GENERAL EXPRESSIONS

4.3.1 SEGMENT EVENT LEVEL L_{SEG}

The segment values are determined by applying adjustments to the baseline (infinite path) values read from the NPD data. The maximum noise level from one flight path segment $L_{max,seg}$ can be expressed in general as

$$L_{max,seg} = L_{max}(P,d) + \Delta_I(\varphi) - \Lambda(\beta,\ell) \tag{4-8a}$$

and the contribution from one flight path segment to L_E as

$$L_{E,seg} = L_{E\infty}(P,d\ ) + \Delta_V + \Delta_I(\varphi) - \Lambda(\beta,\ell) + \Delta_F \tag{4-8b}$$

The 'correction terms' in equations 4-8 - which are described in detail in **Section 4.5** - account for the following effects:

Δ_V *Duration correction:* the NPD data relate to a reference flight speed. This adjusts exposure levels to non-reference speeds. (It is not applied to $L_{max,seg}$.)

$\Delta_I(\varphi)$ *Installation effect:* describes a variation in *lateral directivity* due to shielding, refraction and reflection caused by the airframe, engines and surrounding flow fields.

$\Lambda(\beta,\ell)$ *Lateral attenuation:* significant for sound propagating at low angles to the ground, this accounts for the interaction between direct and reflected sound waves (ground effect) and for the effects of atmospheric non-uniformities (primarily caused by the ground) that refract sound waves as they travel towards the observer to the side of the flight path.

Δ_F *Finite segment correction (Noise Fraction):* accounts for the finite length of the segment which obviously contributes less noise exposure than an infinite one. It is only applied to exposure metrics.

If the segment is part of the takeoff or landing ground roll, special steps are taken, depending on whether the observer is located behind the start or ahead of the end of the segment under consideration, to represent the directivity of engine noise. These special steps result in the use of a start-of-roll directivity correction term and a particular form of the noise fraction for the exposure level:

$$L_{max,seg} = L_{max}(P,d) + \Delta_I(\varphi) - \Lambda(\beta,\ell) + \Delta_{SOR} \tag{4-9a}$$

$$L_{E,seg} = L_{E\infty}(P,d) + \Delta_V + \Delta_I(\varphi) - \Lambda(\beta,\ell) + \Delta'_F + \Delta_{SOR} \tag{4-9b}$$

Δ'_F Particular form of the *Segment correction*

Δ_{SOR} *Directivity correction*: accounts for the pronounced directionality of jet engine noise behind the ground roll segment

The specific treatment of ground roll segments is described in **Sections 4.5.6** and **4.5.7**.

Sections 4.4 to 4.5 describe in detail the calculation of segment noise levels.

4.3.2 EVENT NOISE LEVEL L OF AN AIRCRAFT MOVEMENT

Maximum level L_{max} is simply the greatest of the segment values $L_{max,seg}$ (see equation 4-8a)

$$L_{max} = \max(L_{max,seg}) \tag{4-10}$$

where each segment value is determined from the aircraft NPD data for power P and distance d. These parameters and the modifier terms $\Delta_I(\varphi)$ and $\Lambda(\beta,\ell)$ are explained below.

Exposure level L_E is calculated as the decibel sum of the contributions $L_{E,seg}$ from each noise-significant segment of its flight path; i.e.

$$L_E = 10 \cdot \lg\left(\sum 10^{L_{E,seg}/10}\right) \tag{4-11}$$

The summation proceeds step by step through the flight path segments.

The remainder of this chapter is concerned with the determination of the segment noise levels $L_{max,seg}$ and $L_{E,seg}$.

4.4 FLIGHT PATH SEGMENT PARAMETERS

The power P and distance d, for which the baseline levels $L_{max,seg}(P,d)$ and $L_{E\infty}(P,d)$ are interpolated from the NPD tables, are determined from geometric and operational parameters that define the segment. How this is done is explained below with the aid of illustrations of the plane containing the segment and the observer.

4.4.1 GEOMETRIC PARAMETERS

Figures 4-2a to **4-2c** show the source-receiver geometries when the observer **O** is (a) behind, (b) alongside and (c) ahead of the segment $\mathbf{S_1S_2}$ where the flight direction is from $\mathbf{S_1}$ to $\mathbf{S_2}$. In these diagrams:

O	is the observer location
S_1 , **S_2**	are the start and end of the segment
S_p	is the point of perpendicular closest approach to the observer on the segment or its extension
d_1 , d_2	are the distances between start, end of segment and observer
d_s	is the shortest distance between observer and segment
d_p	is the perpendicular distance between observer and extended segment *(minimum slant range)*
λ	is the length of flight path segment
q	is the distance from **S_1** to **S_p** (negative if the observer position is behind the segment)

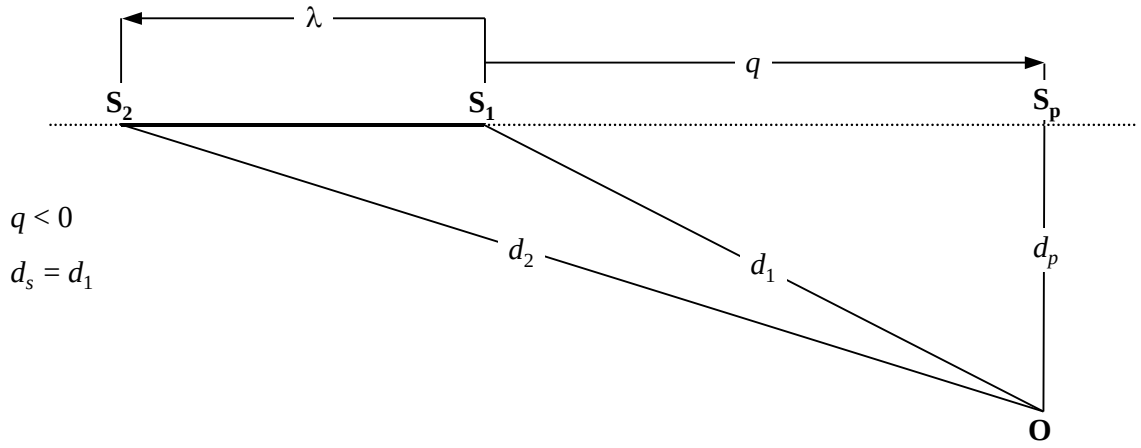

Figure 4-2a: Flight path segment geometry for observer behind segment

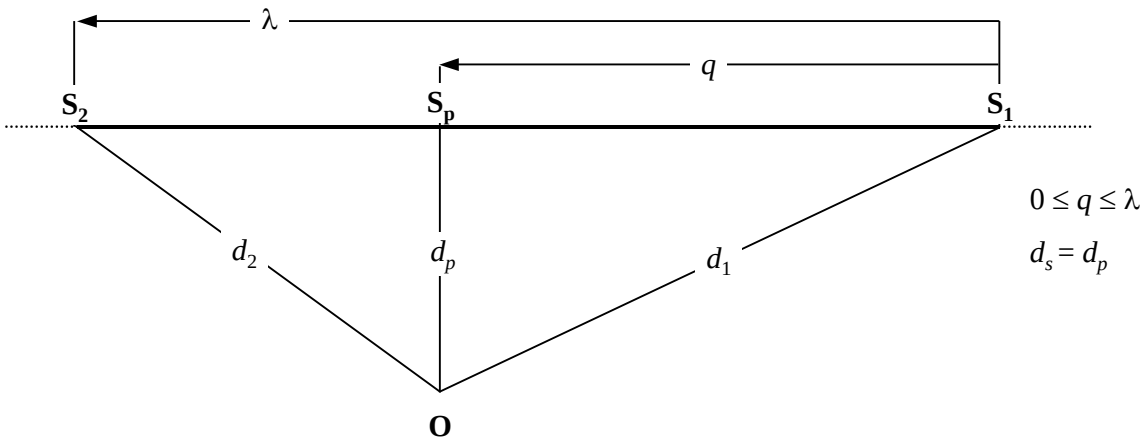

Figure 4-2b: Flight path segment geometry for observer alongside segment

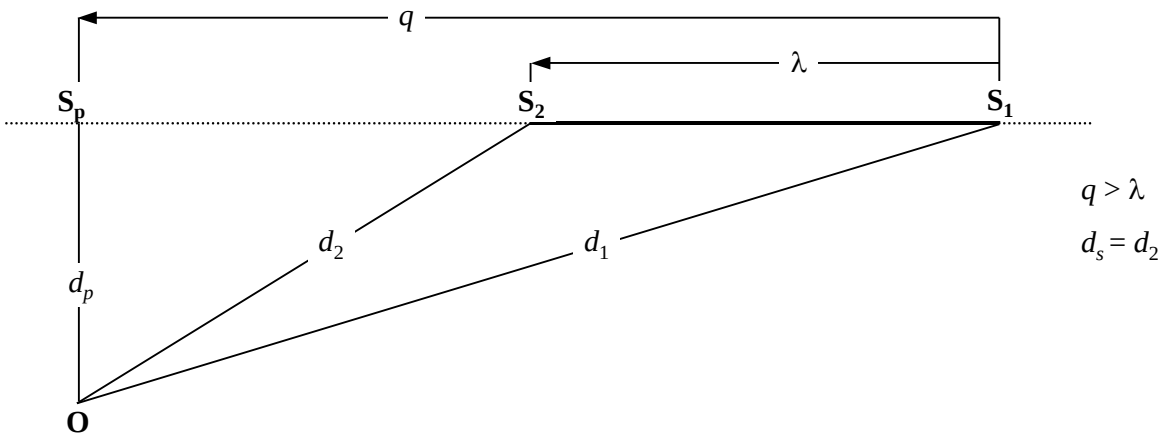

Figure 4-2c: Flight path segment geometry for observer ahead of segment

The flight path segment is represented by a bold, solid line. The dotted line represents the *flight path extension* which stretches to infinity in both directions. For airborne segments, when the event metric is an exposure level L_E, the NPD distance parameter d is the distance d_p between $\mathbf{S_p}$ and the observer, called the *minimum slant range* (i.e. the perpendicular distance from the observer to the segment or its extension, in other words to the hypothetical, infinite flight path of which the segment is considered to be part).

However, for exposure level metrics where observer locations are behind the ground segments during the takeoff roll and locations ahead of ground segments during the landing roll, the NPD distance parameter d becomes the distance d_s, the shortest distance from the observer to the segment (i.e. the same as for maximum level metrics).

For maximum level metrics, the NPD distance parameter d is d_s, the shortest distance from the observer to the segment.

4.4.2 SEGMENT POWER P

The tabulated NPD data describe the noise of an aircraft in steady straight flight on an infinite flight path, i.e. at constant engine power P. The recommended methodology breaks actual flight paths, along which speed and direction vary, into a number of finite segments, each of which is then taken to be part of a uniform, infinite flight path for which the NPD data are valid. But the methodology provides for changes of power along the length of a segment; it is taken to change quadratically with distance from P_1 at its start to P_2 at its end. It is therefore recommended to define an equivalent steady segment value P. This is taken to be the value at the point on the segment that is closest to the observer. If the observer is alongside the segment (**Figure 4.2b**) it is obtained by interpolation as given by equation 3-2d between the end values, i.e.

$$P = \sqrt{P_1^2 + \frac{q}{\lambda} \cdot \left(P_2^{\,2} - P_1^{\,2}\right)} \qquad (4\text{-}12)$$

If the observer is behind or ahead of the segment, it is that at the nearest end point, P_1 or P_2.

4.5 SEGMENT EVENT LEVEL CORRECTION TERMS

The NPD data define noise event levels as a function of distance perpendicularly beneath an idealised straight level path of infinite length along which the aircraft flies with steady power at a fixed reference speed[15]. The event level interpolated from the NPD table for a specific power setting and slant distance is thus described as a *baseline level*. It applies to an infinite flight path and has to be corrected to account for the effects of (1) non-reference speed, (2) engine installation effects (lateral directivity), (3) lateral attenuation, (4) finite segment length and (5) longitudinal directivity behind start of roll on takeoff - see equations 4-8.

4.5.1 THE DURATION CORRECTION Δ_V (EXPOSURE LEVELS L_E ONLY)

This correction[16] accounts for a change in exposure levels if the actual segment speed is different to the aircraft reference speed V_{ref} to which the basic NPD data relate.

Like engine power, speed varies along the flight path segment (from V_{T1} to V_{T2}, which are the speeds output from Appendix B or from a previously pre-calculated flight profile).

For airborne segments, V_{seg} is the segment speed at the closest point of approach, **S**, interpolated between the segment end-point values assuming it varies quadratically with time; i.e. if the observer is alongside the segment:

$$V_{seg} = \sqrt{V_{T1}{}^2 + \frac{q}{\lambda} \cdot \left(V_{T2}{}^2 - V_{T1}{}^2\right)} \qquad (4\text{-}13a)$$

If the observer is behind or ahead of the segment, it is that at the nearest end point, V_{T1} or V_{T2}.

For runway segments (parts of the takeoff or landing ground rolls) V_{seg} is taken to be simply the average of the segment start and end speeds; i.e.

$$V_{seg} = (V_{T1} + V_{T2})/2 \qquad (4\text{-}13b)$$

In either case the additive duration correction is then:

$$\Delta_V = 10 \cdot \log(V_{ref} / V_{seg}) \qquad (4\text{-}14)$$

4.5.2 SOUND PROPAGATION GEOMETRY

Figure 4-3 shows the basic geometry in the plane normal to the aircraft flight path. The ground line is the intersection of the normal plane and the level ground plane. (If the flight path is level the ground line is an end view of the ground plane.) The aircraft is banked at angle ε measured counter-clockwise about its roll axis (i.e. starboard wing up). It is therefore positive for left turns and negative for right turns.

---

[15] NPD specifications require that the data be based on measurements of steady *straight* flight, not necessarily level; to create the necessary flight conditions, the test aircraft flight path can be inclined to the horizontal. However, as will be seen, inclined paths lead to computational difficulties and, when using the data for modelling, it is convenient to visualise the source paths as being both straight and level.

[16] This is known as the *duration correction* because it makes allowance for the effects of aircraft *speed* on the duration of the sound event - implementing the simple assumption that, other things being equal, duration, and thus received event sound energy, is inversely proportional to source velocity.

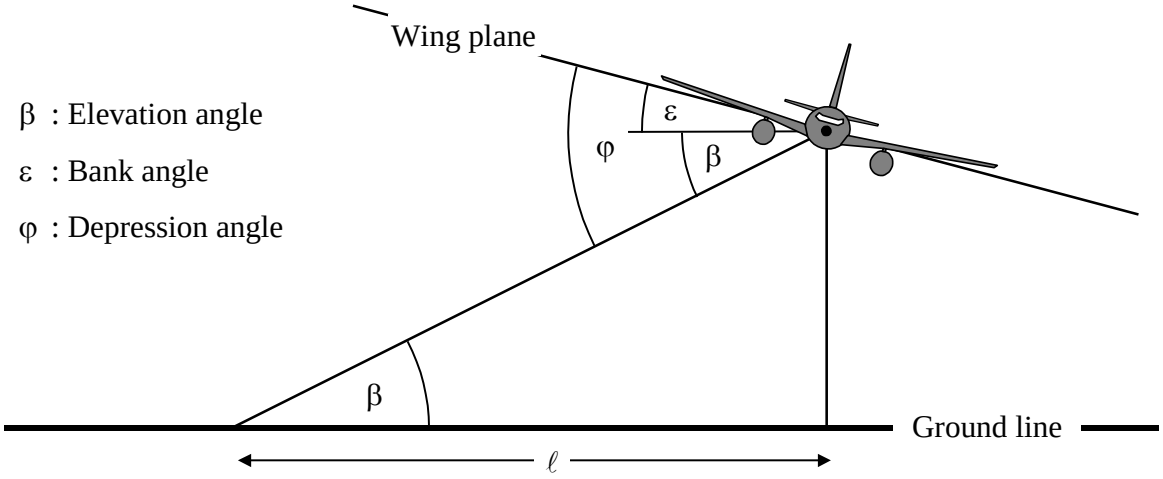

Figure 4-3: Aircraft-observer angles in plane normal to flight path

- The *elevation angle* β (between 0 and 90°) between the direct sound propagation path and the level ground line[17] determines, together with the flight path inclination and the lateral displacement ℓ of the observer from the ground track, the lateral attenuation. This is explained in **Sections 4.5.4** and **4.5.5**.
- The *depression angle* φ between the wing plane and the propagation path, determines the engine installation effects. With respect to the convention for the bank angle $\varphi = \beta \pm \varepsilon$, with the sign positive for observers to starboard (right) and negative for observers to port (left). The correction for engine installation effects is explained in **Section 4.5.3**. The *elevation angle* β, which is required to determine the *depression angle* φ, is defined in **Section 4.5.5**.

4.5.3 ENGINE INSTALLATION CORRECTION Δ_I

An aircraft in flight is a complex sound source. Not only are the engine (and airframe) sources complex in origin, but the airframe configuration, particularly the location of the engines, influences the noise radiation patterns through the processes of reflection, refraction and scattering by the solid surfaces and aerodynamic flow fields. This results in a non-uniform directionality of sound radiated laterally about the roll axis of the aircraft, referred to here as *lateral directivity*.

There are significant differences in lateral directivity between aircraft with fuselage-mounted and underwing-mounted engines and these are allowed for in the following expression:

$$\Delta_I(\varphi) = 10 \cdot \lg\left[\left(a \cdot \cos^2\varphi + \sin^2\varphi\right)^b / \left(c \cdot \sin^2 2\varphi + \cos^2 2\varphi\right)\right] \text{ dB} \qquad (4\text{-}15)$$

where $\Delta_I(\varphi)$ is the correction, in dB, at depression angle φ (see **Figure 4-3**) and

a = 0.0039,	b = 0.062,	c = 0.8786	for wing-mounted engines and
a = 0.1225,	b = 0.329,	c = 1	for fuselage-mounted engines.

[17] In the case of non-flat terrain there can be different definitions of elevation angle. Here it is defined by the aircraft height above the observation point and the slant distance - hence neglecting local terrain gradients as well as obstacles on the sound propagation path (see **Sections 2.4.5** and **3.3.4**). In the event that, due to ground elevation, the receiver point is above the aircraft, elevation angle β is set equal to zero.

For propeller aircraft directivity variations are negligible and for these it may be assumed that

$$\Delta_I(\varphi) = 0 \qquad (4\text{-}16)$$

Figure 4-4 shows the variation of $\Delta_I(\varphi)$ about the aircraft roll axis for the three engine installations. These empirical relationships have been derived by the SAE from experimental measurements made mainly beneath the wing [ref. 11]. Until above-wing data have been analysed it is recommended that, for negative φ, $\Delta_I(\varphi) = \Delta_I(0)$ for all installations.

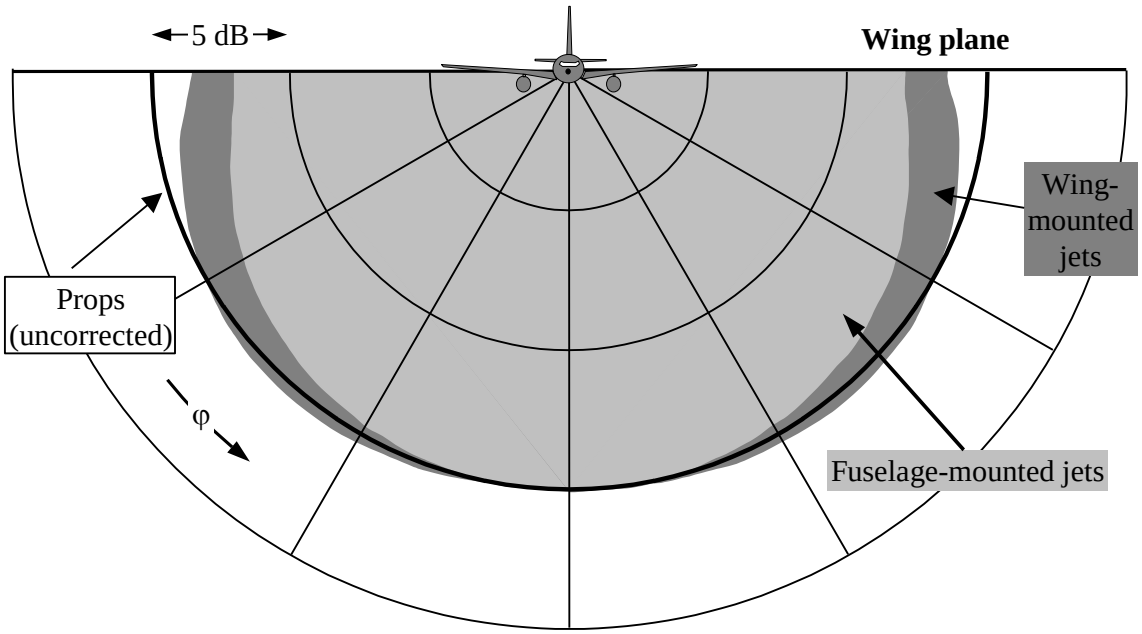

Figure 4-4: Lateral directivity of installation effects

It is assumed that $\Delta_I(\varphi)$ is two-dimensional; i.e. it does not depend on any other parameter, and in particular that it does not vary with the longitudinal distance of the observer from the aircraft. This is for modelling convenience until there is a better understanding of the mechanisms; in reality, installation effects are bound to be substantially three-dimensional. Despite that, a two-dimensional model is justified by the fact that event levels tend to be dominated by noise radiated sideways from the nearest segment.

4.5.4 LATERAL ATTENUATION $\Lambda(\beta,\ell)$ (INFINITE FLIGHT PATH)

Tabulated NPD event levels relate to steady level flight and are generally based on measurements made 1.2m above soft level ground beneath the aircraft; the distance parameter is effectively height above the surface. Any effect of the surface on event noise levels beneath the aircraft, that might cause the tabulated levels to differ from free-field values[18], is assumed to be inherent in the data (i.e. in the shape of the level vs. distance relationships).

To the side of the flight path, the distance parameter is the minimum slant distance – the length of the normal from the receiver to the flight path. At any lateral position the noise level will generally be less than at the same distance immediately below the aircraft. Apart from *lateral directivity* or 'installation effects' described in **Section 4.5.3** this is due to an excess *lateral attenuation* which causes the sound level to fall more rapidly with distance than

[18] A 'free-field' level is that which would be observed if the ground surface were not there.

indicated by the NPD curves. A previous, widely used method for modelling lateral propagation of aircraft noise was developed by the Society of Automotive Engineers (SAE) in AIR-1751 [ref. 12] and the algorithms described below are based on improvements that SAE now recommends AIR-5662 [ref. 11]. Lateral attenuation is a reflection effect, due to interference between directly radiated sound and that which reflects from the surface. It depends on the nature of the surface and can cause significant reductions in observed sound levels at low elevation angles. It is also very strongly affected by sound refraction, steady and unsteady, caused by wind and temperature gradients and turbulence which are themselves attributable to the presence of the surface[19]. The mechanism of surface reflection is well understood and, for uniform atmospheric and surface conditions, it can be described theoretically with some precision. However, atmospheric and surface non-uniformities - which are not amenable to simple theoretical analysis - have a profound effect on the reflection effect, tending to 'spread' it to higher elevation angles; thus the theory is of limited applicability. SAE work to develop a better understanding of surface effects is continuing and this is expected to lead to better models. Until these are developed, the following methodology, described in AIR-5662 [ref. 11], is recommended for calculating lateral attenuation. It is confined to the case of sound propagation over soft level ground which is appropriate for the great majority of civil airports. Adjustments to account for the effects of a hard ground surface (or, acoustically equivalent, water) are still under development.

The methodology is built on the substantial body of experimental data on sound propagation from aircraft with fuselage-mounted engines in straight (non-turning), steady, level flight reported originally in AIR-1751 [ref. 12]. Making the assumption that, for level flight, air-to-ground attenuation depends on (i) elevation angle β measured in the vertical plane and (ii) lateral displacement from the aircraft ground track ℓ, the data were analysed to obtain an empirical function for the *total* lateral adjustment $\Lambda_T(\beta,\ell)$ (i.e. the lateral event level minus the level at the same distance beneath the aircraft).

As the term $\Lambda_T(\beta,\ell)$ accounted for lateral directivity as well as lateral attenuation, the latter can be extracted by subtraction. Describing lateral directivity by equation 4-15, with the fuselage-mount coefficients and with φ replaced by β (appropriate to non-turning flight), the lateral attenuation becomes:

$$\Lambda(\beta,\ell) = \Lambda_T(\beta,\ell) - \Delta_I(\beta) \tag{4-17}$$

where β and ℓ are measured as depicted in **Figure 4-3** in a plane normal to the infinite flight path which, for level flight, is also vertical.

Although $\Lambda(\beta,\ell)$ could be calculated directly using equation 4-17 with $\Lambda_T(\beta,\ell)$ taken from AIR-1751, a more efficient relationship is recommended. This is the following empirical approximation adapted from AIR-5662:

$$\Lambda(\beta,\ell) = \Gamma(\ell)\cdot\Lambda(\beta) \tag{4-18}$$

where $\Gamma(\ell)$ is a distance factor given by

$$\Gamma(\ell) = 1.089\cdot\left[1-\exp(-0.00274\ell)\right] \quad \text{for} \quad 0 \le \ell \le 914 \text{ m} \tag{4-19a}$$

$$\Gamma(\ell) = 1 \quad \text{for} \quad \ell > 914 \text{ m} \tag{4-19b}$$

and $\Lambda(\beta)$ is long-range air-to-ground lateral attenuation given by

[19] The wind and temperature gradients and turbulence depend in part upon the roughness and heat transfer characteristics of the surface.

$$\Lambda(\beta) = 1.137 - 0.0229\beta + 9.72 \cdot \exp(-0.142\beta) \quad \text{for} \quad 0° \le \beta \le 50° \qquad \text{(4-19c)}$$

$$\Lambda(\beta) = 0 \quad \text{for} \quad 50° \le \beta \le 90° \qquad \text{(4-19d)}$$

The expression for lateral attenuation $\Lambda(\beta,\ell)$, equation 4-18, which is assumed to hold true for all aircraft, i.e. propeller aircraft as well as fuselage-mounted and wing-mounted jets, is shown graphically in **Figure 4-5**.

Under certain circumstances (with terrain), it is possible for β to be less than zero. In such cases it is recommended that $\Lambda(\beta)$ = 10.857.

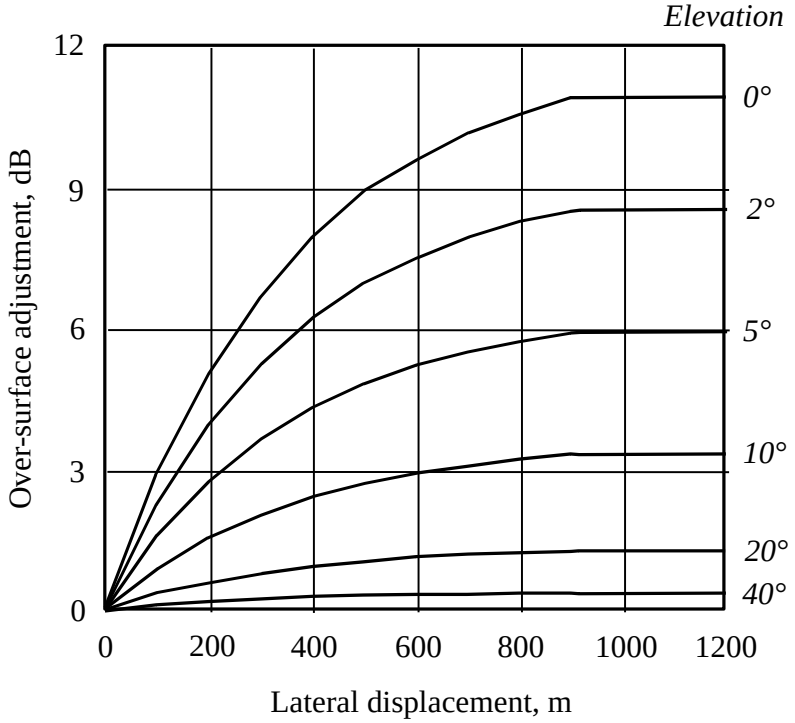

Figure 4-5: Variation of lateral attenuation Λ(β, ℓ) with elevation angle and distance

4.5.5 FINITE SEGMENT LATERAL ATTENUATION

Equations 4-19 describe the lateral attenuation $\Lambda(\beta,\ell)$ of sound arriving at the observer from an aeroplane in steady flight along an infinite, level flight path. When applying them to finite path segments that are not level, the attenuation has to be calculated for an *equivalent* level path - as the closest point on a simple extension of the inclined segment (that passes through the ground surface at some point) generally does not yield an appropriate elevation angle β.

The determination of lateral attenuation for finite segments differs markedly for L_{max} and L_E metrics. Segment maximum levels L_{max} are determined from NPD data as a function of propagation distance d from the nearest point on the segment; no corrections are required to account for the dimensions of the segment. Likewise, lateral attenuation of L_{max} is assumed to depend only on the elevation angle of, and ground distance to, the same point. Thus only the coordinates of that point are required. But for L_E, the process is more complicated.

The baseline event level $L_E(P,d)$ that is determined from the NPD data, even though for finite segment parameters, applies nevertheless to an infinite flight path. The event exposure level from a segment, $L_{E,seg}$, is of course less than the baseline level - by the amount of the finite segment correction defined later in **Section 4.5.6**. That correction, a function of the geometry of triangles OS_1S_2 in **Figure 4-2**, defines what proportion of the total infinite path noise energy received at O comes from the segment; the same correction applies, whether or not there is any lateral attenuation. But any lateral attenuation must be calculated for the infinite flight path, i.e. as a function of its displacement and elevation, not those of the finite segment.

Adding the corrections Δ_V and Δ_I, and subtracting lateral attenuation $\Lambda(\beta,\ell)$ from the NPD *baseline level* gives the adjusted event noise level for equivalent steady *level* flight on an adjacent, infinite straight path. But the actual flight path segments being modelled, those that affect the noise contours, are rarely level; aircraft are usually climbing or descending.

Figure 4-6 illustrates a departure segment $\mathbf{S_1S_2}$ - the aircraft is climbing at an angle γ - but the considerations remain very similar for an arrival. The remainder of the 'real' flight path is not shown; suffice it to state that $\mathbf{S_1S_2}$ represents just a part of the whole path (which in general will be curved). In this case, the observer **O** is alongside, and to the left of, the segment. The aircraft is banked (anti-clockwise about the flight path) at an angle ε to the lateral horizontal axis. The depression angle φ from the wing plane, of which the installation effect Δ_I is a function (equation 4-17), lies in the plane normal to the flight path in which ε is defined. Thus $\varphi = \beta - \varepsilon$ where $\beta = \tan^{-1}(h/\ell)$ and ℓ is the perpendicular distance **OR** from the observer to the ground track; i.e. the lateral displacement of the observer[20]. The aeroplane's closest point of approach to the observer, **S**, is defined by the perpendicular **OS**, of length (slant distance) d_p. The triangle $\mathbf{OS_1S_2}$ accords with **Figure 4-2b**, the geometry for calculating the segment correction Δ_F.

[20] For an observer located on the right side to the segment φ would become $\beta + \varepsilon$ (see **Section 4.5.2**).

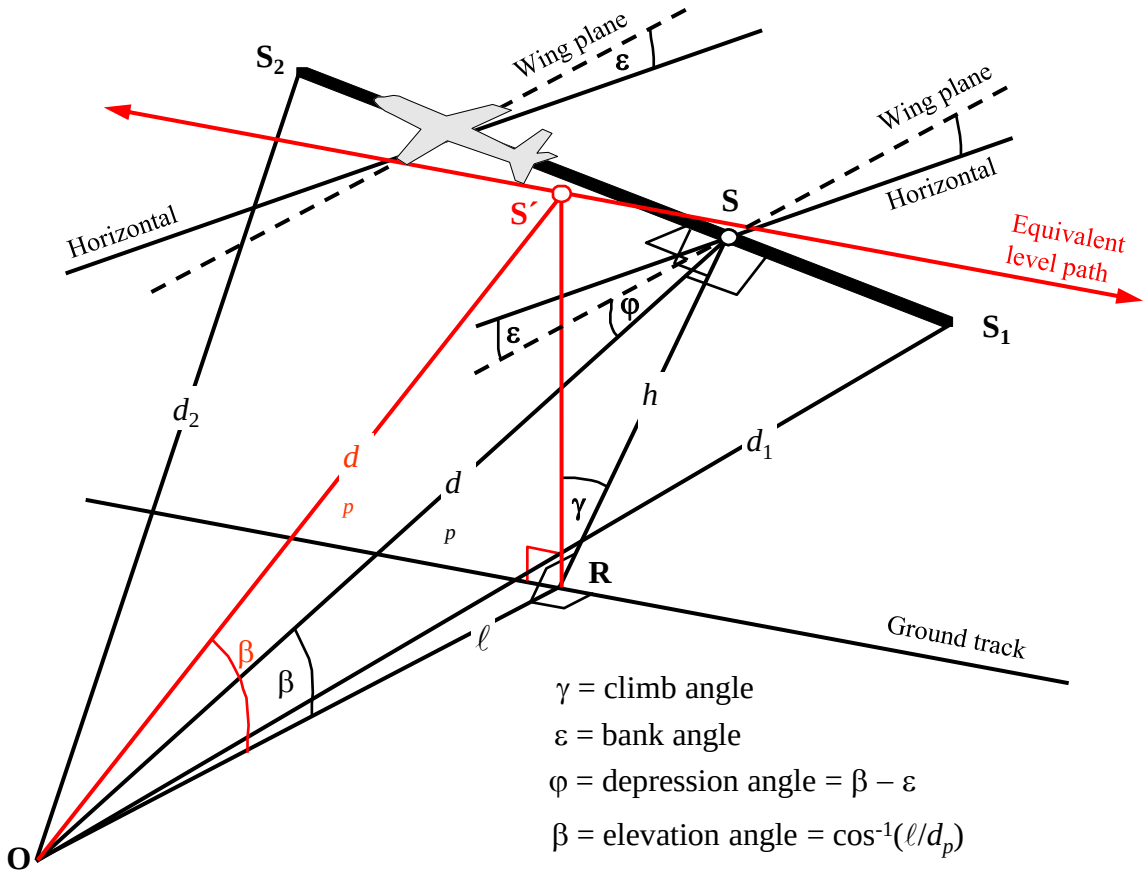

Figure 4-6: Observer alongside segment

To calculate the lateral attenuation using equation 4-18 (where β is measured in a vertical plane), an extended *level* flight path is recommended. An extended level flight path is defined in the vertical plane through $\mathbf{S_1S_2}$ and with the same perpendicular slant distance d_p from the observer. This is visualised by rotating the triangle **ORS**, and its attached flight path about **OR** (see **Figure 4-6**) through angle γ thus forming the triangle **ORS´**. The elevation angle of this equivalent level path (now in a vertical plane) is $\beta = \tan^{-1}(h/\ell)$ (ℓ remains unchanged). In this case, for an observer alongside, angle β and the resulting lateral attenuation $\Lambda(\beta,\ell)$ are the same for L_E and L_{max} metrics.

Figure 4.7 illustrates the situation when the observer point **O** lies *behind the finite segment*, not alongside. Here the segment is observed as a more distant part of an infinite path; a perpendicular can only be drawn to point $\mathbf{S_p}$ on its extension. The triangle $\mathbf{OS_1S_2}$ accords with **Figure 4-2a** which defines the segment correction Δ_F. But in this case the parameters for lateral directivity and attenuation are less obvious.

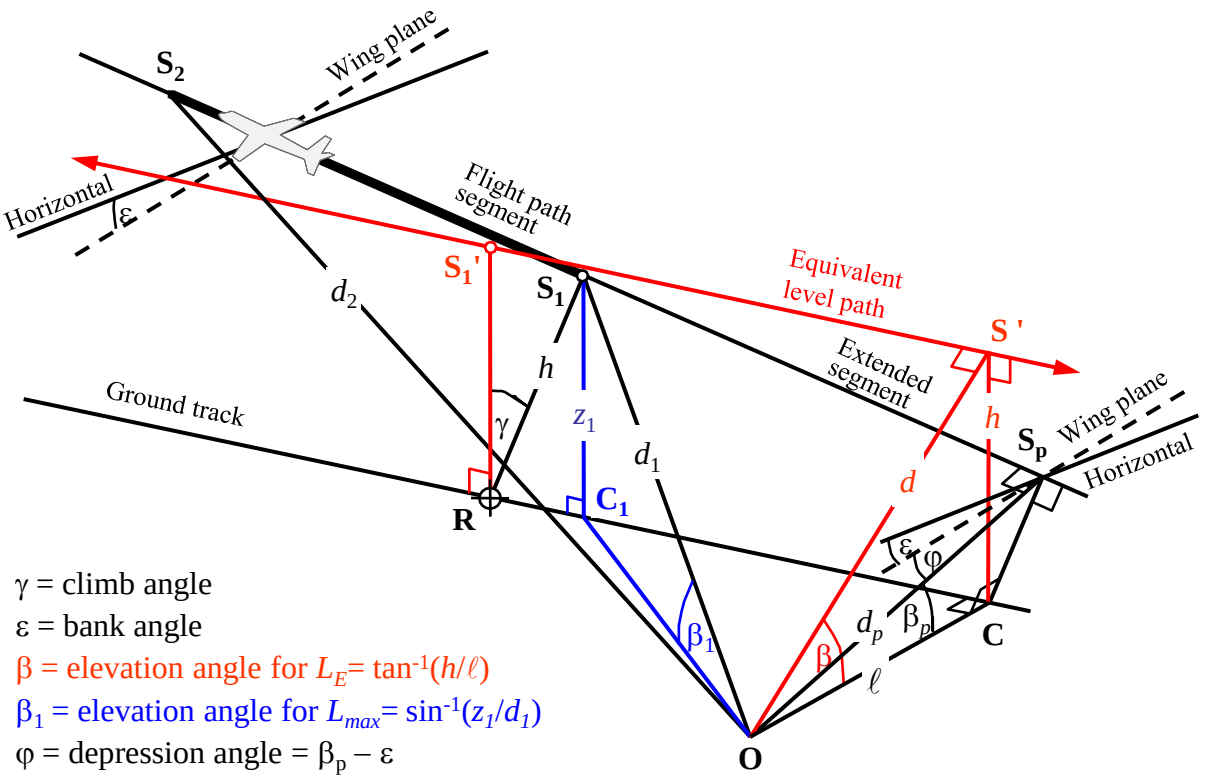

Figure 4-7: Observer behind segment

For maximum level metrics, the NPD distance parameter is taken as the shortest distance to the segment, i.e. $d = d_1$. For exposure level metrics, it is the shortest distance d_p from **O** to $\mathbf{S_p}$ on the extended flight path; i.e. the level interpolated from the NPD table is $L_{E\infty}(P_1, d_p)$.

The geometrical parameters for lateral attenuation also differ for maximum and exposure level calculations. For *maximum level* metrics the adjustment $\Lambda(\beta,\ell)$ is given by equation 4-18 with $\beta = \beta_1 = \sin^{-1}(z_1/d_1)$ and $\ell = \mathbf{OC_1} = \sqrt{d_1^2 - z_1^2}$ where β_1 and d_1 are defined by the triangle $\mathbf{OC_1S_1}$ in the vertical plane through **O** and $\mathbf{S_1}$.

When calculating the lateral attenuation for exposure level metrics, ℓ remains the shortest lateral displacement from the segment extension (**OC**). But to define an appropriate value of β it is again necessary to visualise an (infinite) *equivalent level flight path* of which the segment can be considered part. This is drawn through $\mathbf{S_1'}$, height *h* above the surface, where h is equal to the length of $\mathbf{RS_1}$ the perpendicular from the ground track to the segment. This is equivalent to rotating the actual extended flight path through angle γ about point **R** (see **Figure 4-7**). Insofar as **R** is on the perpendicular to $\mathbf{S_1}$, the point on the segment that is closest to **O**, the construction of the equivalent level path is the same as when **O** is alongside the segment.

The closest point of approach of the equivalent level path to the observer **O** is at **S´**, slant distance *d*, so that the triangle **OCS´** so formed in the vertical plane then defines the elevation angle $\beta = \cos^{-1}(\ell/d)$. Although this transformation might seem rather convoluted, it should be noted that the basic source geometry (defined by d_1, d_2 and φ) remains untouched, the sound travelling from the segment *towards* the observer is simply what it would be if the

entire flight along the infinitely extended inclined segment (of which for modelling purposes the segment forms part) were at constant speed V and power P_1. The lateral attenuation of sound from the segment *received* by the observer, on the other hand, is related not to β_p, the elevation angle of the extended path, but to β, that of the equivalent level path.

Remembering that, as conceived for modelling purposes, the engine installation effect Δ_I is two-dimensional, the defining depression angle φ is still measured laterally from the aircraft wing plane (the baseline event level is still that generated by the aircraft traversing the infinite flight path represented by the extended segment). Thus the depression angle is determined at the closest point of approach, i.e. $\varphi = \beta_p - \varepsilon$ where β_p is angle **S_pOC**.

The case of an observer ahead of the segment is not described separately; it is evident that this is essentially the same as the case of the observer behind.

However, for exposure level metrics *where observer locations are behind ground segments during the takeoff roll and ahead of ground segments during the landing roll*, the value of β becomes the same as that for maximum level metrics.

For locations behind takeoff roll segments:

$$\beta = \beta_1 = \sin^{-1}(z_1/d_1) \text{ and } \ell = OC_1 = \sqrt{d_1^2 - z_1^2}$$

For locations ahead of landing roll segments:

$$\beta = \beta_2 = \sin^{-1}(z_2/d_2) \text{ and } \ell = OC_2 = \sqrt{d_2^2 - z_2^2}$$

The rationale for using these particular expressions is related to the application of the start-of-roll directivity function behind takeoff roll segments and a semi-circular directivity assumption ahead of landing roll segments (see **Sections 4.5.6** and **4.5.7** for further details).

4.5.6 THE FINITE SEGMENT CORRECTION Δ_F (EXPOSURE LEVELS L_E ONLY)

The adjusted baseline noise exposure level relates to an aircraft in continuous, straight, steady level flight (albeit with a bank angle ε that is inconsistent with straight flight). Applying the (negative) *finite segment correction* $\Delta_F = 10 \cdot \lg(F)$, where F is the *energy fraction*, further adjusts the level to what it would be if the aircraft traversed the finite segment only (or were completely silent for the remainder of the infinite flight path).

The energy fraction term accounts for the pronounced longitudinal directivity of aircraft noise and the angle subtended by the segment at the observer position. Although the processes that cause the directionality are very complex, studies have shown that the resulting contours are quite insensitive to the precise directional characteristics assumed. The expression for Δ_F below is based on a fourth-power 90-degree dipole model of sound radiation. It is assumed to be unaffected by lateral directivity and attenuation. How this correction is derived is described in detail in **Appendix E**.

The energy fraction F is a function of the 'view' triangle **OS_1S_2** defined in **Figures 4-2a** to **4-2c** such that:

$$\Delta_F = 10 \cdot \log\left[\frac{1}{\pi}\left(\frac{\alpha_2}{1+\alpha_2^2} + \arctan\alpha_2 - \frac{\alpha_1}{1+\alpha_1^2} - \arctan\alpha_1\right)\right] \qquad (4\text{-}20)$$

with

$$\alpha_1 = -\frac{q}{d_\lambda} \; ; \quad \alpha_2 = -\frac{q-\lambda}{d_\lambda} \; ; \quad d_\lambda = d_0 \cdot 10^{[L_{E\infty}(P,d_p) - L_{max}(P,d_p)]/10} \; ; \quad d_0 = \frac{2}{\pi} \cdot V_{ref} \cdot t_0.$$

where d_λ is known as the 'scaled distance' (see **Appendix E**) and V_{ref} = 270.05 ft/s (for the 160 knots reference speed). Note that $L_{max}(P, d_p)$ is the maximum level, from NPD data, for perpendicular distance d_p, *not* the segment L_{max}. It is advised to apply a lower limit of -150 dB to Δ_F.

In the particular case of observer locations behind <u>every</u> takeoff ground-roll segment, a reduced form of the noise fraction expressed in equation 4-20 is used, which corresponds to the specific case of q = 0. This is denoted $\Delta'_{F,d}$ where 'd' clarifies its use for departure operations, and is computed as:

$$\Delta'_{F,d} = 10 \cdot \log_{10}\left[\frac{1}{\pi}\left(\frac{\alpha_2}{1+\alpha_2^2} + \arctan\alpha_2\right)\right] \qquad (4\text{-}21a)$$

where $\alpha_2 = \lambda / d_\lambda$.

This particular form of the noise fraction is used in conjunction with the start-of-roll directivity function, whose application method is further explained in **Section 4.5.7** below.

In the particular case of observer locations ahead of <u>every</u> landing ground-roll segment, a reduced form of the noise fraction expressed in equation 4-20 is used, which corresponds to the specific case of q = λ. This is denoted $\Delta'_{F,a}$ where 'a' clarifies its use for arrival operations, and is computed as:

$$\Delta'_{F,a} = 10 \cdot \log_{10}\left[\frac{1}{\pi}\left(-\frac{\alpha_1}{1+\alpha_1^2} - \arctan\alpha_1\right)\right] \qquad (4\text{-}21b)$$

where $\alpha_1 = -\lambda / d_\lambda$.

The use of this form, without the application of any further horizontal directivity adjustment (unlike the case of locations behind takeoff ground-roll segments – see **Section 4.5.7**), implicitly assumes a semi-circular horizontal directivity ahead of landing ground roll segments.

4.5.7 THE START-OF-ROLL DIRECTIVITY FUNCTION Δ_{SOR}

The noise of aircraft, especially jet aircraft equipped with lower bypass ratio engines, exhibits a lobed radiation pattern in the rearward arc, which is characteristic of jet exhaust noise. This pattern is more pronounced the higher the jet velocity and the lower the aircraft speed. A less pronounced radiation pattern may be observed for turboprop aircraft, as well. This is of special significance for observer locations behind the start of roll, where both conditions are fulfilled. This effect is taken into account by a directivity function Δ_{SOR}.

The function Δ_{SOR} has been derived from several noise measurement campaigns [ref. 13] using microphones adequately positioned behind and to the side of the SOR of departing jet aircraft. Separate functions were derived for jet and turbo-prop aircraft.

Figure 4-8 shows the relevant geometry. The azimuth angle ψ between the aircraft longitudinal axis and the vector to the observer is defined by:

$$\psi = \arccos\left(\frac{q}{d_{SOR}}\right) \qquad (4\text{-}22)$$

The relative distance q is negative (see **Figure 4-2a**) so that ψ ranges from 90° relative to the aircraft forward heading, to 180° in the reverse direction.

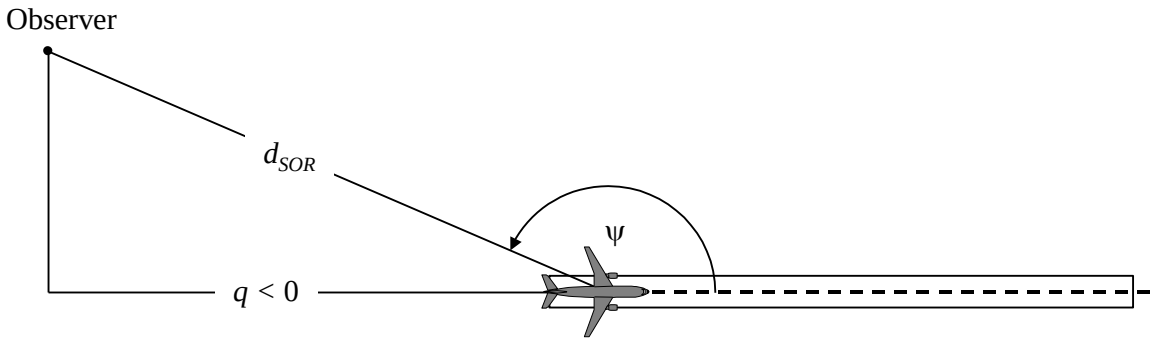

Figure 4-8: Aircraft-observer geometry for estimation of directivity correction

The function Δ_{SOR} represents the variation of the overall noise emanating from the takeoff ground roll measured behind the start of roll, relative to the overall noise from takeoff ground roll measured to the side of the SOR, at the same distance:

$$L_{TGR}(d_{SOR},\psi) = L_{TGR}(d_{SOR},90°) + \Delta_{SOR}(d_{SOR},\psi) \tag{4-23}$$

where $L_{TGR}(d_{SOR},90°)$ is the overall takeoff ground roll noise level at the point distance d_{SOR} to the side of the SOR. Δ_{SOR} is implemented as an adjustment to the noise level from one flight path segment (e.g. $L_{max,seg}$ or $L_{E,seg}$), as described in equation 4-9b.

The SOR directivity function, in decibels, for *turbofan-powered jet aircraft* is given by the following equation:

For 90° ≤ Ψ < 180° then:

$$\Delta^0_{SOR} = 2329.44 - (8.0573\cdot\psi) + \left(11.51\cdot\exp\left(\frac{\pi\cdot\psi}{180}\right)\right) - \left(\frac{3.4601\cdot\psi}{\ln\left(\frac{\pi\cdot\psi}{180}\right)}\right) - \left(\frac{17403338.3\cdot\ln\left(\frac{\pi\cdot\psi}{180}\right)}{\psi^2}\right) \tag{4-24a}$$

The SOR directivity function, in decibels, for *turboprop-powered aircraft* is given by the following equation:

For 90° ≤ Ψ < 180° then:

$$\Delta^0_{SOR} = -34643.898 + \left(\frac{30722161.987}{\psi}\right) - \left(\frac{11491573930.510}{\psi^2}\right) + \left(\frac{2349285669062}{\psi^3}\right) - \left(\frac{283584441904272}{\psi^4}\right) + \left(\frac{20227150391251300}{\psi^5}\right) - \left(\frac{790084471305203000}{\psi^6}\right) + \left(\frac{13050687178273800000}{\psi^7}\right) \tag{4-24b}$$

If the distance d_{SOR} exceeds the normalising distance $d_{SOR,0}$, the directivity correction is multiplied by a correction factor to account for the fact that the directivity becomes less pronounced for greater distances from the aircraft; i.e.

$$\Delta_{SOR} = \Delta^0_{SOR} \qquad \text{if} \qquad d_{SOR} \le d_{SOR,0} \tag{4-25a}$$

$$\Delta_{SOR} = \Delta^0_{SOR} \cdot \frac{d_{SOR,0}}{d_{SOR}} \qquad \text{if} \qquad d_{SOR} > d_{SOR,0} \tag{4-25b}$$

The normalising distance $d_{SOR,0}$ equals 762 m (2500 ft).The Δ_{SOR} function described above mostly captures the pronounced directivity effect of the initial portion of the takeoff roll at locations behind the SOR (because it is the closest to the receivers, with the highest jet velocity to aircraft speed ratio). However, the use of the hence established Δ_{SOR} is 'generalised' to positions behind *each* individual takeoff ground roll segment, so not only behind the start-of-roll point (in the case of takeoff). *The established Δ_{SOR} is not applied to positions ahead of individual takeoff ground roll segments, nor is it applied to positions behind or ahead of individual landing ground roll segments*.

The parameters d_{SOR} and ψ are calculated relative to the start of each individual ground roll segment. The event level L_{SEG} for a location behind a given takeoff ground-roll segment is calculated to comply with the formalism of the Δ_{SOR} function: it is essentially calculated for the reference point located on the side of the start point of the segment, at the same distance d_{SOR} as the actual point, and is further adjusted with Δ_{SOR} to obtain the event level at the actual point.

5 CALCULATION OF CUMULATIVE LEVELS

Chapter 4 describes the calculation of the event sound noise level of a single aircraft movement at a single observer location. The total noise exposure at that location is calculated by accumulating the event levels of all noise-significant aircraft movements, i.e. all movements, inbound or outbound, that influence the cumulative level. Some of the basic measures of cumulative noise are outlined below; for a general description of noise scales, metrics and indices, see **Section 3.2** of **Volume 1**.

5.1 WEIGHTED EQUIVALENT SOUND LEVELS

Time-weighted equivalent sound levels, which account for all significant aircraft sound energy received, can be expressed in a generic manner by the formula

$$L_{eq,W} = 10 \cdot \lg\left[\frac{t_0}{T_0} \cdot \sum_{i=1}^{N} g_i \cdot 10^{L_{E,i}/10}\right] + C \qquad (5\text{-}1a)$$

The summation is performed over all N noise events during the time interval T_0 to which the noise index applies. $L_{E,i}$ is the single event noise exposure level of the i-th noise event. g_i is a time-of-day dependent weighting factor (usually defined for day, evening and night periods). Effectively g_i is a multiplier for the number of flights occurring during the specific periods. The constant C can have different meanings (normalising constant, seasonal adjustment etc.).

Using the relationship:

$$g_i = 10^{\Delta_i/10}$$

where Δ_i is the decibel weighting for the i-th period, equation 5-1a can be rewritten as

$$L_{eq,W} = 10 \cdot \lg\left[\frac{t_0}{T_0} \sum_{i=1}^{N} 10^{(L_{E,i}+\Delta_i)/10}\right] + C \qquad (5\text{-}1b)$$

i.e. the time-of-day weighting is expressed by an additive level offset.

Some (nationally used) noise indices are based on maximum noise event levels rather than on time integrated metrics. An example is the average maximum sound level:

$$\overline{L_{max}} = 10 \cdot \lg\left[\frac{1}{N} \sum_{i=1}^{N} 10^{L_{max,i}/10}\right] \qquad (5\text{-}2)$$

Common applications are situations with a relative low equivalent sound level but high maximum levels (e.g. aerodromes with a relatively small number of jet operations).

Once popular but now largely supplanted by equivalent continuous sound levels L_{eq}, some indices account for both $\overline{L_{max}}$ and event numbers N by a relationship of the form:

$$Index = \overline{L_{max}} + K \cdot \lg N \qquad (5\text{-}3)$$

where the constant K defines the relative weight given to event numbers.

A special index is the *"Number Above Threshold"* – abbreviated *NAT*. Thus NAT_X is the number of noise events with maximum sound levels reaching or exceeding a threshold value X (dB). *NAT*-criteria can be defined for specific times of day (e.g. $NAT_{Night,70}$).

5.2 THE WEIGHTED NUMBER OF OPERATIONS

The cumulative noise level is estimated by summing the contributions from all different types or categories of aircraft using the different flight routes which comprise the airport scenario.

To describe this summation process the following subscripts are introduced:

i index for aircraft type or category

j index for flight track or subtrack (if subtracks are defined)

k index for flight track segment

Many noise indices – especially equivalent sound levels – include time-of-day weighting factors g_i in their definition (equation 5.1). For average maximum levels (equation 5.2) the weighting factors g_i are usually 1 or 0, depending on whether the metric covers specific times of the day or the whole 24 hours.

The summation process can be simplified by introducing a 'weighted number of operations':

$$M_{ij} = \left(g_{day} \cdot N_{ij,day} + g_{evening} \cdot N_{ij,evening} + g_{night} \cdot N_{ij,night}\right) \tag{5-4}$$

The values N_{ij} represent the numbers of operations of aircraft type/category *i* on track (or subtrack) *j* during the day, evening and night period respectively[21].

From equation 5-1b the (generic) cumulative equivalent sound level L_{eq} at the observation point *(x,y)* is:

$$L_{eq,W}(x,y) = 10 \cdot \lg\left[\frac{t_0}{T_0} \cdot \sum_i \sum_j \sum_k M_{ij} \cdot 10^{L_{E,ijk}(x,y)/10}\right] + C \tag{5-5}$$

T_0 is the reference time period. It depends on – as well as the weighting factors g_i – the specific definition of the weighted index used (e.g. L_{den} or L_{DN} - see **Volume 1** for definitions of weighted equivalent sound levels). $L_{E,ijk}$ is the single event noise level contribution from segment *k* of track or subtrack *j* for an operation of aircraft of category *i*. The estimation of $L_{E,ijk}$ is described in detail in **Chapter 4**.

5.3 ESTIMATION OF CUMULATIVE MAXIMUM LEVEL BASED METRICS

Calculating a cumulative equivalent sound level is a straightforward aggregation of the event levels L_E of all noise-significant aircraft movements. Cumulative maximum level metrics are less straightforward; care is required when estimating maximum sound levels. By definition a maximum sound level is tied to a single noise event. However, a single aircraft movement can generate more than one sound event at a given observer location (when its flight path causes more than one rise and fall in the received sound intensity).

Additionally different metrics assign different meanings to the generic expression 'maximum sound level' as illustrated by the following alternative definitions:

(a) The average maximum sound level, defined by equation 5-2, of all noise events occurring at the observer location.

(b) The average maximum sound level, defined by equation 5-2, of all noise events exceeding a specified threshold level L_T at the observer location.

[21] The time periods may differ from these three, depending on the definition of the noise index used.

(c) The absolute maximum level (i.e. the 'maximum' maximum level). In this case *only one noise event* contributes.

This points to a need for metric-specific aggregation of the maximum sound levels.

With no threshold, the average maximum sound level (a) occurring at the observer location (*x*,*y*) can be expressed as:

$$\overline{L_{max}}(x,y) = 10 \cdot \lg\left[\sum_i \sum_j \sum_k 10^{L_{max,ijk}/10} \cdot \mathrm{u}(k)\right] - 10 \cdot \lg\left[\sum_i \sum_j \sum_k M_{ij} \cdot \mathrm{u}(k)\right] \quad (5\text{-}6a)$$

$$\text{where: } \mathrm{u}(k) = \begin{Bmatrix} 0 \\ 1 \end{Bmatrix} \text{ if } L_{max,ijk} \begin{Bmatrix} \text{is not} \\ \text{is} \end{Bmatrix} \text{the maximum level of a noise event} \quad (5\text{-}6b)$$

The function u(*k*) determines whether the maximum segment level $L_{max,ijk}$ is the maximum level of a noise event or not (how this function is derived is described in detail in **Appendix F**).

With a threshold L_T, the average maximum sound level (b) can be expressed as:

$$\overline{L_{max}}(x,y) = 10 \cdot \lg\left[\sum_i \sum_j \sum_k 10^{L_{max,ijk}/10} \cdot v(k)\right] - 10 \cdot \lg\left[\sum_i \sum_j \sum_k M_{ij} \cdot v(k)\right] \quad (5\text{-}7a)$$

$$\text{where: } \mathrm{v}(k) = \begin{Bmatrix} 0 \\ 1 \end{Bmatrix} \text{ if } \begin{Bmatrix} L_{max,ijk} < L_T \\ L_{max,ijk} \geq L_T \end{Bmatrix} \quad (5\text{-}7b)$$

which guarantees that only noise events with maximum levels reaching or exceeding the threshold value L_T are included in the summation process.

If only the highest maximum level (c) of all noise events occurring at the observation point has to be calculated, the corresponding equation is quite simple:

$$L_{max}(x,y) = \max\left(L_{max,ijk}\right) \quad (5\text{-}8)$$

The equation for estimation of a number above threshold criterion is similar to that for an average maximum sound level. However the weighted operations have to be summed rather than the level contributions:

$$NAT_{L_T}(x,y) = \sum_i \sum_j \sum_k M_{ij} \cdot \mathrm{u}(k) \cdot \mathrm{v}(k) \quad (5\text{-}9)$$

5.4 THE USE OF LEVEL DISTRIBUTIONS FOR MAXIMUM LEVEL METRICS

The methodology described in **Chapter 4** yields the same maximum sound level for all movements of the same aircraft type on the same track[22]. This can lead to unrealistic discontinuities in $\overline{L_{max}}$ and *NAT* contours. In reality there are no sharp changes; the calculated $\overline{L_{max}}$ is just an estimated average of event levels that are scattered about a central value L_0. This scatter can be realistically described by a Gaussian distribution function with a standard deviation *S*:

[22] Assuming the same operating procedures and weight.

$$w(L_{max}, L_0, S) = \frac{1}{\sqrt{2\pi} \cdot S} \cdot \exp\left[-\frac{1}{2}\left(\frac{L_{max} - L_0}{S} \right)^2 \right] \quad (5\text{-}10)$$

Figure 5-1 shows a sketch of such a level distribution.

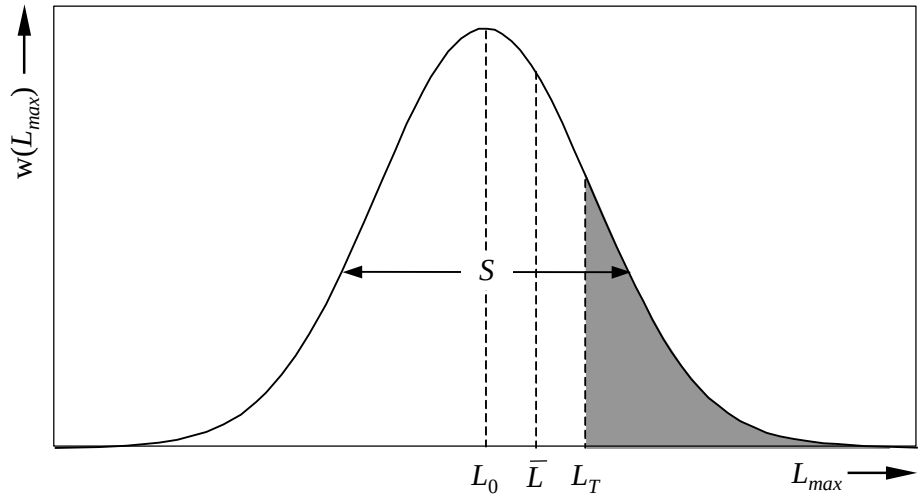

Figure 5-1: Maximum sound level distribution

It must be noted that the median value L_0 of the distribution function is generally not equal to the value $\bar{L}$ stored in NPD databases as that is normally derived from measurements by decibel averaging. This is higher than the median value of the distribution by an amount which depends on the standard deviation:

$$\bar{L} = L_0 + \frac{S^2 \cdot \ln 10}{20} = L_0 + 0.115 \cdot S^2 \quad (5\text{-}11)$$

A characteristic type-specific value for the standard deviation S is observed from operational measurements to be around 2 dB[23]. This results in a level difference between logarithmic and arithmetic averages of about 0.5 dB.

For similar reasons, distributed levels should be taken into account when estimating *NAT* values. The reason is clear from **Figure 5-1**: for this case both L_0 and $\bar{L}$ are less than the threshold level L_T. If the distribution is not taken into account, the contribution to *NAT* will equal zero. However with distributed levels some are higher than the threshold and thus contribute to the total *NAT*. To account for the distribution, equation 5-9 has to be modified by replacing the discrete step represented by the function v(k) by an integral over a continuous distribution function:

$$NAT_{L_T}(x, y) = \sum_i \sum_j \sum_k M_{ij} \cdot u(k) \cdot \int_{L_T}^{\infty} w\left(L_{max,ijk}, L_{0,k}, s\right) dL_{max,ijk} \quad (5\text{-}12)$$

Polynomial approximations of this integral for programming purposes can be found in mathematical handbooks (e.g. ref. 14).

[23] Rather lower scatter is achieved in certification tests.

It should be noted that the arithmetic mean $L_{0,k}$ has to be derived according to equation 5-11 if, as in the ANP database the maximum values are estimated from measured data by logarithmic averaging.

6 CALCULATION OF NOISE CONTOURS

6.1 STANDARD GRID CALCULATION AND REFINEMENT

When noise contours are obtained by interpolation between index values at rectangularly spaced grid points, their accuracy depends on the choice of the grid spacing (or mesh size) Δ_G, especially within cells where large gradients in the spatial distribution of the index cause tight curvature of the contours (see **Figure 6-1**). Interpolation errors are reduced by narrowing the grid spacing, but since this increases the number of grid points, the computation time is increased. Optimising a regular grid mesh involves balancing modelling accuracy and run time.

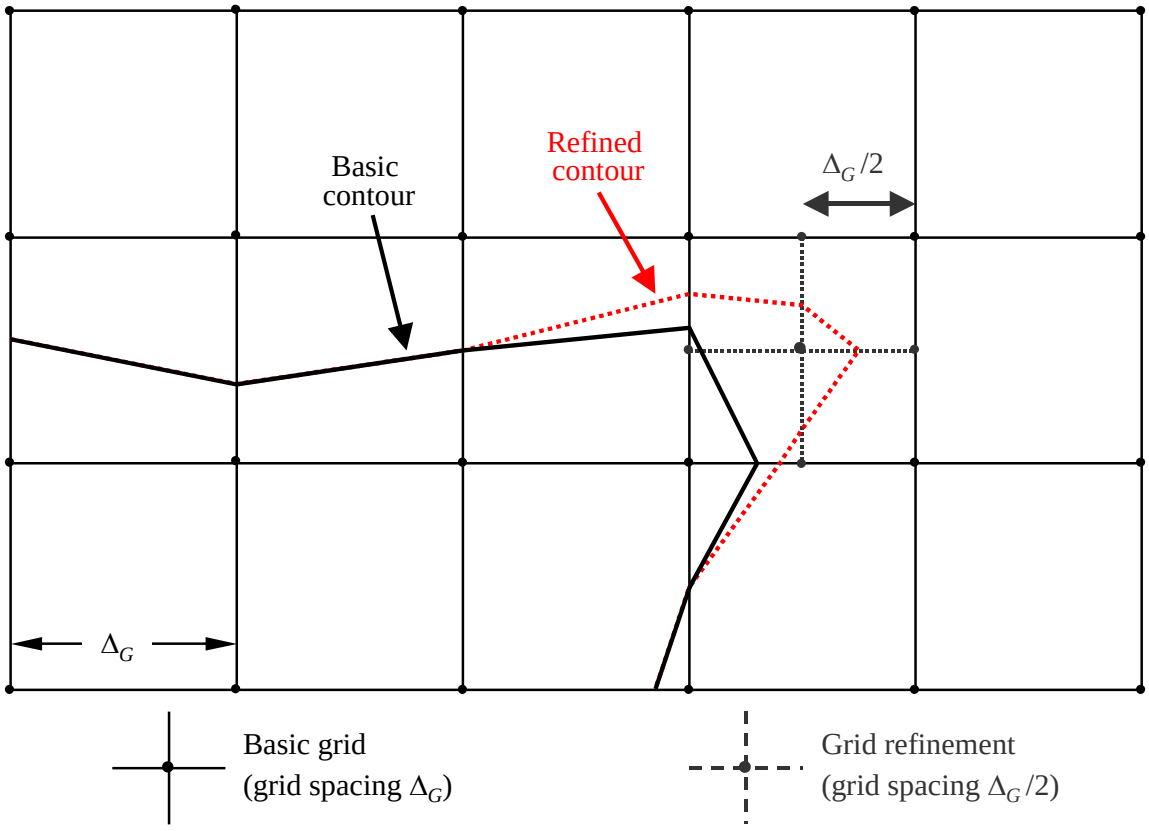

Figure 6-1: Standard grid and grid refinement

A marked improvement in computing efficiency that delivers more accurate results is to use an irregular grid to refine the interpolation in critical cells. The technique, depicted in **Figure 6-1**, is to tighten the mesh locally, leaving the bulk of the grid unchanged. This is very straightforward and achieved by the following steps:

1. Define a refinement threshold difference ΔL_R for the noise index.
2. Calculate the basic grid for a spacing Δ_G.
3. Check the differences ΔL of the index values between adjacent grid nodes.
4. If there are any differences $\Delta L > \Delta L_R$, define a new grid with a spacing $\Delta_G/2$ and estimate the levels for the new nodes in the following way:

$$\text{If} \begin{cases} \Delta L \le \Delta L_R \\ \Delta L > \Delta L_R \end{cases} \text{ calculate the new value } \begin{cases} \text{by linear interpolation from the adjacent ones.} \\ \text{completely anew from the basic input data.} \end{cases}$$

5. Repeat steps 1–4 until all differences are less than the threshold difference.
6. Estimate the contours by linear interpolation.

If the array of index values is to be aggregated with others (e.g. when calculating weighted indices by summing separate day, evening and night contours), care is required to ensure that the separate grids are identical.

6.2 USE OF ROTATED GRIDS

In many practical cases, the true shape of a noise contour tends to be symmetrical about a ground track. However if the direction of this track is not aligned with the calculation grid, this can cause result in an asymmetric contour shape:

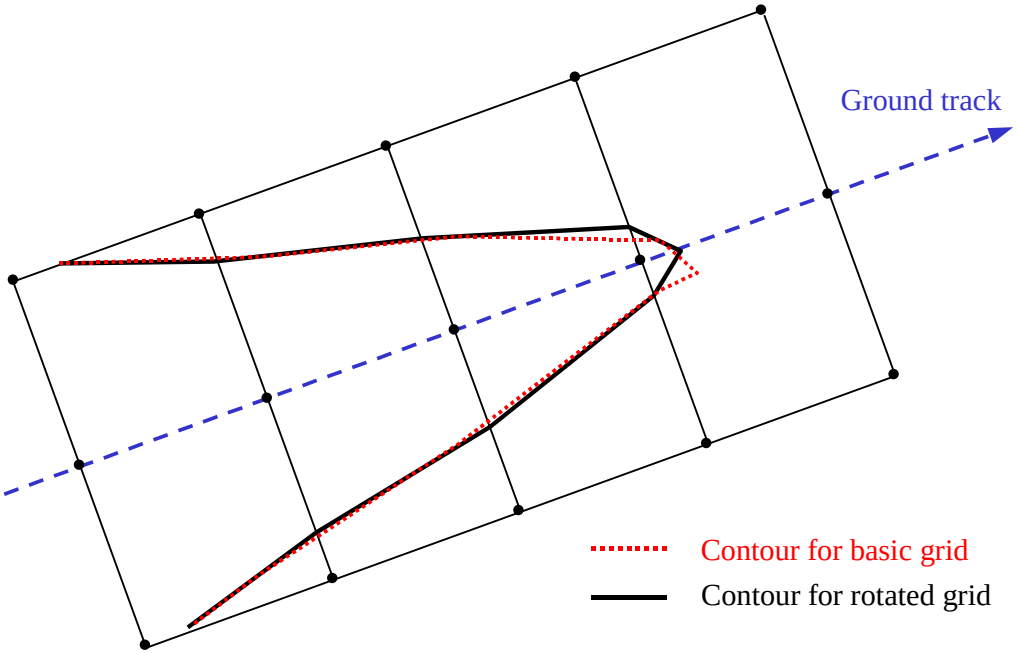

Figure 6-2: Use of a rotated grid

The straightforward way to avoid this effect is to tighten the grid. However this increases computation time. A more elegant solution is to rotate the computation grid so that its direction is parallel to the main ground tracks (i.e. usually parallel to the main runway). **Figure 6-2** shows the effect of such a grid rotation on the contour shape.

6.3 TRACING OF CONTOURS

A very time-efficient algorithm that eliminates the need to calculate a complete grid array of index values at the expense of a little more computational complexity is to trace the path of the contour, point by point. This option requires two basic steps to be performed and repeated (see **Figure 6-3**):

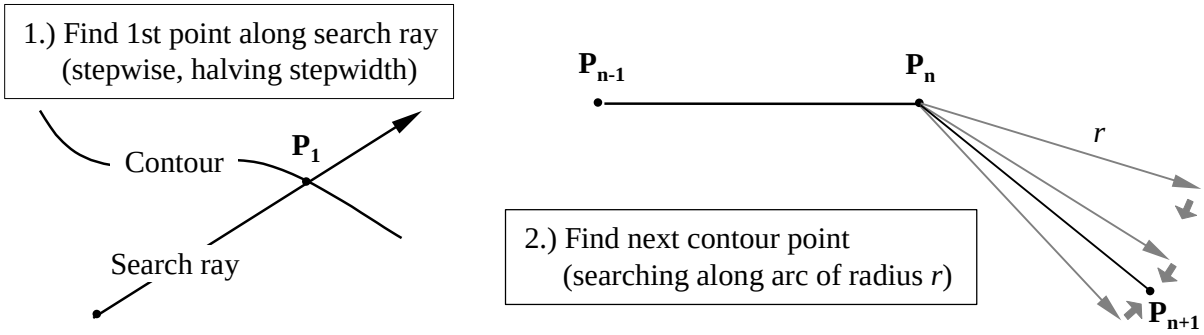

Figure 6-3: Concept of tracing algorithm

Step 1 is to find a first point $\mathbf{P_1}$ on the contour. This is done by calculating the noise index levels L in equidistant steps along a 'search ray' that is expected to cross the required contour of level L_C. When the contour is crossed, the difference $\delta = L_C - L$ changes sign. If this happens, the step-width along the ray is halved and the search direction is reversed. This is done until δ is smaller than a pre-defined accuracy threshold.

Step 2, which is repeated until the contour is sufficiently well defined, is to find the next point on the contour L_C - which is at a specified straight line distance r from the current point. During consecutive angular steps, index levels and differences δ are calculated at the ends of vectors describing an arc with radius r. By similarly halving and reversing the increments, this time in the directions of the vector, the next contour point is determined within a predefined accuracy.

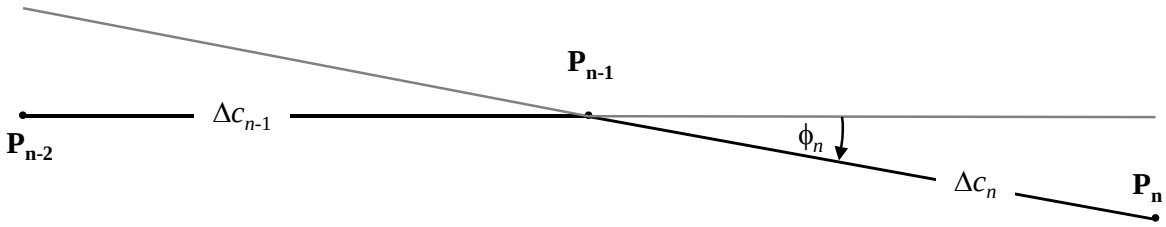

Figure 6-4: Geometric parameters defining conditions for the tracing algorithm

Some constraints should be imposed to guarantee that the contour is estimated with a sufficient degree of accuracy (see **Figure 6-4**):

1. The length of the chord Δc (the distance between two contour points) should be within an interval $[\Delta c_{min}, \Delta c_{max}]$, e.g. [10 m, 200 m].
2. The length ratio between two adjacent chords of lengths Δc_n and Δc_{n+1} should be limited, e.g. $0.5 < \Delta c_n / \Delta c_{n+1} < 2$.
3. With respect to a good fit of the chord length to the contour curvature, the following condition should be fulfilled:

$$\phi_n \cdot \max(\Delta c_{n-1}, \Delta c_n) \leq \varepsilon \quad (\varepsilon \approx 15\,\mathrm{m})$$

where ϕ_n is the difference in the chord headings.

Experience with this algorithm has shown that, on an average, between 2 and 3 index values have to be calculated to determine a contour point with an accuracy of better than 0.01 dB.

Especially when large contours have to be calculated this algorithm speeds up computation time dramatically. However it should be noted that its implementation requires experience, especially when a contour breaks down into separate 'islands'.

6.4 POST-PROCESSING

Commonly the post-processing of calculated noise indices involves the following:

- Interpolation and, if necessary, smoothing of noise contours (if the index was estimated for a grid).
- Performing grid operations such as merging, adding, subtracting or converting.
- Plotting (including representation of contours, runways, tracks, specific observer locations and/or topography).
- Integration of noise data into geographic information systems (GIS) to estimate enclosed population numbers for example.

Currently several post-processing tools and standardised data formats are in use, which are suitable for processing data from aircraft noise calculation programs. Examples of such tools are:

- NMPLOT: this program is designed to view and edit sets of geo-referenced data sets such as noise data stored in grids.
- GIS software such as ArcView or MicroStation GeoGraphics (usually commercial software).

Data formats which are widely used are:

- ARC/INFO shapefile format used by ArcView.
- AutoCAD data exchange format DXF.
- Intergraph and MicroStation standard file format ISFF (also known as DGN).
- Noise model grid format, NMGF. The NMGF was originally developed for use in conjunction with different noise models. It is used by NMPLOT.

Hence a lot of possibilities for the definition of interfaces exist. This should be taken into account when a computer model based on this document is developed.

REFERENCES

[1] International Civil Aviation Organization: *Manual of the ICAO Standard Atmosphere*, ICAO Doc. 7488 (1993).

[2] International Organization for Standardization: *Acoustics – Description, measurement and assessment of environmental noise – Part 1: Basic quantities and assessment procedures.* ISO 1996-1 (2001).

[3] International Organization for Standardization*: Acoustics – Procedure for describing aircraft noise heard on the ground.* ISO 3891 (1978).

[4] European Civil Aviation Conference (ECAC): *Methodology for Computing Noise Contours around Civil Airports. Volume 1: Applications Guide.* Proposal by the AIRMOD Subgroup, 2004.

[5] European Civil Aviation Conference (ECAC): *Report on Standard Method of Computing Noise Contours around Civil Airports.* ECAC.CEAC Doc.29, 1st Edition, 1986 (2nd Edition 1997 and 3rd Edition 2007).

[6] Society of Automotive Engineers: *Procedure for the Calculation of Aircraft Noise in the Vicinity of Airports.* SAE AIR-1845 (1986).

[7] Gulding, J.M.; Olmstead, J.R; Fleming, G.G.: *Integrated Noise Model (INM) Version 6.0 User's Guide.* Department of Transportation, Federal Aviation Administration, Report No. FAA-AEE-99-03, September 1999.

[8] Society of Automotive Engineers: *Monitoring Noise from Aircraft Operations in the Vicinity of Airports Aerodromes.* SAE ARP 4721 (Draft).

[9] Roberts, S., McLeod, R., Vermij, M., Heaslip, T. and MacWilliam, G.: *RAP (Radar Analysis Program) - An Interactive Computer Program for Radar Based Flight Path Reconstruction and Analysis*, p.27-45, Seminar Proceedings, ISASI Forum 1994.

[10] Orloff, K. L. & Bruno, A. E.: *An Improved Technique for Flight Path and Groundspeed Analysis Using Recorded Radar Data*, ICAS Paper 98-6,5,3, 21st ICAS Congress, Melbourne, Australia, 13-18 September 1998.

[11] Society of Automotive Engineers: AIR-5662, update to AIR-1751 (2006).

[12] Society of Automotive Engineers: *Prediction Method for Lateral Attenuation of Airplane Noise during Takeoff and Landing.* SAE AIR-1751 (1981).

[13] U.S. Department of Transportation: *Behind Start of Take-off Roll Aircraft Sound Level Directivity Study – Revision 1.* DOT-VNTSC-NASA-12-01 NASA/TM-2012-217783 (Final Report April 2015)

[14] Abramovitz, M., Stegun, I.A.: *Handbook of Mathematical Functions*. Dover publications, New York. 1972.

[15] Committee on Aircraft Noise (CAN): *Seventh Meeting Report on Agenda Item 3*. ICAO CAN/7-WP/59, May 1983. (Referring to: ICAO CAN/7-WP/19: *A revision to the definition of the reference atmosphere in Annex 16 to improve data quality and reliability and ease technical problems*. March 1983.)

[16] Society of Automotive Engineers: *Standard values of atmospheric absorption as a function of temperature and humidity.* SAE ARP 866A (1975).

[17] Society of Automotive Engineers: Aerospace Recommended Practice, Application of pure-tone atmospheric absorption losses to one-third octave-band level. SAE-ARP-5534 (2013).

APPENDIX A: DATA REQUIREMENTS

Section 2.4 of the main text describes in general terms the requirements for case-specific data describing an airport and its operations that are needed for noise contour calculations. The following datasheets are filled with example data for a hypothetical airport. Specific data formats will generally depend on the requirements and needs for the particular noise modelling system as well as the study scenario.

Note: It is recommended that geographic information (reference points etc.) be specified in Cartesian co-ordinates. The choice of the particular co-ordinate system usually depends on the maps available.

A1 GENERAL AIRPORT DATA

Aerodrome designation	Hypothetical Airport	
Co-ordinate system	UTM, Zone 15, Datum WGS-84	
Aerodrome reference point, ARP	3 600 000 m E Mid-point of runway 09L-27R	6 300 000 m N
Altitude of ARP	120 m	
Average air temperature at ARP*	12.0 ºC	
Average relative humidity at ARP*	60 %	
Average wind speed & direction*	5 kt	270 degrees
Source of topographical data	Unknown	

* Repeat for each time interval of interest (time of day, season etc.)

A2 RUNWAY DESCRIPTION

Runway designation	09L	
Start of runway	3 599 000 m E	6 302 000 m N
End of runway	3 603 000 m E	6 302 000 m N
Start of roll	3 599 000 m E	6 302 000 m N
Landing threshold	3 599 700 m E	6 302 000 m N
Altitude of start of runway	110 m	
Mean runway gradient	0.001	

For displaced thresholds, runway description may be repeated or displaced thresholds can be described in the ground track description section.

A3 GROUND TRACK DESCRIPTION

In the absence of radar data the following information is needed to describe particular ground tracks.

Track No.	001
Track designation	Dep 01 – 09L
From runway	09L
Type of track	Departure
Displacement from start of roll	0 m
Number of subtracks:	7

Backbone track description

Segment no.	Straight [m]	Curve			Standard deviation for lateral dispersion at segment end [m]
		L/R	Heading change [°]	Radius [m]	
1	10000				2000
3		R	90.00	3000	2500
4	20000				3000

Track No.	002
Track designation	App 01 – 09L – Disp 300
From runway	09L
Type of track	Approach
Displacement from landing threshold	300 m
Number of subtracks:	1

Backbone track description

Segment no.	Straight [m]	Curve			Standard deviation for lateral dispersion at segment end [m]
		L/R	Heading change [°]	Radius [m]	
1	30000				0

Approach track information

Glide angle for approach tracks	2.7°
Flight altitude at glide slope interception	4000 ft

A4 AIR TRAFFIC DESCRIPTION

Reference time period	366 d = 8748 h (01-01-2000 to 31-12-2000)
Time of day period I	From 0600 to 1800 h = 12 h
Time of day period II	From 1800 to 2200 h = 4 h
Time of day period III	From 2200 to 0600 h = 8 h

AIR TRAFFIC DESCRIPTION DATA SHEET – MOVEMENTS PER TRACK			
Ground track no.	001		
Track designation	Dep 01 – 09L		
Aircraft designation	**Movements during time period**		
	I	**II**	**III**
A/C 1, Dep.1	20000	4000	1000
A/C 2, Dep.4	10000	5000	500
A/C 4, Dep.3	2000	300	0
Ground track no.	002		
Track designation	Dep 01 – 09L – Disp 300		
Aircraft designation	**Movements during time period**		
	I	**II**	**III**
A/C 1, App.1	18000	2000	5000
A/C 2, App.1	10000	3000	2500
A/C 4, App.1	1300	0	1000

A5 FLIGHT PROCEDURE DATA SHEET

Example aircraft for a Chapter 3 Boeing 727-200 as derived from radar using the guidance set out in vol. 2.

Aircraft designation	B727C3
NPD-Identifier from ANP database	JT8E5
No. of engines	3
Mode of operation	Departure
Actual aircraft mass [t]	71.5
Headwind [m/s]	5
Temperature [°C]	20
Airport elevation [m]	83

Segment No.	Dist. from RP[24] [m]	Height [m]	Ground speed [m/s]	Engine Power [[25]]
1	0	0	0	14568
2	2500	0	83	13335
3	3000	117	88	13120
4	4000	279	90	13134
5	4500	356	90	13147
6	5000	431	90	13076
7	6000	543	90	13021
8	7000	632	93	12454
9	8000	715	95	10837
10	10000	866	97	10405
11	12000	990	102	10460
12	14000	1122	111	10485
13	16000	1272	119	10637
14	18000	1425	125	10877
15	20000	1581	130	10870
16	25000	1946	134	10842
17	30000	2242	142	10763

[24] The reference point RP is the start of roll for departures and the landing threshold for approaches.

[25] Units corresponding to units in ANP database

Example for a procedural profile based on aircraft data stored in ANP database:

Aircraft designation from ANP database	B727C3
NPD-Identifier from ANP database	JT8E5
No. of engines	3
Mode of operation	Departure
Actual aircraft mass [t]	71.5
Headwind [m/s]	5
Temperature [°C]	15
Airport elevation [m]	100

Segment No.	Mode	Target	Flaps	Engine Power
1	Takeoff		5	Takeoff
2	Initial Climb	Altitude 1500 ft	5	Takeoff
3	Retract Flaps	210 kts IAS ROC 750 ft/min	0	Max Climb
4	Accelerate	250 kts IAS ROC 1500 ft/min	0	Max Climb
5	Climb	10000 ft	0	Max Climb

APPENDIX B: FLIGHT PERFORMANCE CALCULATIONS

TERMS AND SYMBOLS

The terms and symbols used in this appendix are consistent with those conventionally used by aircraft performance engineers. Some basic terms are explained briefly below for the benefit of users not familiar with them. To minimise conflict with the main body of the document, symbols are mostly defined separately within this appendix. Quantities that are referenced in the main body are assigned common symbols; a few that are used differently in this appendix are marked with an asterix (*). There is some juxtaposition of US and SI units; again this is to preserve conventions that are familiar to users from different disciplines.

Terms

Break point	See Flat Rating
Calibrated airspeed	(Otherwise termed equivalent or indicated airspeed.) The speed of the aircraft relative to the air as indicated by a calibrated instrument on the aircraft. The true airspeed, which is normally greater, can be calculated from the calibrated airspeed knowing the air density.
Corrected net thrust	Net thrust is the propulsive force exerted by an engine on the airframe. At a given power setting (*EPR* or N_1) this falls with air density as altitude increases; corrected net thrust is the thrust at sea level.
Flat rating	For specific maximum component temperatures, the engine thrust falls as the ambient air temperature rises, and *vice-versa*. This means that there is a critical air temperature above which the *rated thrust* cannot be achieved. For most modern engines this is called the 'flat rated temperature' because, at lower air temperatures the thrust is automatically limited to the rated thrust to maximise service life. The thrust falls anyway at temperatures above the flat rated temperature - which is often called the *break point* or *break temperature*.
Speed	Magnitude of aircraft velocity vector (relative to aerodrome coordinate system).
Rated thrust	The service life of an aircraft engine is very dependent upon the operating temperatures of its components. The greater the power or thrust generated, the higher the temperatures and the shorter the life. To balance performance and life requirements flat rated engines are assigned *thrust ratings* for takeoff, climb and cruise which define normal maximum power settings.
Thrust setting parameter	The pilot cannot select a particular engine thrust, but instead chooses an appropriate setting of this parameter which is displayed in the cockpit. It is usually either the engine pressure ratio (*EPR*) or low-pressure rotor (or fan) rotational speed (N_1).

Symbols

Quantities are dimensionless unless otherwise stated. Symbols and abbreviations not listed below are used only locally and defined in the text. Subscripts 1 and 2 denote conditions at the start and end of a segment respectively. Overbars denote segment mean values, i.e. the average of start and end values.

a	Average acceleration, ft/s^2
a_{max}	Maximum acceleration available, ft s^2
A, B, C, D	Flap coefficients
$E, F, G_{A,B}, H$	Engine thrust coefficients
F_n	Net thrust per engine, lbf
F_n/δ	Corrected net thrust per engine, lbf
G	Climb gradient
$G´$	Engine-out climb gradient
G_R	Mean runway gradient, positive uphill
g	Gravitational acceleration, ft/s^2
ISA	International Standard Atmosphere
N *	Number of engines supplying thrust
R	Drag-to-lift ratio C_D/C_L
ROC	Segment rate of climb (ft/min)
s	Ground distance covered along ground track, ft
s_{TO8}	Takeoff distance into an 8 kt headwind, ft
s_{TOG}	Takeoff distance corrected for w and G_R, ft
s_{TOw}	Takeoff distance into headwind w, ft
T	Air temperature, °C
T_B	Breakpoint temperature, °C
V	Groundspeed, kt
V_C	Calibrated airspeed, kt
V_T	True airspeed, kt
W	Aeroplane weight, lb
w	Headwind speed, kt
Δs	Still air segment length projected onto ground track, ft
Δs_w	Segment length ground projection corrected for headwind, ft
δ	p/p_O, the ratio of the ambient air pressure at the aeroplane to the standard air pressure at mean sea level: p_O = 101.325 kPa (or 1013.25 mb) [ref. 1]
ε	Bank angle, radians
γ	Climb/descent angle, radians

θ	$(T + 273.15)/(T_0 + 273.15)$ the ratio of the air temperature at altitude to the standard air temperature at mean sea level: T_0 = 15.0 °C [ref. 1]
σ *	ρ/ρ_0 = Ratio of air density at altitude to the mean sea level value (also, $\sigma = \delta/\theta$)

B1 INTRODUCTION

Flight path synthesis

In the main, this appendix recommends procedures for calculating an aeroplane flight profile, based on specified aerodynamic and powerplant parameters, aircraft weight, atmospheric conditions, ground track and operating procedure (flight configuration, power setting, forward speed, vertical speed etc). The operating procedure is described by a set of *procedural steps* that prescribe how to fly the profile.

The flight profile, for takeoff or approach, is represented by a series of straight-line segments, the ends of which are termed *profile points*. It is calculated using aerodynamic and thrust equations containing numerous coefficients and constants which must be available for the specific combination of airframe and engine. This calculation process is described in the text as the process of flight path *synthesis*.

Apart from the aircraft performance parameters, which can be obtained from the ANP database (see **Appendix G**), these equations require specification of (1) aeroplane gross weight, (2) the number of engines, (3) air temperature, (4) runway elevation, and (5) the procedural steps (expressed in terms of power settings, flap deflections, airspeed and, during acceleration, average rate-of-climb/descent) for each segment during takeoff and approach. Each segment is then classified as a ground roll, takeoff or landing, constant speed climb, power cutback, accelerating climb with or without flap retraction, descent with or without deceleration and/or flap deployment, or final landing approach. The flight profile is built up step by step, the starting parameters for each segment being equal to those at the end of the preceding segment.

The aerodynamic-performance parameters in the ANP database are intended to yield a reasonably accurate representation of an aeroplane's actual flight path for the specified reference conditions (see **Section 2.5**). But the aerodynamic parameters and engine coefficients have been shown to be adequate for air temperatures up to 43 °C, aerodrome altitudes up to 4,000 ft and across the range of weights specified in the ANP database. The equations thus permit the calculation of flight paths for other conditions; i.e. non-reference aeroplane weight, windspeed, air temperature, and runway elevation (air pressure), normally with sufficient accuracy for computing contours of average sound levels around an airport.

Section B-4 explains how the effects of turning flight are taken into account for departures. This allows bank angle to be accounted for when calculating the effects of lateral directivity (installation effects). Also, during turning flight, climb gradients will generally be reduced depending on the radius of the turn and the speed of the aeroplane. (The effects of turns during the landing approach are more complex and are not covered at present. However these will rarely influence noise contours significantly.)

Sections B-5 to **B-9** describe the recommended methodology for generating departure flight profiles, based on ANP database coefficients and procedural steps.

Sections B-10 and **B-11** describe the methodology used to generate approach flight profiles, based on ANP database coefficients and flight procedures.

Section B-12 provides worked examples of the calculations.

Separate sets of equations are provided to determine the net thrust produced by jet engines and propellers respectively. Unless noted otherwise, the equations for aerodynamic performance of an aeroplane apply equally to jet and propeller-powered aeroplanes.

Mathematical symbols used are defined at the beginning of this appendix and/or where they are first introduced. *In all equations the units of coefficients and constants must of course be*

consistent with the units of the corresponding parameters and variables. For consistency with the ANP database, the conventions of aircraft performance engineering are followed in this appendix; distances and heights in feet (ft), speed in knots (kt), mass in pounds (lb), force in pounds-force (lbf), and so on - even though some dimensions (e.g. atmospheric ones) are expressed in SI units. Modellers using other unit systems should be very careful to apply appropriate conversion factors when adopting the equations to their needs.

Flight path analysis

In some modelling applications the flight path information is provided not as procedural steps but as coordinates in position and time, usually determined by analysis of radar data. This is discussed in **Chapter 3** of the text. In this case the equations presented in this appendix are used 'in reverse'; the engine thrust parameters are derived from the aircraft motion rather than vice-versa. In general, once the flight path data have been averaged and reduced to segment form, each segment being classified by climb or descent, acceleration or deceleration, and thrust and flap changes, this is relatively straightforward by comparison with synthesis which often involves iterative processes.

B2 ENGINE THRUST

The propulsive force produced by each engine is one of five quantities that need to be defined at the ends of each flight path segment (the others being height, speed, power setting and bank angle). Net thrust represents the component of engine gross thrust that is available for propulsion. For aerodynamic and acoustical calculations, the net thrust is referred to standard air pressure at mean sea level. This is known as *corrected net thrust, F_n/δ*.

This will be either the net thrust available when operating at a specified *thrust rating*, or the net thrust that results when the *thrust-setting parameter* is set to a particular value. For a turbojet or turbofan engine operating at a specific thrust rating, corrected net thrust is given by the equation

$$F_n/\delta = E + F \cdot V_C + G_A \cdot h + G_B \cdot h^2 + H \cdot T \qquad \text{(B-1)}$$

where:

F_n	is the net thrust per engine, lbf
δ	is the ratio of the ambient air pressure at the aeroplane to the standard air pressure at mean sea level, i.e., to 101.325 kPa (or 1013.25 mb) [ref. 1]
F_n/δ	is the corrected net thrust per engine, lbf
V_C	is the calibrated airspeed, kt
T	is the ambient air temperature in which the aeroplane is operating, °C, and
E, F, G_A, G_B, H	are engine thrust constants or coefficients for temperatures below the engine flat rating temperature at the thrust rating in use (on the current segment of the takeoff/climbout or approach flight path), lb.s/ft, lb/ft, lb/ft^2, lb/°C. Obtainable from the ANP database.

Data are also provided in the ANP database to allow calculation of non-rated thrust as a function of a thrust setting parameter. This is defined by some manufacturers as engine pressure ratio *EPR*, and by others as low-pressure rotor speed, or fan speed, N_1. When that parameter is *EPR*, equation B-1 is replaced by

$$F_n/\delta = E + F \cdot V_C + G_A \cdot h + G_B \cdot h^2 + H \cdot T + K_1 \cdot EPR + K_2 \cdot EPR^2 \qquad \text{(B-2)}$$

where K_1 and K_2 are coefficients from the ANP database that relate corrected net thrust and engine pressure ratio in the vicinity of the engine pressure ratio of interest for the specified aeroplane Mach number.

When engine rotational speed N_1 is the parameter used by the cockpit crew to set thrust, the generalised thrust equation becomes:

$$F_n/\delta = E + F \cdot V_C + G_A \cdot h + G_B \cdot h^2 + H \cdot T + K_3 \cdot \left(\frac{N_1}{\sqrt{\theta}}\right) + K_4 \cdot \left(\frac{N_1}{\sqrt{\theta}}\right)^2 \qquad \text{(B-3)}$$

where:

N_1	is the rotational speed of the engine's low-pressure compressor (or fan) and turbine stages, %
θ	= (T + 273)/288.15, the ratio of the absolute total temperature at the engine inlet to the absolute standard air temperature at mean sea level [ref. 1]
$\frac{N_1}{\sqrt{\theta}}$	is the corrected low pressure rotor speed, %, and
K_3, K_4	are constants derived from installed engine data encompassing the N_1 speeds of interest.

Note that for a particular aeroplane *E*, *F*, G_A, G_B and *H* in equations B-2 and B-3 might have different values from those in equation B-1.

Not every term in the equation will always be significant. For example, for flat-rated engines operating in air temperatures below the break point (typically 30 °C), the temperature term may not be required. For engines not flat rated, ambient temperature must be considered when designating rated thrust. Above the engine flat rating temperature, a different set of engine thrust coefficients (*E*, *F*, G_A, G_B and $H)_{high}$ must be used to determine the thrust level available. Normal practice would then be to compute F_n/δ using both the low temperature and high temperature coefficients and to use the higher thrust level for temperatures *below* the flat rating temperature and use the lower calculated thrust level for temperature *above* the flat rating temperature.

Where only low temperature thrust coefficients are available, the following relationship may be used:

$$(F_n/\delta)_{high} = F \cdot V_C + (E + H \cdot T_B) \cdot (1 - 0.006 \cdot T)/(1 - 0.006 \cdot T_B) \qquad \text{(B-4)}$$

where:

$(F_n/\delta)_{high}$	high-temperature corrected net thrust (pounds)
T_B	breakpoint temperature (in the absence of a definitive value

assume a default value of 30 °C)

The ANP database provides values for the constants and coefficients in equations B-1 to B-4.

For propeller-driven aeroplanes, corrected net thrust per engine should be read from graphs or calculated using the equation

$$F_n/\delta = \left(326 \cdot \eta \cdot P_p / V_T\right)/\delta \qquad \text{(B-5)}$$

where:

η	is the propeller efficiency for a particular propeller installation and is a function of propeller rotational speed and aeroplane flight speed
V_T	is the true airspeed, kt
P_p	is net propulsive power for the given flight condition, e.g. max takeoff or max climb power, hp

Parameters in equation B-5 are provided in the ANP database for maximum takeoff thrust and maximum climb thrust settings.

True airspeed V_T is estimated from the calibrated airspeed V_C using the relationship

$$V_T = V_C/\sqrt{\sigma} \qquad \text{(B-6)}$$

where σ is the ratio of the air density at the aeroplane to the mean sea level value.

Guidance on operation with reduced takeoff thrust

Often, aircraft takeoff weights are below maximum allowable and/or the available runway field length exceeds the minimum required with the use of maximum takeoff thrust. In these cases, it is common practice to reduce engine thrust below maximum levels in order to prolong engine life and, sometimes, for noise abatement purposes. Engine thrust can only be reduced to levels that maintain a required margin of safety. The calculation procedure used by airline operators to determine the amount of thrust reduction is regulated accordingly; it is complex and takes into account numerous factors including takeoff weight, ambient air temperature, declared runway distances, runway elevation and runway obstacle clearance criteria. Therefore the amount of thrust reduction varies from flight to flight.

As they can have a profound effect upon departure noise contours, modellers should take reasonable account of reduced thrust operations and, to make best possible provision, to seek practical advice from operators.

If such advice is not available it is still advisable to make some allowance by alternative means. It is impractical to mirror the operators' calculations for noise modelling purposes; nor would they be appropriate alongside the conventional simplifications and approximations which are made for the purposes of calculating long term average noise levels. As a practicable alternative the following guidance is provided. It should be emphasised that considerable research is ongoing in this area and thus, this guidance is subject to change.

Analysis of FDR data has shown that the level of thrust reduction is strongly correlated with ratio of the actual takeoff weight to the Regulated Takeoff Weight (RTOW), down to a fixed lower limit[26]; i.e.

$$F_n / \delta = (F_n / \delta)_{max} \cdot W / W_{RTOW} \quad \text{(B-7)}$$

where $(F_n/\delta)_{max}$ is the maximum rated thrust, W is the actual gross takeoff weight and W_{RTOW} is the Regulated Takeoff Weight.

The RTOW is the maximum takeoff weight that can be safely used, whilst satisfying takeoff field length, engine-out and obstacle requirements. It is a function of the available runway length, airfield elevation, temperature, headwind, and flap angle. This information can be obtained from operators and should be more readily available than data on actual levels of reduced thrust. Alternatively, it may be computed using data contained in aircraft flight manuals.

Reduced Climb Thrust

When employing reduced takeoff thrust, operators often, but not always, reduce climb thrust from below maximum levels[27]. This prevents situations occurring where, at the end of the initial climb at takeoff thrust, power has to be increased rather than cut back. However, it is more difficult to establish a rationale for a common basis here. Some operators use fixed detents below maximum climb thrust, sometimes referred to as Climb 1 and Climb 2, typically reducing climb thrust by 10 and 20 percent respectively relative to maximum. It is recommended that whenever reduced takeoff thrust is used, climb thrust levels also be reduced by 10 percent.

B3 VERTICAL PROFILES OF AIR TEMPERATURE, PRESSURE, DENSITY AND WINDSPEED

For the purposes of this document, the variations of temperature, pressure and density with height above mean sea level are taken to be those of the International Standard Atmosphere (ISA) [ref. 1]. The methodologies described below have been validated for aerodrome altitudes up to 4000 ft above sea level and for air temperatures up to 43 °C (109 °F).

Although, in reality, mean wind velocity varies with both height and time, it is not usually practicable to take account of this for noise contour modelling purposes. Instead, the flight performance equations given below are based on the common assumption that the aeroplane is heading directly into a (default) headwind of 8 kt at all times - regardless of compass bearing (although no explicit account of mean wind velocity is taken in sound propagation calculations). Methods for adjusting the results for other headwind speeds are provided.

B4 THE EFFECTS OF TURNS

The remainder of this appendix explains how to calculate the required properties of the segments joining the profile points *s,z* that define the two-dimensional flight path in the vertical plane above the flight track. Segments are defined in sequence in the direction of motion. At the end of any one segment (or at the start of roll in the case of the first for a departure) where the operational parameters and the next procedural step are defined, the need

[26] Airworthiness authorities normally stipulate a lower thrust limit, often 25 percent below maximum.

[27] To which thrust is reduced after the initial climb at takeoff power.

is to calculate the climb angle and track distance to the point where the required height and/or speed are reached.

If the track is straight, this will be covered by a single profile segment, the geometry of which can then be determined directly (albeit sometimes with a degree of iteration). But if a turn starts or ends, or changes in radius or direction, before the required end-conditions are reached, a single segment would be insufficient because the aircraft lift and drag change with bank angle. *To account for the effects of the turn on the climb*, additional profile segments are required to implement the procedural step - as follows.

The construction of the ground track is described in **Section 3.6.1** of the text. This is done independently of any aircraft flight profile (although with care not to define turns that could not be flown under normal operating constraints). But as the flight profile (height and speed as a function of track distance) is affected by turns, the flight profile cannot be determined independently of the ground track.

To maintain speed in a turn the aerodynamic wing lift has to be increased to balance centrifugal force as well as the aircraft weight. This in turn increases drag and consequently the propulsive thrust required. The effects of the turn are expressed in the performance equations as functions of bank angle ε which, for an aircraft in level flight turning at constant speed on a circular path, is given by

$$\varepsilon = \tan^{-1}\left\{\frac{2.85 \cdot V^2}{r \cdot g}\right\} \qquad \text{(B-8)}$$

where V is the groundspeed, kt

r is the turn radius, ft

and g is the acceleration due to gravity, ft/s^2

All turns are assumed to have a constant radius and second-order effects associated with non-level flight paths are disregarded; bank angles are based on the turn radius *r* of the ground track only.

To implement a procedural step a provisional profile segment is first calculated using the bank angle ε at the start point - as defined by equation B-8 for the track segment radius *r*. If the calculated length of the provisional segment is such that it does not cross the start or end of a turn, the provisional segment is confirmed and attention turns to the next step.

But if the provisional segment crosses one or more starts or ends of turns (where ε changes)[28], the flight parameters at the first such point are estimated by interpolation (see **Section 3.6.2**), saved along with its coordinates as end-point values, and the segment truncated. The second part of the procedural step is then applied from that point - once more assuming provisionally that it can be completed in a single segment with the same end conditions but with the new start point and new bank angle. If this second segment then passes another change of turn radius/direction, a third segment will be required - and so on until the end-conditions are achieved.

[28] To avoid contour discontinuities caused by instantaneous changes of bank angle at the junctions between straight and turning flight, sub-segments are introduced into the noise calculations to allow linear transitions of bank angle over the first and last 5° of the turn. These are not necessary in the performance calculations; the bank angle is always given by equation B-8.

Approximate method

It will be apparent that accounting fully for the effects of turns, as described above, involves considerable computational complexity because the climb profile of any aircraft has to be calculated separately for each ground track that it follows. But changes to the vertical profile caused by turns usually have a markedly smaller influence on the contours than the changes of bank angle, and some users may prefer to avoid the complexity - at the cost of some loss of precision - by disregarding the effects of turns on profiles while still accounting for the bank angle in the calculation of lateral sound emission (see **Sections 4.5.2** and **4.5.3**). Under this approximation, profile points for a particular aircraft operation are calculated once only, assuming a straight ground track (for which $\varepsilon = 0$).

B5 TAKEOFF GROUND ROLL

Takeoff thrust accelerates the aeroplane along the runway until lift-off. Calibrated airspeed is then assumed to be constant throughout the initial part of the climbout. Landing gear, if retractable, is assumed to be retracted shortly after lift-off.

For the purpose of this document, the actual takeoff ground-roll is approximated by an equivalent takeoff distance (into a default headwind of 8 kt), s_{TO8}, defined as shown in **Figure B-1**, as the distance along the runway from brake release to the point where a straight line extension of the initial landing-gear-retracted climb flight path intersects the runway.

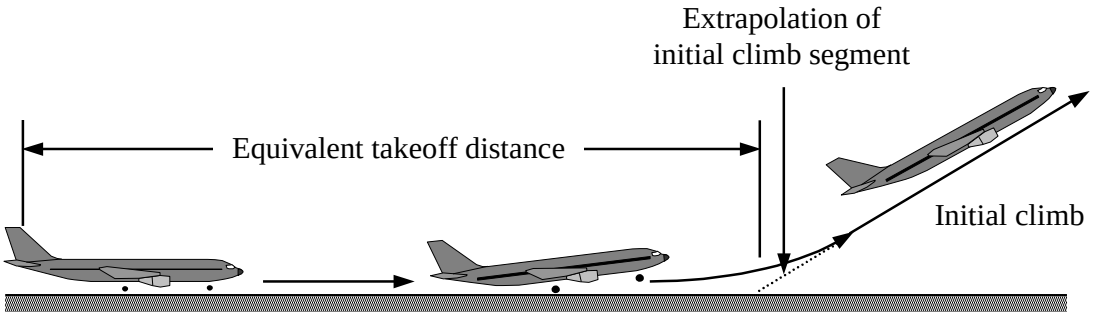

Figure B-1: Equivalent takeoff distance

On a level runway, the equivalent takeoff ground-roll distance s_{TO8} in feet is determined from:

$$s_{TO8} = \frac{B_8 \cdot \theta \cdot (W/\delta)^2}{N \cdot (F_n/\delta)} \qquad \text{(B-9)}$$

where

B_8	is a coefficient appropriate to a specific aeroplane/flap-deflection combination for the ISA reference conditions, including the 8 kt headwind, ft/lbf
W	is the aeroplane gross weight at brake release, lbf
N	is the number of engines supplying thrust.

Note: Since equation B-9 accounts for variation of thrust with airspeed and runway elevation, for a given aeroplane the coefficient B_8 depends only on flap deflection.

For headwind other than the default 8 kt, the takeoff ground-roll distance is corrected by using:

$$s_{TOw} = s_{TO8} \cdot \frac{(V_C - w)^2}{(V_C - 8)^2} \qquad \text{(B-10)}$$

where

S_{TOw} is the ground-roll distance corrected for headwind w, ft

V_C (in this equation) is the calibrated speed at takeoff rotation, kt

w is the headwind, kt

The takeoff ground-roll distance is also corrected for runway gradient as follows:

$$s_{TOG} = s_{TOw} \cdot \frac{a}{(a - g \cdot G_R)} \qquad \text{(B-11)}$$

where

S_{TOG} is the ground-roll distance (ft) corrected for headwind and runway gradient,

a is the average acceleration along the runway, equal to $\left(V_C \cdot \sqrt{\sigma}\right)^2 / (2 \cdot s_{TOw})$, ft/s^2

G_R is the runway gradient; positive when taking-off uphill

B6 CLIMB AT CONSTANT SPEED

This type of segment is defined by the aeroplane's calibrated airspeed, flap setting, and the height and bank angle at its end, together with the headwind speed (default 8 kt). As for any segment, the segment start parameters including corrected net thrust are put equal to those at the end of the preceding segment - there are no discontinuities (except of flap angle and bank angle which, in these calculations, are allowed to change in steps). The net thrusts at the segment end are first calculated using the appropriate equation from B-1 to B-5. The average geometric climb angle γ (see **Figure B-1**) is then given by

$$\gamma = \arcsin\left(K \cdot \left[N \cdot \frac{\overline{F_n/\delta}}{\overline{W/\delta}} - \frac{R}{\cos\varepsilon} \right] \right) \qquad \text{(B-12)}$$

where the over-bars denote mid-segment values (= average of start-point and end-point values - generally the mid-segment values) and

K is a speed-dependent constant equal to 1.01 when $V_C \leq 200$ kt or 0.95 otherwise. This constant accounts for the effects on climb gradient of climbing into an 8-knot headwind and the acceleration inherent in climbing at constant calibrated airspeed (true speed increases as air density diminishes with height).

R is the ratio of the aeroplane's drag coefficient to its lift coefficient appropriate to the given flap setting. The landing gear is assumed to be retracted.

ε Bank angle, radians

The climb angle is corrected for headwind *w* using:

$$\gamma_w = \gamma \cdot \frac{(V_C - 8)}{(V_C - w)} \tag{B-13}$$

where γ_w is the average climb angle corrected for headwind.

The distance that the aeroplane traverses along the ground track, Δs, while climbing at angle γ_w, from an initial altitude h_1 to a final altitude h_2 is given by:

$$\Delta s = \frac{(h_2 - h_1)}{\tan \gamma_w} \tag{B-14}$$

As a rule, two distinct phases of a departure profile involve climb at constant airspeed. The first, sometime referred to as the *initial climb segment* is immediately after lift-off, where safety requirements dictate that the aeroplane is flown at a minimum airspeed of least the takeoff safety speed. This is a regulated speed and should be achieved by 35 ft above the runway during normal operation. However, it is common practice to maintain an initial climb speed slightly beyond the takeoff safety speed, usually by 10-20 kt, as this tends to improve the initial climb gradient achieved. The second is after flap retraction and initial acceleration, referred to as *continuing climb*.

During the initial climb, the airspeed is dependent on the takeoff flap setting and the aeroplane gross weight. The calibrated initial climb speed V_{CTO} is calculated using the first order approximation:

$$V_{CTO} = C \cdot \sqrt{\mathrm{W}} \tag{B-15}$$

where *C* is a coefficient appropriate to the flap setting (kt/√lbf), read from the ANP database.

For continuing climb after acceleration, the calibrated airspeed is a user input parameter.

B7 POWER CUTBACK (TRANSITION SEGMENT)

Power is reduced, or *cut back*, from takeoff setting at some point after takeoff in order to extend engine life and often to reduce noise in certain areas. Thrust is normally cut back during either a constant speed climb segment (**Section B6)** or an acceleration segment (**Section B8)**. As it is a relatively brief process, typically of only 3 - 5 seconds duration, is it modelled by adding a 'transition segment' to the primary segment. This is usually taken to cover a horizontal ground distance of 1000 ft (305 m).

Amount of thrust reduction

In normal operation the engine thrust is reduced to the maximum climb thrust setting. Unlike the takeoff thrust, climb thrust can be sustained indefinitely, usually in practice until the aeroplane has reached its initial cruise altitude. The maximum climb thrust level is determined with equation B-1 using the manufacturer-supplied maximum thrust coefficients. However, noise abatement requirements may call for additional thrust reduction, sometimes referred to as a 'deep' cutback. For safety purposes the maximum thrust reduction is limited[29] to an amount determined by the performance of the aeroplane and the number of engines.

[29] "Noise Abatement Procedures", ICAO Document 8168 'PANS-OPS' Vol.1 Part V, Chapter 3, ICAO 2004.

The minimum 'reduced-thrust' level is sometimes referred to as the engine-out 'reduced thrust':

$$\left(F_n / \delta\right)_{engineout} = \frac{\left(W / \delta_2\right)}{\left(N-1\right)} \cdot \left[\frac{\sin\left(\arctan\left(0.01 \cdot G'\right)\right)}{K} + \frac{R}{\cos\varepsilon}\right] \qquad \text{(B-16)}$$

where:

δ_2 is the pressure ratio at altitude h_2

G' is the engine-out percentage climb gradient:

= 0% for aeroplanes with automatic thrust restoration systems; otherwise,

= 1.2% for a 2-engine aeroplane

= 1.5% for a 3-engine aeroplane

= 1.7% for a 4-engine aeroplane

Constant speed climb segment with cutback

The climb segment gradient is calculated using equation B-12, with thrust calculated using either B-1 with maximum climb coefficients, or B-16 for reduced thrust. The climb segment is then broken into two sub-segments, both having the same climb angle. This is illustrated in **Figure B-2**.

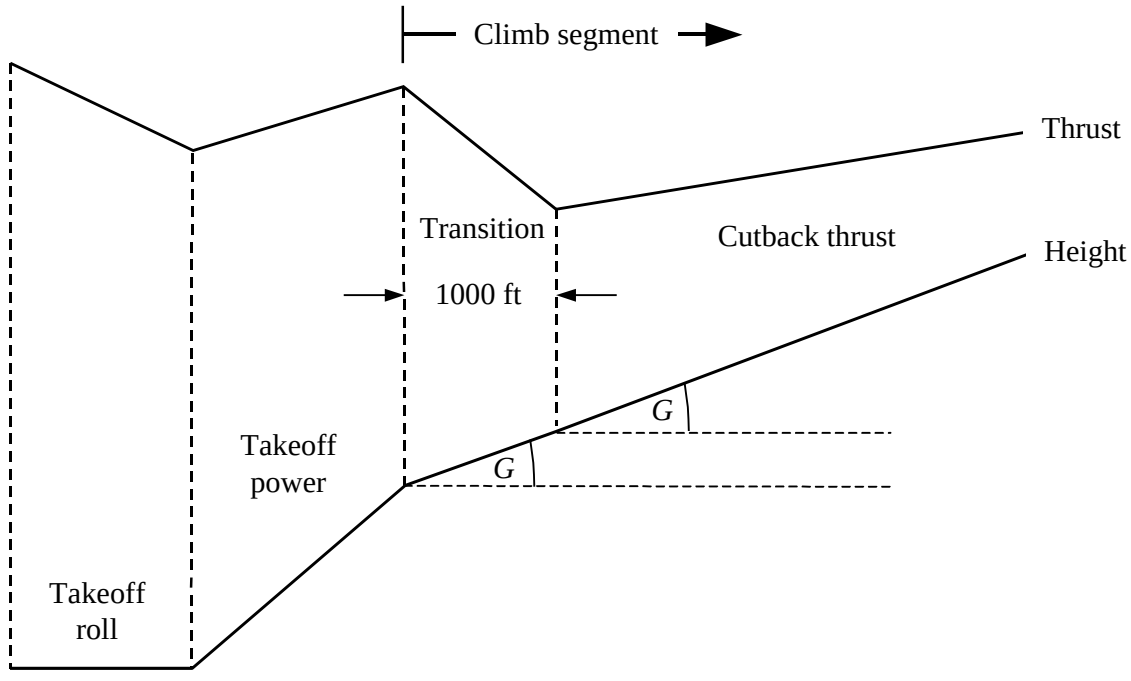

Figure B-2: Constant speed climb segment with cutback (illustration – not to scale)

The first sub-segment is assigned a 1000 ft (304 m) ground distance, and the corrected net thrust per engine at the end of 1000 ft is set equal to the cutback value. (If the original horizontal distance is less than 2000 ft, one half of the segment is used to cutback thrust.) The

final thrust on the second sub-segment is also set equal to the cutback thrust. Thus, the second sub-segment is flown at constant thrust.

B8 ACCELERATING CLIMB AND FLAP RETRACTION

This usually follows the initial climb. As for all flight segments, the start-point altitude h_1, true airspeed V_{T1}, and thrust $(F_n/\delta)_1$ are those from the end of the preceding segment. The end-point calibrated airspeed V_{C2} and the average climb rate *ROC* are user inputs (bank angle ε is a function of speed and radius of turn). As they are interdependent, the end altitude h_2, end true airspeed V_{T2}, end thrust $(F_n/\delta)_2$ and segment track length Δs have to be calculated by iteration; the end altitude h_2 is guessed initially and then recalculated repeatedly using equations B-16 and B-17 until the difference between successive estimates is less than a specified tolerance, e.g. one foot. A practical initial estimate is $h_2 = h_1 + 250$ feet.

The segment track length (horizontal distance covered) is estimated as:

$$s_{seg} = 0.95 \cdot k^2 \cdot (V_{T2}^2 - V_{T1}^2)/2(a_{max} - G \cdot g) \qquad \text{(B-17)}$$

where:

0.95 is a factor to account for effect of 8 kt headwind when climbing at 160 kt

k is a constant to convert knots to ft/sec = 1.688 ft/s per kt

V_{T2} = true airspeed at segment end, kt: $V_{T2} = V_{C2}/\sqrt{\sigma_2}$

where σ_2 = air density ratio at end altitude h_2

a_{max} = maximum acceleration in level flight (ft/s^2)
$= g[N \cdot \overline{F_n/\delta}/(\overline{W/\delta}) - R/\cos\varepsilon]$

G = climb gradient $\approx \dfrac{ROC}{60 \cdot k \cdot \overline{V_T}}$

where *ROC* = climb rate, ft/min

Using this estimate of Δs, the end altitude h_2' is then re-estimated using:

$$h_2' = h_1 + s \cdot G/0.95 \qquad \text{(B-18)}$$

As long as the error $|h_2' - h_2|$ is outside the specified tolerance, the steps B-17 and B-18 are repeated using the current iteration segment-end values of altitude h_2, true airspeed V_{T2}, corrected net thrust per engine $(F_n/\delta)_2$. When the error is within the tolerance, the iterative cycle is terminated and the acceleration segment is defined by the final segment-end values.

Note: If during the iteration process $(a_{max} - G \cdot g) < 0.02$g, the acceleration may be too small to achieve the desired V_{C2} in a reasonable distance. In this case, the climb gradient can be limited to $G = a_{max}/\text{g} - 0.02$, in effect reducing the desired climb rate in order to maintain acceptable acceleration. If $G < 0.01$ it should be concluded there is not enough thrust to achieve the acceleration and climb specified; the calculation should be terminated and the procedure steps revised[30].

The acceleration segment length is corrected for headwind *w* by using:

[30] In either case the computer model should be programmed to inform the user of the inconsistency.

$$\Delta s_w = \Delta s \cdot \frac{(V_T - w)}{(V_T - 8)} \tag{B-19}$$

Accelerating segment with cutback

Thrust cutback is inserted into an acceleration segment in the same way as for a constant speed segment, by turning its first part into a transition segment. The cutback thrust level is calculated as for the constant-speed cutback thrust procedure, using equation B-1 only. Note it is not generally possible to accelerate and climb whilst maintaining the minimum engine-out thrust setting. The thrust transition is assigned a 1000 ft (305 m) ground distance, and the corrected net thrust per engine at the end of 1000 ft is set equal to the cutback value. The speed at the end of the segment is determined by iteration for a segment length of 1000 ft. (If the original horizontal distance is less than 2000 ft, one half of the segment is used for thrust change.) The final thrust on the second sub-segment is also set equal to the cutback thrust. Thus, the second sub-segment is flown at constant thrust.

B9 ADDITIONAL CLIMB AND ACCELERATION SEGMENTS AFTER FLAP RETRACTION

If additional acceleration segments are included in the climbout flight path, equations B-12 to B-19 should be used again to calculate the ground-track distance, average climb angle, and height gain for each. As before, the final segment height must be estimated by iteration.

B10 DESCENT AND DECELERATION

Approach flight normally requires the aeroplane to descend and decelerate in preparation for the final approach segment where the aeroplane is configured with approach flap and gear down. The flight mechanics are unchanged from the departure case; the main difference is that the height and speed profile is generally known, and it is the engine thrust levels that must be estimated for each segment. The basic force balance equation is:

$$F_n / \delta = W \cdot \frac{R \cdot \cos\gamma + \sin\gamma + a/g}{N \cdot \delta} \tag{B-20}$$

Equation B-20 may be used in two distinct ways. First the aeroplane speeds at the start and end of a segment may be defined, along with a descent angle (or level segment distance) and initial and final segment altitudes. In this case the deceleration may be calculated using:

$$a = \frac{(V_2 / \cos\gamma)^2 - (V_1 / \cos\gamma)^2}{(2 \cdot \Delta s / \cos\gamma)} \tag{B-21}$$

where Δs is the ground distance covered and V_1 and V_2 and are the initial and final groundspeeds calculated using

$$V = \frac{V_C \cdot \cos\gamma}{\sqrt{\sigma}} - w \tag{B-22}$$

Equations B-20, B-21 and B-22 confirm that whilst decelerating over a specified distance at a constant rate of descent, a stronger headwind will result in more thrust being required to maintain the same deceleration, whilst a tailwind will require less thrust to maintain the same deceleration.

In practice most, if not all decelerations during approach flight are performed at idle thrust. Thus for the second application of equation B-20, thrust is defined at an idle setting and the equation is solved iteratively to determine (1) the deceleration and (2) the height at the end of the deceleration segment - in a similar manner to the departure acceleration segments. In this case, deceleration distance can be very different with head and tailwinds and it is sometimes necessary to reduce the descent angle in order to obtain reasonable results.

For most aeroplanes, idle thrust is not zero and, for many, it is also a function of flight speed. Thus, equation B-20 is solved for the deceleration by inputting an idle thrust; the idle thrust is calculated using an equation of the form:

$$\left(F_n/\delta\right)_{idle} = E_{idle} + F_{idle} \cdot V_C + G_{A,idle} \cdot h + G_{B,idle} \cdot h^2 + H_{idle} \cdot T \qquad \text{(B-23)}$$

where (E_{idle}, $F_{idle,}$ $G_{A,idle}$, $G_{B,idle}$ and H_{idle}) are idle thrust engine coefficients available in the ANP database.

B11 LANDING APPROACH

The landing approach calibrated airspeed, V_{CA}, is related to the landing gross weight by an equation of the same form as equation B-11, namely

$$V_{CA} \approx D \cdot \sqrt{W} \qquad \text{(B-24)}$$

where the coefficient D (kt/√lbf) corresponds to the landing flap setting.

The corrected net thrust per engine during descent along the approach glideslope is calculated by solving equation B-12 for the landing weight W and a drag-to-lift ratio R appropriate for the flap setting with landing gear extended. The flap setting should be that typically used in actual operations. During landing approach, the glideslope descent angle γ may be assumed constant. For jet-powered and multi-engine propeller aeroplanes, γ is typically –3°. For single-engine, propeller-powered aeroplanes, γ is typically –5°.

The average corrected net thrust is calculated by inverting equation B-12 using K=1.03 to account for the deceleration inherent in flying a descending flight path into an 8 kt reference headwind at the constant calibrated airspeed given by equation B-24, i.e.

$$\overline{F_n/\delta} = \frac{\overline{W/\delta}}{N} \cdot \left(R + \frac{\sin\gamma}{1.03}\right) \qquad \text{(B-25)}$$

For headwinds other than 8kt, average corrected net thrust becomes

$$\left(\overline{F_n/\delta}\right)_w = \overline{F_n/\delta} + 1.03 \cdot \overline{W/\delta} \cdot \frac{\sin\gamma \cdot (w-8)}{N \cdot V_{CA}} \qquad \text{(B-26)}$$

The horizontal distance covered is calculated by:

$$\Delta s = \frac{(h_2 - h_1)}{\tan\gamma} \qquad \text{(B-27)}$$

(positive since $h_1 > h_2$ and γ is negative).

B12 WORKED EXAMPLES

The following worked examples for the Boeing 737-300 illustrate how the various equations are used with parameters defining aeroplane departure and approach 'procedures' to construct flight profiles together with power settings.

Departure Profile

Boeing 737-300: takeoff mass of 53,968 kg (119,000 lb), ISA conditions at sea level, headwind component 8 kt.

The procedural steps are:

1. Takeoff, flap 5, full takeoff thrust
2. Maintain takeoff power, climb at V_2 + 10 kt to 1000ft
3. Maintain takeoff power, accelerate to 185 kt CAS, climbing at 1544 ft/min
4. Maintain takeoff power, select flap 1, accelerate to 190 kt CAS, climbing at 1544 ft/min.
5. Reduce thrust to maximum climb thrust, select zero flap, accelerate to 220 kt CAS, climbing at 1000 ft/min
6. Maintain maximum climb thrust, 220 kt CAS, zero flap and climb to 3000 ft
7. Maintain maximum climb thrust, accelerate to 250 kt CAS, climbing at 1000 ft/min
8. Maintain maximum climb thrust and 250 kt CAS, zero flap and climb to 5500 ft
9. Maintain maximum climb thrust, 250 kt CAS, zero flap and climb to 7500 ft[31]
10. Maintain maximum climb thrust, 250 kt CAS, zero flap and climb to 10000 ft

The calculation steps and results are shown in **Table B-1**. Note that step 5 is split into two parts, the initial part including a 1000 ft long segment to account for thrust reduction. The length of the segment following acceleration at the specified climb rate determines the end speed for this segment.

[31] Although apparently redundant as Step 10 supplants it, Step 9, like much ANP content, dates from a time when models had to be less sophisticated. In this particular case the original need was to reduce the risk of using excessively long segments. Modern tools designed for more capable computers can be designed to warn of such risks automatically.

Approach Profile

Boeing 737-300: landing mass 46,636 kg (102600 lb), ISA conditions at sea level, 8 kt headwind. Relatively conventional approach with a long decelerating segment in level flight.

The procedural steps are:

1. Descend from 6000 ft to 3000 ft with a descent angle of 3°, whilst maintaining 250 kt CAS, flap code zero.
2. At 3000 ft, level off, select flap code 5 and decelerate to 170 kt CAS over a distance of 21000 ft.
3. Maintain altitude of 3000 ft, flap code 5 and decelerate to 148.6 kt CAS over a distance of 5000 ft.
4. Descend at 3°, select flap code D-15 and decelerate to 139 kt CAS by an altitude of 2500 ft.
5. Descend at 3°, select flap code D-30 and maintain 139 kt (reference landing speed).
6. Touchdown roll out for 294 ft, decelerate to 132.1 kt.
7. Touchdown roll for 2940 ft, thrust at 60% maximum.
8. End of procedure, speed at 30 kt, thrust at 10% maximum.

Note: The approach example features a level flight segment at 3000 ft along which speed is reduced and illustrates how the improved methodology may be applied. However the specified 'procedural steps' are not at present tabulated in the ANP database[32]. Data for the Boeing 737-300 were generated some years ago when the SAE data specification called only for a continuous 3° descent from 6000 ft to touchdown, whilst continuously decelerating. Such a flight profile is rarely typical of operations at most airports. Although the aerodynamic coefficients necessary to calculate more realistic approach profiles have still not been provided, more recent data entries remedy the problem via tabulations of 'profile points' data for an approach with a 3000 ft level flight segment. (A remaining difficulty with 'profile points' is that they are fixed; alternative profiles cannot be created.) In future, the methodology described in **Section B-10** will enable the provision of 'procedural steps' data for profiles incorporating level flight segments and deceleration.

[32] However it is consistent with the current ANP database 'procedural steps' to the extent that the flap deployment has been sequenced based on the same speeds.

Table B-1: Example departure profile

Segment		Start of roll	Takeoff ground roll	Climb to 1000ft	Accelerate to 185kt	Accelerate to 190kt	Thrust cutback (Accelerate to 220 kt)	Accelerate to 220kt	Climb to 3000ft	Accelerate to 250kt	Climb to 5500ft	Climb to 7500ft	Climb to 10000ft
Start speed (CAS)	(kt)		0	164.6	164.6	185.0	190.0	196.7	220.0	220.0	250.0	250.0	250.0
End speed (CAS)	(kt)		164.6	164.6	185.0	190.0	196.7	220.0	220.0	250.0	250.0	250.0	250.0
Start height	(ft)		-	-	-	-	-	-	-	-	-	-	-
End height	(ft)		-	1000	1331	1408	1461	1646	3000	3268	5500	7500	10000
Input climb rate	(ft/min)		-	-	1544	1544	1000	1000	-	1000	-	-	-
Flap	(°)		5	5	5	1	zero	zero	zero	zero	zero	zero	zero
Thrust rating	(-)		Max takeoff	Max takeoff	Max takeoff	Max takeoff	Max climb	Max climb	Max climb	Max climb	Max climb	Max climb	Max climb
Start FN/δ	(lb/eng)	18745	18745	15433	15837	15561	14376	14269	13894	14105	13627	13974	14286
End FN/δ	(lb/eng)	-	15433	15837	15561	15492	14269	13894	14105	13627	13974	14286	14675
Start θ	(-)	1.000	1.000	1.000	0.993	0.991	0.990	0.990	0.989	0.979	0.978	0.962	0.948
End θ	(-)	1.000	1.000	0.993	0.991	0.990	0.990	0.989	0.979	0.978	0.962	0.948	0.931
Start δ	(-)	1.000	1.000	1.000	0.964	0.953	0.950	0.948	0.942	0.896	0.887	0.817	0.757
End δ	(-)	1.000	1.000	0.964	0.953	0.950	0.948	0.942	0.896	0.887	0.817	0.757	0.688
Start σ	(-)	1.000	1.000	1.000	0.971	0.962	0.959	0.958	0.953	0.915	0.908	0.849	0.798
End σ	(-)	1.000	1.000	0.971	0.962	0.959	0.958	0.953	0.915	0.908	0.849	0.798	0.738
Weight/δ (mean)	(lb)	119000	119000	121173	124140	125067	125365	125910	129509	133435	139768	151324	164882
Climb factor	(-)	-	-	1.01	1.01	1.01	1.01	0.95	0.95	0.95	0.95	0.95	0.95
Climb gradient	(-)	-	-	0.1817	0.1765	0.1748	0.1690	0.1542	0.1470	0.1390	0.1291	0.1188	0.1082
Wind adjustment	(-)	1.00	1.00	1.00	1.00	1.00	1.00	1.00	1.00	1.00	1.00	1.00	1.00
Eq. takeoff distance	(ft)	-	5506	-	-	-	-	-	-	-	-	-	-
Start VTAS	(kt)	0.0	0.0	164.6	167.1	188.7	194.0	201.0	225.4	230.0	262.4	271.4	279.8
End VTAS	(kt)	-	164.6	167.1	188.7	194.0	201.0	225.4	230.0	262.4	271.4	279.8	290.9
Sector distance gain	(ft)	0	5506	5441	3671	926	999	3801	9143	6357	17197	16757	23021
Sector height gain	(ft)	0	0	1000	331	78	53	185	1354	268	2232	2000	2500
Total distance gain	(ft)	0	5506	10947	14618	15544	16543	20344	29487	35844	53041	69798	92818
Total height gain	(ft)	0	0	1000	1331	1408	1461	1646	3000	3268	5500	7500	10000

Table B-2: Example approach profile

	Units	Step 1	Step 2		Step 3		Step 4		Step 5		Step 6	Step 7	Step 8
Flap code		zero	5	5	5	5	D-15	D-15	D-15	D-30	D-30	D-30	D-30
D		0	0	0	0	0	0	0	0	0.434	0.434	0.434	0.434
R		0.062	0.0791	0.0791	0.0791	0.0791	0.1103	0.1103	0.1103	0.1247	0.1247	0.1247	0.1247
Segment:		Descend	Level	Level	Level	Level	Descend	Descend	Descend	Descend	Land	Decelerate	Decelerate
Descent angle	(°)	-3	-	-	-	-	-3	-3	-3	-3	-3	-	-
Distance	(ft)		1000	20000	1000	4000	-	-	-	-	294	2940	0
Ground thrust	(%)	-	-	-	-	-	-	-	-	-	-	60	10
Start:													
CAS	(kt)	250.0	250.0	246.2	170.0	165.7	148.6	147.6	139.0	139.0	139.0	132.1	30.0
Altitude (h)	(ft)	6000	3000	3000	3000	3000	3000	2948	2500	2448	0	0	0
Δ h	(ft)	3000	0	0	0	0	52.4	447.6	52.4	2447.6	0	0	0
θ	(-)	0.959	0.979	0.979	0.979	0.979	0.979	0.980	0.983	0.983	1.000	1.000	1.000
δ	(-)	0.801	0.896	0.896	0.896	0.896	0.896	0.898	0.913	0.915	1.000	1.000	1.000
σ	(-)	0.836	0.915	0.915	0.915	0.915	0.915	0.917	0.929	0.930	1.000	1.000	1.000
TAS	(kt)	273.4	261.3	257.4	177.7	173.2	155.3	154.2	144.2	144.1	139.0	132.1	30.0
GSP	(kt)	265.5	253.3	249.4	169.7	165.2	147.3	146.2	136.2	136.1	131.0	0.0	0.0
RoD (ft/min)	(ft/min)	-1258.6	0.0	0.0	0.0	0.0	-745.6	-721.4	-699.8	-699.8	0.0	0.0	0.0
Mid-values:													
θ	(-)	0.969	0.979	0.979	0.979	0.979	0.980	0.981	0.983	0.992	1.000	1.000	1.000
δ	(-)	0.849	0.896	0.896	0.896	0.896	0.897	0.905	0.914	0.957	1.000	1.000	1.000
σ	(-)	0.875	0.915	0.915	0.915	0.915	0.916	0.923	0.930	0.965	1.000	1.000	1.000
Calculation:													
Segment length (ft)	(ft)	57243	1000	20000	1000	4000	1000	8541	1000	46703	-294	-2940	0
Deceleration (m/s²)	(m/s²)	-0.048	-0.731	-0.731	-0.731	-0.615	0.000	-0.143	-0.143	0.000	-	-	-
Track distance	(ft)	140487	83243	82243	62243	61243	57243	56243	47703	46703	0	-294	-3234
FN/δ	(lb/eng)	302.1	260.8	260.8	260.8	936.5	936.5	2467.6	2427.3	4144.0	3790.4	12000.0	2000.0

Note: Blue figures are input procedural step values, other numbers are calculated

APPENDIX C: MODELLING OF LATERAL GROUND TRACK SPREADING

It is recommended that, in the absence of radar data, lateral ground track dispersion be modelled on the assumption that the spread of tracks perpendicular to the backbone track follows a Gaussian normal distribution. Experience has shown that this assumption is a reasonable one in most cases.

Assuming a Gaussian distribution with a standard deviation *S*, illustrated in **Figure C-1**, about 98.8 percent of all movements fall within boundaries of ±2.5·*S* (i.e. within a swathe of width of 5·*S*).

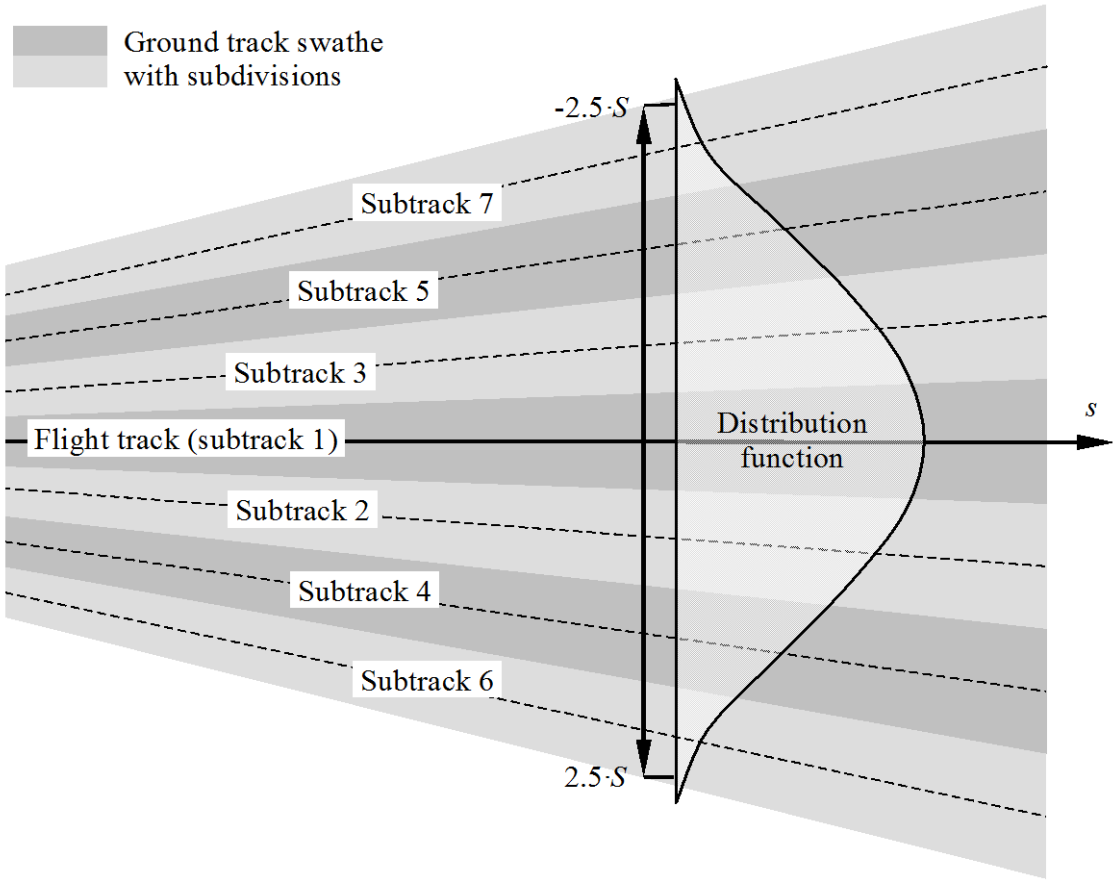

Figure C-1: Subdivision of a ground track into 7 subtracks. The width of the swathe is 5 times the standard deviation of the flight track spreading

A Gaussian distribution can normally be modelled adequately using 7 discrete sub-tracks evenly spaced between the ±2.5·*S* boundaries of the swathe as shown in **Figure C-1**.

However, the adequacy of the approximation depends on the relationship of the sub-track track separation to the heights of the aircraft above. There may be situations (very tight or very dispersed tracks) where a different number of subtracks is more appropriate. Too few subtracks cause 'fingers' to appear in the contour. **Tables C-1** and **C-2** show the parameters for a subdivision into between 5 and 13 subtracks. **Table C-1** shows the location of the particular subtracks, **Table C-2** the corresponding percentage of movements on each subtrack.

Table C-1: Location of 5, 7, 9, 11 or 13 subtracks. The overall width of the swathe (containing 98% of all movements) is 5 times the standard deviation

Subtrack number	Location of subtracks for subdivision into				
	5 subtracks	7 subtracks	9 subtracks	11 subtracks	13 subtracks
12 / 13					±2.31·*S*
10 / 11				±2.27·*S*	±1.92·*S*
8 / 9			±2.22·*S*	±1.82·*S*	±1.54·*S*
6 / 7		±2.14·*S*	±1.67·*S*	±1.36·*S*	±1.15·*S*
4 / 5	±2.00·*S*	±1.43·*S*	±1.11·*S*	±0.91·*S*	±0.77·*S*
2 / 3	±1.00·*S*	±0.71·*S*	±0.56·*S*	±0.45·*S*	±0.38·*S*
1	0	0	0	0	0

Table C-2: Percentage of movements on 5, 7, 9, 11 or 13 subtracks. The overall width of the swathe (containing 98% of all movements) is 5 times the standard deviation

Subtrack number	Percentage of movements on subtrack for subdivision into				
	5 subtracks	7 subtracks	9 subtracks	11 subtracks	13 subtracks
12 / 13					1.1 %
10 / 11				1.4 %	2.5 %
8 / 9			2.0 %	3.5 %	4.7 %
6 / 7		3.1 %	5.7 %	7.1 %	8.0 %
4 / 5	6.3 %	10.6 %	12.1 %	12.1 %	11.5 %
2 / 3	24.4 %	22.2 %	19.1 %	16.6 %	14.4 %
1	38.6 %	28.2 %	22.2 %	18.6 %	15.6 %

APPENDIX D: RECALCULATION OF NPD DATA FOR NON-REFERENCE CONDITIONS

The noise level contributions from each segment of the flight path are derived from the NPD data stored in the international ANP database. However it must be noted that these data have been normalised using average atmospheric attenuation rates defined in SAE AIR-1845 [ref. 6] and revised in CAN/7-WP/59 [ref. 15]. Those rates are averages of values determined during aircraft noise certification testing in Europe and the USA. The wide variation of atmospheric conditions (temperature and relative humidity) in those tests is shown in **Figure D-1** (taken from [ref. 15]).

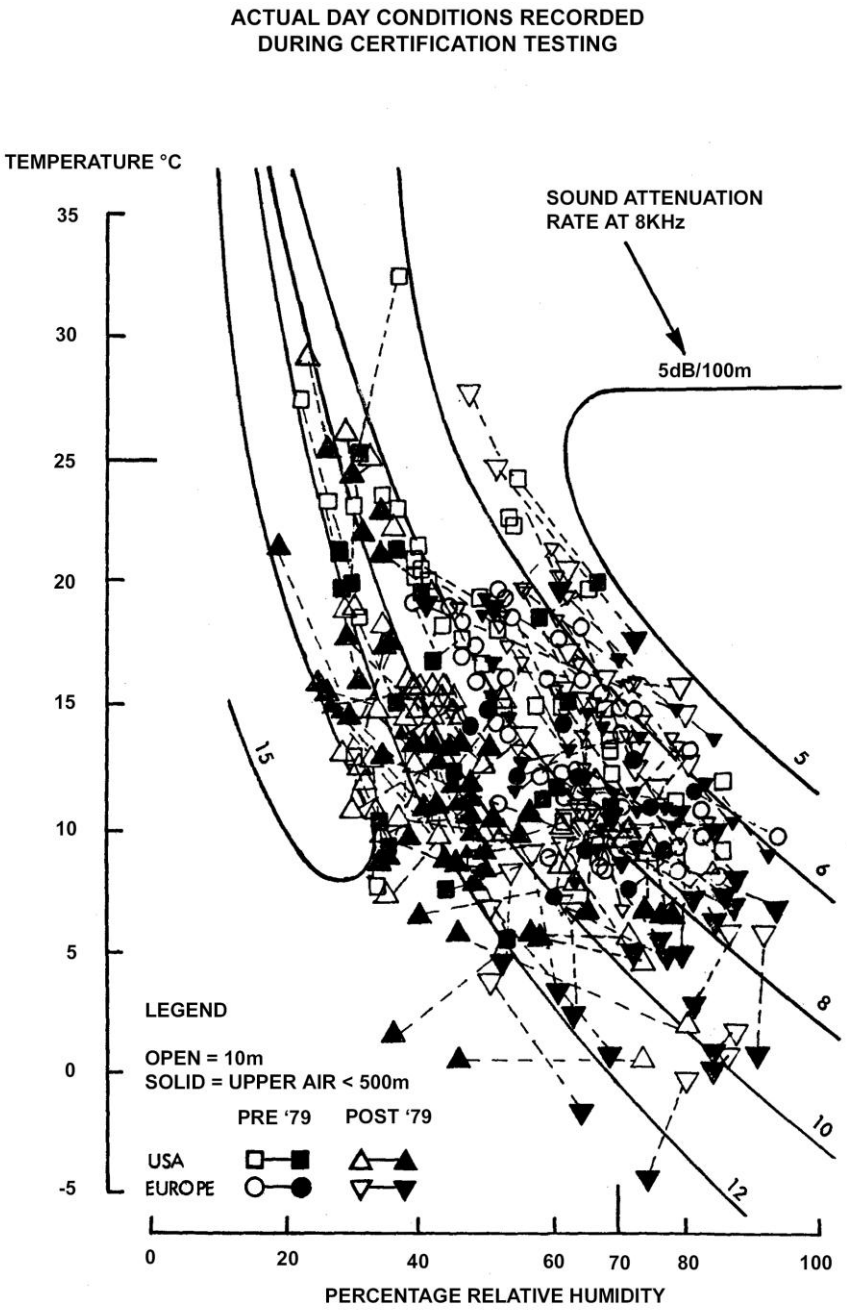

Figure D-1: Meteorological conditions recorded during noise certification tests

An atmospheric absorption adjustment accounts for changes in noise levels due to the atmospheric absorption for study or airport-specific atmospheric conditions that differ from the reference atmospheric conditions. The curves overlaid on **Figure D-1**, calculated using an industry standard atmospheric attenuation model SAE-ARP-866A [ref. 16], illustrate that across the test conditions a substantial variation of high frequency (8 kHz) sound absorption would be expected (although the variation of overall absorption would be rather less).

SAE-ARP-5534 [ref. 17] provides an updated methodology (2013) to calculate atmospheric absorption which is consistent with current scientific information, and is the recommended method. However, the flexibility is given for transition purposes to model non-standard atmospheric conditions with the legacy SAE-ARP-866A method (1975).

Because the attenuation rates [ref. 6], given in **Table D-1**, are arithmetic averages, the complete set cannot be associated with a single reference atmosphere (i.e. with specific values of temperature and relative humidity). They should be thought of as properties of a purely notional atmosphere - referred to as the 'AIR-1845 atmosphere'.

Table D-1: Average atmospheric attenuation rates used to normalise NPD data in the ANP database [ref. 6]

Centre frequency of 1/3-octave band [Hz]	Attenuation rate [dB/100 m]	Centre frequency of 1/3-octave band [Hz]	Attenuation rate [dB/100 m]
50	0.033	800	0.459
63	0.033	1 000	0.590
80	0.033	1 250	0.754
100	0.066	1 600	0.983
125	0.066	2 000	1.311
160	0.098	2 500	1.705
200	0.131	3 150	2.295
250	0.131	4 000	3.115
315	0.197	5 000	3.607
400	0.230	6 300	5.246
500	0.295	8 000	7.213
630	0.361	10 000	9.836

The attenuation coefficients in **Table D-1** may be assumed valid over reasonable ranges of temperature and humidity. However, to check whether adjustments may be necessary, SAE-ARP-5534 or SAE-ARP-866A should be used to calculate the atmospheric absorption for the specific airport temperature *T*, relative humidity RH and atmospheric pressure *p*. If a comparison of these attenuation rates with those in **Table D-1** indicates that adjustment is required, the following methodology should be used.

The ANP database provides the following NPD data for each power setting:

- maximum sound level versus slant distance, $L_{max}(d)$
- time integrated level versus distance for the reference airspeed, $L_E(d)$, and

- unweighted reference sound spectrum at a slant distance of 305 m (1000 ft), $L_{n,ref}(d_{ref})$ where n = frequency band (ranging from 1 to 24 for 1/3-octave bands with centre frequencies from 50 Hz to 10 kHz),

all data being normalised to the SAE-AIR-1845 atmosphere.

Adjustment of the NPD curves to specified conditions (temperature, pressure and relative humidity) is performed in three steps:

1. The reference spectrum is corrected to remove the SAE AIR-1845 atmospheric attenuation $\alpha_{n,ref}$:

$$L_n\left(d_{ref}\right) = L_{n,ref}\left(d_{ref}\right) + \alpha_{n,ref} \cdot d_{ref} \qquad \text{(D-1)}$$

   where $L_n(d_{ref})$ is the unattenuated spectrum at d_{ref} = 305 m and $\alpha_{n,ref}$ is the coefficient of atmospheric absorption for the frequency band n taken from **Table D-1** (but expressed in dB/m).

2. The corrected spectrum is adjusted to each of the ten standard NPD distances[33] d_i using attenuation rates for both (i) the SAE AIR-1845 atmosphere and (ii) the specified atmosphere (based on either SAE-ARP-5534 or SAE-ARP-866A).

   (i) For the SAE AIR-1845 atmosphere:

$$L_{n,ref}\left(d_i\right) = L_n\left(d_{ref}\right) - 20.lg(d_i / d_{ref}) - \alpha_{n,ref} \cdot d_i \qquad \text{(D-2)}$$

   (ii) For the specified atmosphere:

$$L_{n,atm}\left(T, p_a, h_{rel}, d_i\right) = L_n\left(d_{ref}\right) - 20 \cdot \log\left(\frac{d_i}{d_{ref}}\right) - \delta_n\left(T, p_a, h_{rel}\right) \cdot d_i \qquad \text{(D-3)}$$

   where $\delta_n(T, p_a, h_{rel})$ is the coefficient of atmospheric absorption for the frequency band n (expressed in dB/m) calculated using SAE ARP-5534 or SAE-ARP-866A with temperature T, atmospheric pressure p_a and relative humidity h_{rel}.

3. At each NPD distance d_i the two spectra are A-weighted and decibel-summed to determine the resulting A-weighted levels $L_{A,atm}$ and $L_{A,ref}$, which are then subtracted arithmetically:

$$\begin{aligned} \Delta L(T, p_a, h_{rel}, d_i) &= L_{A,atm}(T, p_a, h_{rel}, d_i) - L_{A,ref}(d_i) \\ &= 10 \cdot \lg \sum_{n=17}^{40} 10^{(L_{n,atm}(T, p_a, h_{rel}, d_i) - A_n)/10} - 10 \cdot \lg \sum_{n=17}^{40} 10^{(L_{n,ref}(d_i) - A_n)/10} \end{aligned} \qquad \text{(D-4)}$$

The increment $\Delta L(T,p_a,h_{rel},d_i)$ is the difference between the NPDs in the specified atmosphere and the reference atmosphere at the NPD distance d_i. This is added to the ANP database NPD data value to derive the adjusted NPD data.

Applying $\Delta L(T,p_a,h_{rel},d_i)$ to adjust both L_{max} and L_E NPDs effectively assumes that different atmospheric conditions affect the reference spectrum only and have no effect on the shape of the level time-history. This may be considered valid for typical propagation ranges and typical atmospheric conditions.

Example:

33. The NPD distances are 200, 400, 630, 1000, 2000, 4000, 6300, 10000, 16000 and 25000 ft.

The following is an example of the application of the NPD spectral adjustment: Adjust standard NPD data to the atmosphere 10 °C, 80% relative humidity and sea level atmospheric pressure using both the SAE-ARP-5534 and SAE-ARP-866A methodologies.

Using the SEL NPD data presented in **Appendix G** for the V2527A, the matching spectral classes in the ANP database are 103 and 205 for departure and arrival respectively. The spectra data are tabulated in **Table D-2**.

First the spectrum levels (which are referenced to 305 m (1000 ft)) are corrected back to the source to remove the SAE AIR-1845 atmosphere, ignoring spherical spreading effects. This is done using equation D-1. The corresponding spectra at source are also tabulated in **Table D-2**.

Table D-2: Spectra for V2527 NPD from ANP database and calculated source spectra

	At 1000 ft		At source	
Frequency (Hz)	**DEP_103 (dB)**	**ARR_205 (dB)**	**DEP_103 (dB)**	**ARR_205 (dB)**
50	56.7	68.3	56.8	68.4
63	66.1	60.7	66.2	60.8
80	70.1	64.6	70.2	64.7
100	72.8	67.4	73.0	67.6
125	76.6	78.4	76.8	78.6
160	73.0	74.8	73.3	75.1
200	74.5	71.4	74.9	71.8
250	77.0	72.4	77.4	72.8
315	75.3	72.0	75.9	72.6
400	72.2	72.4	72.9	73.1
500	72.2	71.6	73.1	72.5
630	71.2	72.0	72.3	73.1
800	70.2	71.0	71.6	72.4
1000	70.0	70.0	71.8	71.8
1250	69.6	68.9	71.9	71.2
1600	71.1	67.2	74.1	70.2
2000	70.6	65.8	74.6	69.8
2500	67.1	64.4	72.3	69.6
3150	63.4	63.0	70.4	70.0
4000	63.5	62.0	73.0	71.5
5000	58.2	60.6	69.2	71.6
6300	51.5	54.4	67.5	70.4
8000	42.3	48.5	64.3	70.5
10000	37.7	39.0	67.7	69.0

The source spectral data are then propagated out to the standard NPD data distances (200, 400, 630, 1000, 2000, 4000, 6300, 10000, 16000 and 25000 ft) using equations D-2 and D-3, together with the absorption coefficients in **Table D-1** for the AIR-1845 atmosphere and using absorption coefficients calculated using SAE-ARP-5534 and SAE-ARP-866A for the specified atmosphere: 10°C, 80% relative humidity and 101.325 kPa (sea level). All three sets of absorption coefficients are listed in **Table D-3**.

Table D-3: AIR-1845 absorption coefficients (from Table D-1) and coefficients for 10°C/80% relative humidity/101.325 kPa calculated using SAE-ARP-5534 and SAE-ARP-866A.

Frequency (Hz)	AIR-1845 Absorption (dB/100 m)	SAE-ARP-5534 10 °C/80% relative humidity/101.325 kPa (dB/100 m)	SAE-ARP-866A 10 °C/80% relative humidity (dB/100 m)
50	0.033	0.007	0.021
63	0.033	0.011	0.027
80	0.033	0.017	0.034
100	0.066	0.026	0.043
125	0.066	0.039	0.053
160	0.098	0.056	0.068
200	0.131	0.078	0.086
250	0.131	0.104	0.107
315	0.197	0.134	0.135
400	0.230	0.166	0.172
500	0.295	0.201	0.216
630	0.361	0.241	0.273
800	0.459	0.292	0.349
1000	0.590	0.364	0.439
1250	0.754	0.471	0.552
1600	0.983	0.636	0.738
2000	1.311	0.893	0.985
2500	1.705	1.297	1.322
3150	2.295	1.931	1.853
4000	3.115	2.922	2.682
4500	3.607	4.461	3.216
6300	5.246	6.826	4.580
8000	7.213	10.398	6.722
10000	9.836	15.661	9.774

At each NPD distance, the 1/3-octave band levels are A-weighted and decibel-summed to give the overall A-weighted level at each distance. This is repeated for both the departure spectrum (103) and the approach spectrum (205). For each NPD distance the A-weighted levels are then subtracted to give the increment, ΔL. The A-weighted levels and increments ΔL are shown in **Table D-4** for SAE-ARP-5534 and **Table D-5** for SAE-ARP-866A.

Table D-4: A-weighted levels for reference and SAE-ARP-5534 specified atmosphere and difference between each atmosphere, ΔL

Distance (ft)	DEP_103 $L_{A,ref}$ (dBA)	DEP_103 $L_{A,atm}$ (dBA)	DEP_103 ΔL (dB)	ARR_205 $L_{A,ref}$ (dBA)	ARR_205 $L_{A,atm}$ (dBA)	ARR_205 ΔL (dB)
200	97.0	97.1	+0.1	95.8	95.8	0.0
400	90.3	90.6	+0.3	88.9	89.1	+0.2
630	85.6	86.1	+0.4	84.2	84.6	+0.3
1000	80.6	81.3	+0.7	79.2	79.8	+0.6
2000	72.5	73.7	+1.2	71.3	72.4	+1.1
4000	63.6	65.4	+1.8	62.7	64.4	+1.7
6300	57.4	59.6	+2.1	56.4	58.6	+2.2
10000	50.7	53.2	+2.4	49.5	52.2	+2.7
16000	43.3	46.2	+2.9	41.8	45.0	+3.2
25000	35.3	38.9	+3.6	34.0	37.7	+3.7

Table D-5: A-weighted levels for reference and SAE-ARP-866A specified atmosphere and difference between each atmosphere, ΔL

Distance (ft)	DEP_103 $L_{A,ref}$ (dBA)	DEP_103 $L_{A,atm}$ (dBA)	DEP_103 ΔL (dB)	ARR_205 $L_{A,ref}$ (dBA)	ARR_205 $L_{A,atm}$ (dBA)	ARR_205 ΔL (dB)
200	97.0	97.2	0.2	95.8	95.9	+0.1
400	90.3	90.6	0.3	88.9	89.2	+0.3
630	85.6	86.0	0.4	84.2	84.6	+0.4
1000	80.6	81.2	0.6	79.2	79.8	+0.5
2000	72.5	73.4	0.9	71.3	72.2	+0.8
4000	63.6	64.9	1.3	62.7	63.9	+1.2
6300	57.4	59.0	1.5	56.4	58.0	+1.6
10000	50.7	52.5	1.8	49.5	51.4	+2.0
16000	43.3	45.5	2.2	41.8	44.1	+2.3
25000	35.3	38.2	2.8	34.0	36.7	+2.7

The departure and approach increments shown in **Table D-4** or **D-5** are then added to the departure and approach ANP database NPD noise levels (**Table D-6a**) to construct the revised

NPD data with SAE-ARP-5534 atmospheric absorption shown in **Table D-6b** or revised NPD data with SAE-ARP-866A atmospheric absorption shown in **Table D-6c**.

Table D-6a: Original NPD data

NPD Identifier	Noise Descriptor	Op Mode	Power Setting	L_200ft	L_400ft	L_630ft	L_1000ft	L_2000ft	L_4000ft	L_6300ft	L_10000ft	L_16000ft	L_25000ft
V2527A	SEL	A	2000	93.1	89.1	86.1	82.9	77.7	71.7	67.1	61.9	55.8	49.2
V2527A	SEL	A	2700	93.3	89.2	86.2	83.0	77.7	71.8	67.2	62.0	55.8	49.3
V2527A	SEL	A	6000	94.7	90.5	87.4	83.9	78.5	72.3	67.7	62.5	56.3	49.7
V2527A	SEL	D	10000	95.4	90.7	87.3	83.5	77.7	71.1	66.3	60.9	54.6	47.4
V2527A	SEL	D	14000	100.4	96.1	93.0	89.4	83.5	77.0	72.2	66.7	60.1	53.0
V2527A	SEL	D	18000	103.2	99.1	96.2	92.9	87.4	81.1	76.5	71.1	64.9	57.9
V2527A	SEL	D	22500	105.1	101.2	98.5	95.4	90.3	84.3	79.9	74.8	68.7	62.0

Table D-6b: Revised NPD data using SAE-ARP-5534

NPD Identifier	Noise Descriptor	Op Mode	Power Setting	L_200ft	L_400ft	L_630ft	L_1000ft	L_2000ft	L_4000ft	L_6300ft	L_10000ft	L_16000ft	L_25000ft
V2527A	SEL	A	2000	93.1	89.3	86.4	83.5	78.8	73.4	69.3	64.6	59.0	52.9
V2527A	SEL	A	2700	93.3	89.4	86.5	83.6	78.8	73.5	69.4	64.7	59.0	53.0
V2527A	SEL	A	6000	94.7	90.7	87.7	84.5	79.6	74.0	69.9	65.2	59.5	53.4
V2527A	SEL	D	10000	95.5	91.0	87.7	84.2	78.9	72.9	68.4	63.3	57.5	51.0
V2527A	SEL	D	14000	100.5	96.4	93.4	90.1	84.7	78.8	74.3	69.1	63.0	56.6
V2527A	SEL	D	18000	103.3	99.4	96.6	93.6	88.6	82.9	78.6	73.5	67.8	61.5
V2527A	SEL	D	22500	105.2	101.5	98.9	96.1	91.5	86.1	82.0	77.2	71.6	65.6

Table D-6c: Revised NPD data using SAE-ARP-866A

NPD Identifier	Noise Descriptor	Op Mode	Power Setting	L_200ft	L_400ft	L_630ft	L_1000ft	L_2000ft	L_4000ft	L_6300ft	L_10000ft	L_16000ft	L_25000ft
V2527A	SEL	A	2000	93.2	89.4	86.5	83.4	78.5	72.9	68.7	63.9	58.1	51.9
V2527A	SEL	A	2700	93.4	89.5	86.6	83.5	78.5	73.0	68.8	64.0	58.1	52.0
V2527A	SEL	A	6000	94.8	90.8	87.8	84.4	79.3	73.5	69.3	64.5	58.6	52.4
V2527A	SEL	D	10000	95.6	91.0	87.7	84.1	78.6	72.4	67.8	62.7	56.8	50.2
V2527A	SEL	D	14000	100.6	96.4	93.4	90.0	84.4	78.3	73.7	68.5	62.3	55.8
V2527A	SEL	D	18000	103.4	99.4	96.6	93.5	88.3	82.4	78.0	72.9	67.1	60.7
V2527A	SEL	D	22500	105.3	101.5	98.9	96.0	91.2	85.6	81.4	76.6	70.9	64.8

APPENDIX E: THE FINITE SEGMENT CORRECTION

This appendix outlines the derivation of the finite segment correction and the associated energy fraction algorithm described in **Section 4.5.6**.

E1 GEOMETRY

The energy fraction algorithm is based on the sound radiation of a 'fourth-power' 90-degree dipole sound source. This has directional characteristics which approximate those of jet aircraft sound, at least in the angular region that most influences sound event levels beneath and to the side of the aircraft flight path.

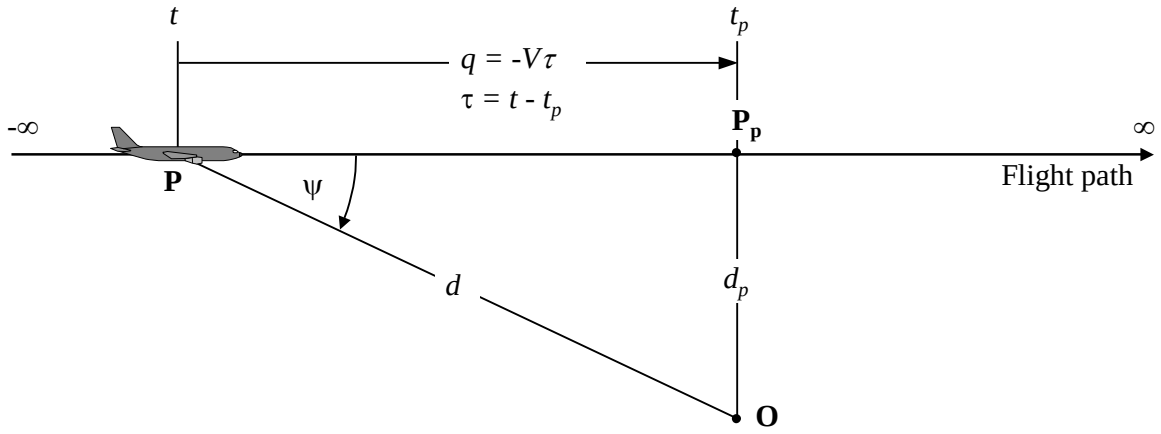

Figure E-1: Geometry between flight path and observer location O

Figure E-1 illustrates the geometry of sound propagation between the flight path and the observer location **O**. The aircraft at **P** is flying in still uniform air with a constant speed on a straight, level flight path. Its closest point of approach to the observer is $\mathbf{P_p}$. The parameters are:

d	distance from the observer to the aircraft
d_p	perpendicular distance from the observer to the flight path (slant distance)
q	distance from **P** to $\mathbf{P_p} = -V \cdot \tau$
V	speed of the aircraft
t	time at which the aircraft is at point **P**
t_p	time at which the aircraft is located at the point of closest approach $\mathbf{P_p}$
τ	flight time = time relative to time at $\mathbf{P_p}$ = $t - t_p$
ψ	angle between flight path and aircraft-observer vector

It should be noted that since the flight time τ relative to the point of closest approach is negative when the aircraft is before the observer position (as shown in **Figure E-1**), the relative distance q to the point of closest approach becomes positive in that case. If the aircraft is ahead of the observer, q becomes negative.

E2 ESTIMATION OF THE ENERGY FRACTION

The basic concept of the energy fraction is to express the noise exposure E produced at the observer position from a flight path segment $\mathbf{P_1P_2}$ (with a start-point $\mathbf{P_1}$ and an end-point $\mathbf{P_2}$) by multiplying the exposure E_∞ from the whole infinite path flyby by a simple factor – the *energy fraction* factor F:

$$E = F \cdot E_\infty \tag{E-1}$$

Since the exposure can be expressed in terms of the time-integral of the mean-square (weighted) sound pressure level, i.e.

$$E = const \cdot \int p^2(\tau) d\tau \tag{E-2}$$

to calculate E, the mean-square pressure has to be expressed as a function of the known geometric and operational parameters. For a 90° dipole source,

$$p^2 = p_p^2 \cdot \frac{d_p^2}{d^2} \cdot \sin^2 \psi = p_p^2 \cdot \frac{d_p^4}{d^4} \tag{E-3}$$

where p^2 and $p_p{}^2$ are the observed mean-square sound pressures produced by the aircraft as it passes points **P** and $\mathbf{P_p}$.

This relatively simple relationship has been found to provide a good simulation of jet aircraft noise, even though the real mechanisms involved are extremely complex. The term $d_p{}^2/d^2$ in equation E-3 describes just the mechanism of spherical spreading appropriate to a point source, an infinite sound speed and a uniform, non-dissipative atmosphere. All other physical effects - source directivity, finite sound speed, atmospheric absorption, Doppler-shift etc. - are implicitly covered by the $sin^2 \psi$ term. This factor causes the mean square pressure to decrease inversely as d^4; whence the expression "fourth power" source.

Introducing the substitutions:

$$d^2 = d_p^2 + q^2 = d_p^2 + (V \cdot \tau)^2 \qquad \text{and} \qquad \left(\frac{d}{d_p}\right)^2 = 1 + \left(\frac{V \cdot \tau}{d_p}\right)^2$$

the mean-square pressure can be expressed as a function of time (again disregarding sound propagation time):

$$p^2 = p_p^2 \cdot \left(1 + \left(\frac{V \cdot \tau}{d_p}\right)^2\right)^{-2} \tag{E-4}$$

Putting this into equation E-2 and performing the substitution

$$\alpha = \frac{V \cdot \tau}{d_p} \tag{E-5}$$

the sound exposure at the observer from the flypast between the time interval $[\tau_1, \tau_2]$ can be expressed as:

$$E = const \cdot p_p^2 \cdot \frac{d_p}{V} \cdot \int_{\alpha_1}^{\alpha_2} \frac{1}{(1+\alpha^2)^2} d\alpha \tag{E-6}$$

The solution of this integral is:

$$E = const \cdot p_p^2 \cdot \frac{d_p}{V} \cdot \frac{1}{2}\left(\frac{\alpha_2}{1+\alpha_2^2} + \arctan\alpha_2 - \frac{\alpha_1}{1+\alpha_1^2} - \arctan\alpha_1 \right) \qquad \text{(E-7)}$$

Integration over the interval [-∞,+∞] (i.e. over the whole infinite flight path) yields the following expression for the total exposure E_∞:

$$E_\infty = const \cdot \frac{\pi}{2} \cdot p_p^2 \cdot \frac{d_p}{V} \qquad \text{(E-8)}$$

and hence the energy fraction according to equation E-1 is:

$$F = \frac{1}{\pi}\left(\frac{\alpha_2}{1+\alpha_2^2} + \arctan\alpha_2 - \frac{\alpha_1}{1+\alpha_1^2} - \arctan\alpha_1 \right) \qquad \text{(E-9)}$$

E3 CONSISTENCY OF MAXIMUM AND TIME INTEGRATED METRICS – THE SCALED DISTANCE

A consequence of using the simple dipole model to define the energy fraction is that it implies a specific theoretical difference ΔL between the event noise levels L_{max} and L_E. If the contour model is to be internally consistent, this needs to equal the difference of the values determined from the NPD curves. A problem is that the NPD data are derived from actual aircraft noise measurements - which do not necessarily accord with the simple theory. The theory therefore needs an added element of flexibility. But in principle the variables α_1 and α_2 are determined by geometry and aircraft speed – thus leaving no further degrees of freedom. A solution is provided by the concept of a *scaled distance* d_λ as follows.

The exposure level $L_{E,\infty}$ as tabulated as a function of d_p in the ANP database for a reference speed V_{ref}, can be expressed as:

$$L_{E,\infty}\left(V_{ref}\right) = 10 \cdot \lg\left[\frac{\int_{-\infty}^{\infty} p^2.dt}{p_0^2 \cdot t_{ref}} \right] \qquad \text{(E-10)}$$

where p_0 is a standard reference pressure and t_{ref} is a reference time (= 1 s for SEL). For the actual speed V it becomes

$$L_{E,\infty}(V) = L_{E,\infty}\left(V_{ref}\right) + 10 \cdot \lg\left(\frac{V_{ref}}{V} \right) \qquad \text{(E-11)}$$

Similarly the maximum event level L_{max} can be written

$$L_{max} = 10 \cdot \lg\left[\frac{p_p^2}{p_0^2} \right] \qquad \text{(E-12)}$$

For the dipole source, using equations E-8, E-11 and E-12, noting that (from equations E-2 and E-8) $\int_{-\infty}^{\infty} p^2 \cdot dt = \frac{\pi}{2} \cdot p_p^2 \cdot \frac{d_p}{V}$, the difference ΔL can be written:

$$\Delta L = L_{E,\infty} - L_{max} = 10 \cdot \lg\left[\frac{V}{V_{ref}} \cdot \left(\frac{\pi}{2} p_p^2 \frac{d_p}{V}\right) \cdot \frac{1}{p_0^2 \cdot t_{ref}}\right] - 10 \cdot \lg\left[\frac{p_p^2}{p_0^2}\right] \qquad \text{(E-13)}$$

This can only be equated to the value of ΔL determined from the NPD data if the slant distance d_p used to calculate the energy fraction is substituted by a *scaled distance* d_λ given by

$$d_\lambda = \frac{2}{\pi} \cdot V_{ref} \cdot t_{ref} \cdot 10^{(L_{E,\infty} - L_{max})/10} \qquad \text{(E-14a)}$$

or

$$d_\lambda = d_0 \cdot 10^{(L_{E,\infty} - L_{max})/10} \quad \text{with} \quad d_0 = \frac{2}{\pi} \cdot V_{ref} \cdot t_{ref} \qquad \text{(E-14b)}$$

Replacing d_p by d_λ in equation E-5 and using the definition $q = V\tau$ from **Figure E-1** the parameters α_1 and α_2 in equation E-9 can be written (putting $q = q_1$ at the start-point and q–$\lambda = q_2$ at the endpoint of a flight path segment of length λ) as

$$\alpha_1 = \frac{-q_1}{d_\lambda} \quad \text{and} \quad \alpha_2 = \frac{-q_1 + \lambda}{d_\lambda} \qquad \text{(E-15)}$$

Having to replace the slant actual distance by scaled distance diminishes the simplicity of the fourth-power 90° dipole model. But as it is effectively calibrated *in situ* using data derived from measurements, the energy fraction algorithm can be regarded as semi-empirical rather than purely theoretical.

APPENDIX F: MAXIMUM LEVEL OF NOISE EVENTS

In **Chapter 5**, equation 5-9 introduces a step-function u(k) which determines whether the maximum level contribution from flight path segment k is the maximum level of a noise event or not:

$$\mathrm{u}(k) = \begin{Bmatrix} 0 \\ 1 \end{Bmatrix} \quad \text{if} \quad L_{max,k} \begin{Bmatrix} \text{is not} \\ \text{is} \end{Bmatrix} \text{the maximum level of a noise event}$$

In **Figure F-1** a flow-diagram shows the steps by which this function can be estimated for each aircraft type and ground track (or subtrack).

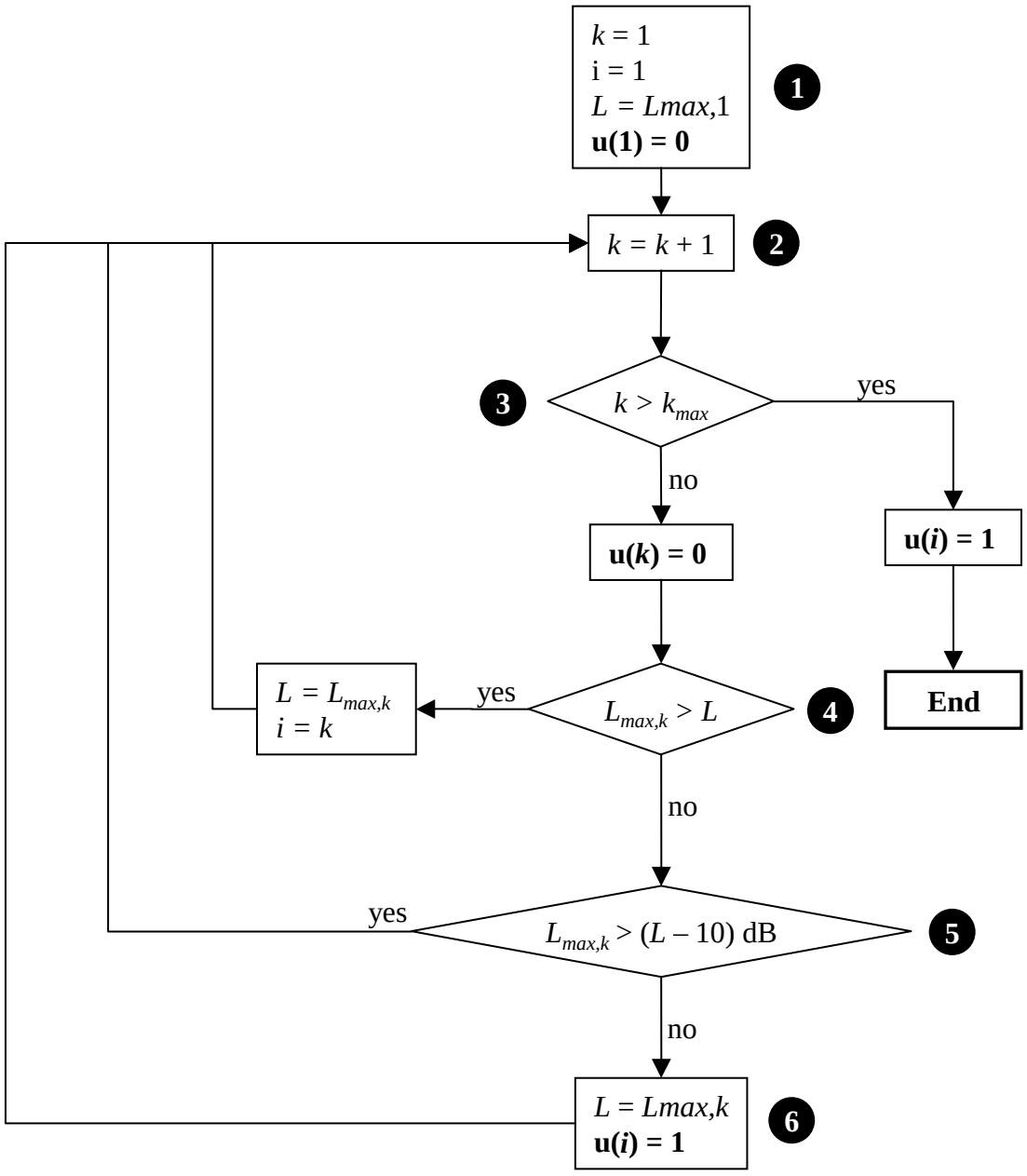

Figure F-1: Flow-diagram for the estimation of the function u(*k*)

The procedure uses four variables:

k is the number of the current track (or subtrack) segment.

$L_{max,k}$ is the maximum level from the current track (or subtrack) segment.

L is the maximum level of the actual noise event.

i is a pointer to the segment which produces the maximum level L.

❶ Initialise the variables: set the subtrack counter k to one, set the pointer i to the actual maximum event level to one and set the variable L representing the maximum level of the actual noise event to $L_{max,1}$. This means that the maximum level of the first track segment is to be assumed the maximum level of the first noise event. Additionally initialise the variable u(1) with zero.

❷ Perform a loop over all segments of the actual ground (sub)track increasing the segment number by one.

❸ If the last segment is processed, leave the loop. Set the variable u(i) for the last marked maximum level to one. If the current segment is not the last one, set the variable u(k) for this segment to zero (i.e. initialise it).

❹ Check if the maximum level $L_{max,k}$ from the actual segment is higher than the maximum level L of the current noise event. If so, set $L = L_{max,k}$ and set the marker i to the current segment number ($i = k$). Then branch to the next segment (i.e. to step❷).

❺ Estimate the difference between the maximum level L of the current noise event and the maximum level of the current segment. If it is less than 10 dB, the event is not yet finished - branch to step ❷.

❻ The actual noise event is finished. Start a new new event by setting the maximum level of this new event to $L = L_{max,k}$ and set the counter $i = k$. This is similar to step ❶.

Steps ❺ and ❻ are not necessary if only the highest maximum level produced by the actual aircraft type on the actual (sub)track has to be estimated. In this case branch directly from step ❹ to step ❷.

APPENDIX G: THE INTERNATIONAL AIRCRAFT NOISE AND PERFORMANCE (ANP) DATABASE

G1 INTRODUCTION

To support the development of accurate aircraft noise contour models that meet present and future requirements of ECAC and other organisations engaged in international harmonisation, an on-line aircraft noise and performance (ANP) database has been established, accessible at www.aircraftnoisemodel.org.

Data sources

The data accord with specifications and formats laid down by the international Society of Automotive Engineers (SAE) in AIR 1845 [ref. 6] and endorsed by ECAC, that are designed to achieve best practicable levels of data quality and consistency. By preference, entries are supplied by the aircraft manufacturers and these cover most of the larger, modern aircraft models and variants in the world's airline fleets and that therefore govern the noise at most major airports. Those entries usually include noise data acquired during noise certification tests carried out under stringent internationally standardised procedures that are regulated by national or international certification agencies. Data for some other aircraft, mainly those of less general noise significance, have been obtained from other sources, principally controlled tests, similar to those of certification, undertaken by national noise modelling agencies in various countries.

An ANP data submittal form is available via the above website which sets out the data requirements for new aircraft entries in the ANP database. Separate forms are provided for turbofan and propeller-driven fixed-wing aircraft due to the differences in some performance parameters.

Aircraft coverage and substitutions

With respect to aircraft entries, the ANP database is identical to that of the INM/AEDT database [ref. 7], excluding at present only data that are not required by ECAC; i.e., currently data for military aircraft and helicopters.

Users will represent 'in-service' aeroplanes, i.e. airframe/engine combinations, by equivalent ones designated in the ANP database. Aircraft models and variants that are not covered by the ANP database have to be represented by substitutes (often referred to as 'proxy' aircraft) - aircraft with similar noise and performance characteristics that are included in the ANP database, and that can be adequately scaled (through the use of either adjusted NPD noise data or 'adjusted number of movements') to represent the missing aircraft.

To facilitate the work of aircraft noise modellers, the ANP database website includes a Substitutions table providing a list of suggested aircraft substitutions which was derived in line with the substitution method described in **Volume 1** - section 6.4.4 - of this ECAC guidance (ref. 4). A detailed description of the Substitutions table content is provided in Section G5.

The database continues to be expanded so that the need for substitution can be reduced over time. Users who consider that their modelling work is compromised by a lack of coverage are urged to communicate their needs to the managers, via the website.

Data scrutiny

With each update the database developers check entries for consistency and reasonableness as resources allow. However, inconsistencies and deficiencies may be discovered by users in their model applications. Users may report these to the ANP database managers.

Terms and conditions for accessing the database

Users have to be registered to access the database (the website includes an online registration form for new users). Use of data is subject to terms and conditions so that any misuse can be clearly identified.

Database content

The ANP data meet in full the requirements of the ECAC contour modelling methodology. The content of the database and the procedures for downloading the data from the ANP website are described below. The data are provided in a near 'ready-to-use' format; it is only necessary for the software developer to match the model parameters and variables to those of the data.

The database includes several tables of data that are described in the following sections, as they are at the time of publication of this guidance. The content and format of these tables are likely to evolve with time, depending on the needs of the aviation community.

Users are cautioned that quantities, dimensions and units are those generally used by the data suppliers; modellers must be especially careful to ensure that, where necessary, appropriate conversions are applied at the point of use.

G2 AIRCRAFT TABLE

This tabulates the aircraft represented along with descriptive parameters. Some parameters are required for noise modelling purposes whilst others are for general information only, enabling the user to further classify the aircraft according to selected criteria (e.g. source of the data, weight categories, noise certification status, etc.), and to assist with establishing aircraft substitutions.

The different fields/parameters of the Aircraft Table are listed below. Parameters that are required inputs to the noise contour model are underlined.

- ACFT_ID: the ANP aircraft identifier which labels the associated performance data and by which it is accessed.
- Description of the aircraft: manufacturer, airframe, engine, etc.
- Engine Type: Jet, Turboprop or Piston.
- Number of Engines: used in various equations of **Appendix B**.
- Weight Class: Small, Large or Heavy.
- Owner Category: Commercial or General Aviation.
- Maximum Gross Takeoff Weight (lb): used to calculate reduced takeoff thrust (see **Appendix B**).
- Maximum Gross Landing Weight (lb): default approach profiles are usually provided for 90% of MGLW.
- Maximum Landing Distance (ft)

- Maximum Sea Level Static Thrust (lb): provided for standard day conditions.
- Noise Chapter (Noise certification standard)
- NPD ID: identifier associating the aircraft (ACFT_ID) with a set of NPD data, stored in the NPD table. (As NPDs tend to be powerplant-related, similar aircraft types may be assigned the same set of NPD data.)
- Power Parameter: indicates which noise-related power parameter is used to access the NPD data (corrected net thrust, shaft horsepower, etc.) and the associated unit (pounds, percent, other).
- Approach and Departure Spectral Class IDs: identifiers associating the aircraft (ACFT_ID) with reference sound spectral shapes, one for approach and one for departure, stored in the Spectral Classes table.
- Lateral Directivity Identifier: Fuselage-mounted, Wing-mounted or Prop. Indicates the engine installation correction to be applied – see **Section 4.5.3**.
- Lateral Level (EPNdB)
- Flyover Level (EPNdB)
- Approach Level (EPNdB)
- Overflight Level (dBA)
- Takeoff Level (dBA)
- Noise Certification Data Source
- The six last fields provide the certified noise levels of each ANP aircraft type. These are required to apply the substitution method described in **Volume 1** - section 6.4.4 - of this ECAC guidance (ref [4]).

G3 AIRCRAFT PERFORMANCE TABLES

These provide the engine and aerodynamic data required to implement the performance equations presented in **Appendix B**. These data (coefficients) may not be available for all the aircraft of the database. For aircraft with missing coefficients, or for specific flight procedures which cannot be well-modelled using the methodology described in **Appendix B**, the database includes a supplementary table providing default fixed-point profiles – a set of height, speed and thrust values as a function of ground distance.

Additionally, the database includes a table providing, for each aircraft, default takeoff weight values as a function of trip length.

G3.1 Reference conditions for performance data

The performance data (engine coefficients) are provided by manufacturers for the following reference conditions:

Atmosphere:	International Standard Atmosphere (ISA) [ref. 1]
Surface Air Temperature:	15 °C (59 °F)

Wind:	4 m/s (8 kt) headwind, constant with height above ground
Runway elevation:	Mean Sea Level (MSL)
Runway gradient:	None
Number of engines supplying thrust:	All

However, the engine coefficients, along with the thrust equations described in **Appendix B**, may also be used for aerodrome conditions other than 15°C, sea level (temperatures up to 43 °C (109 °F) and airport elevations up to 6000 feet above sea level). The database includes high temperature jet coefficients enabling thrust calculations above temperature breakpoint.

G3.2 Jet engine coefficients table

This table provides, for each aircraft and for different rated thrusts, the jet coefficients E, F, G_A, G_B and H for use with thrust equation B-1 of **Appendix B**. The thrust ratings encompass MaxTakeoff, MaxClimb, and IdleApproach (the last one being used for approach procedures - see equation B-23). Some aircraft may also feature jet coefficients for thrust calculation above the temperature breakpoint (the corresponding thrust rating label includes a 'HiTemp' suffix – ex: 'MaxTakeoffHiTemp').

Additionally, the table may provide (depending on the aircraft) a set of general jet coefficients (labelled 'General') enabling the calculation of non-rated thrust as a function of either EPR or N1, using equations B-2 and B-3 of **Appendix B**. These general jet coefficients include in particular the additional coefficients K_1 to K_4.

The table contains the following fields (each field representing a column):

- ACFT_ID
- Thrust Rating: see above
- *E* (lbf)
- *F* (lbf/kt)
- G_A (lbf/ft)
- G_B (lbf/ft^2)
- *H* (lbf/ °C)
- K_1 (lbf/EPR)
- K_2 (lbf/EPR^2)
- K_3 (lbf/(N1/$\sqrt{\theta}$))
- K_4 (lbf/(N1/$\sqrt{\theta}$)^2)

Note: Rated thrust coefficients are provided for at least MaxTakeoff and MaxClimb thrust ratings. The general thrust K-coefficients are provided either for EPR ($K_{1,2}$) or N1 ($K_{3,4}$), depending on the aircraft/engine.

G3.3 Propeller engine coefficients table

This provides propeller efficiency and installed net propulsive power data for the calculation of corrected net thrust for propeller-driven aeroplanes (**Appendix B**, equation B-5). The data are usually provided for two thrust ratings: MaxTakeoff and MaxClimb.

The table contains the following fields (each field representing a column):

- ACFT_ID
- Thrust rating: MaxTakeoff or MaxClimb
- η: Propeller Efficiency
- P_p (hp): Installed Net Propulsive Power

G3.4 Aerodynamic coefficients table

This table provides, for each aircraft, the aerodynamic coefficients B_8, C/D and R (see **Appendix B**, equations B-9, B-12, B-15 and B-24) associated with different flap settings on arrival and departure. The number of flap settings and the flap identifiers are aircraft-specific. The flap settings for which aerodynamic data are available normally cover the complete sequence used by aeroplanes under operational conditions (from clean configuration to full landing configuration/gear down during approach for instance). The flap identifiers include – where necessary - an indication on gear position (up or down).

The table contains the following fields (each field representing a column):

- ACFT_ID
- Op Type: Arrival (A) or Departure (D)
- Flap_ID: flap setting identifier (including gear position information where necessary)
- B_8 (ft/lb)
- C (for initial climb speed calculation) (kt/√lb)
- D (for landing speed calculation) (kt/√lb)
- R

Note: Coefficient B_8 is provided only for flap settings usable during takeoff.

G3.5 Default weights table

This provides, for each aircraft, suggested default takeoff weights assigned to different trip- (or stage-) length ranges. These are for use when the operational takeoff weights at the studied airport are unknown. The trip length stages are defined as follows:

Stage Length	**1**	**2**	**3**	**4**	**5**	**6**	**7**	**8**	**9**
Trip Length Range (nm x 1000)	0-0.5	0.5-1	1-1.5	1.5-2.5	2.5-3.5	3.5-4.5	4.5-5.5	5.5-6.5	> 6.5
Representative Range (nm)	350	850	1350	2200	3200	4200	5200	6200	
Takeoff Weight (lb)									

The Representative Range, for which the takeoff weight is calculated, is defined as follows:

Representative Range = Min Range + 0.70*(Max Range – Min Range)

The assumptions made to arrive at the default takeoff weights associated with each of the above representative ranges may depend on the aircraft category and/or weight class. Additional information may be found in the ANP data submittal form, available on the ANP database website.

The default weights table contains the following fields (each field representing a column):

- ACFT_ID
- Stage Length
- Weight (lb)

G3.6 Default departure procedural steps table

This table provides a description of default departure procedures (i.e. description of successive steps, as flown by the crew). It includes all the required parameters which, combined with data from the performance tables, allow calculation of the resulting flight profiles (altitude, speed and thrust as a function of ground distance) using equations described in **Appendix B**.

The table contains the following fields (each field representing a column):

- ACFT_ID
- Profile_ID: name of the procedure (ex: 'ICAO_A')
- Stage Length: used to obtain the takeoff weight information from the Default Weights table
- Step Number
- Step Type: Takeoff, Climb or Accelerate
- Thrust Rating: MaxTakeoff, MaxClimb, other
- Flap_ID: flap settings used on each step
- End Point Altitude (ft): altitude to be reached at the end of the segment
- Rate of Climb (ft/min)
- End Point CAS (kt): calibrated airspeed to be reached at the end of the segment

Note: Each of the last three parameters may be assigned a value or not (field 'empty'), depending on the step type that is flown (example: a rate of climb value is provided only for an acceleration step, the field being empty for the other step types).

G3.7 Default approach procedural steps table

This table, in a similar way as the previous one, provides a description of default approach procedures, using step-by-step flight instructions. ANP aircraft types have in general a single default procedure. The approach procedure of this table have mostly been supplied by aircraft manufacturers assuming a landing weight of 90% of the Maximum Gross Landing Weight, but their use may be generalized to other user-defined landing weights.

The table contains the following fields (each field representing a column):

- ACFT_ID
- Profile_ID
- Step Number
- Step Type: Descend, Descend-Idle, Level, etc.
- Flap_ID

- Start Altitude(ft)
- Start CAS (kt)
- Descent Angle (deg)
- Touchdown Roll (ft)
- Distance (ft)
- Start Thrust (% Max thrust)

The last three parameters are used to model the runway rolling portion of the procedure.

G3.8 Default fixed-points profiles table

This table provides default fixed-point profiles for aircraft, for which the required performance data to calculate flight profiles based on the methodology described in **Appendix B** are unavailable. This will progressively be phased out (in favour of the procedural profiles) as soon as the aircraft performance data which are required for a full implementation of **Appendix B** become available.

The table contains the following fields (each field representing a column in the table):

- ACFT_ID
- Operation type: Arrival (A) or Departure (D)
- Profile ID
- Stage Length
- Point Number
- Distance (ft)
- Height above field elevation (ft)
- Speed TAS (kt)
- Corrected Net Thrust (lbf)

Note: Some tables have all the coefficients required to calculate departure profiles but no aerodynamic coefficients enabling the calculation of approach profiles. For these aircraft, default fixed-point profiles are provided for approach only.

G4 AIRCRAFT NOISE TABLES

These provide the acoustic data required to calculate the single event noise as described in **Chapter 4**. For each aircraft, there are two sets of data: (1) a Noise-Power-Distance (NPD) table and (2) two Spectral Classes - reference sound spectra (used to adjust NPDs for non-reference atmospheric conditions).

G4.1 NPD table

This table provides, for each aircraft type (through its NPD identifier) and a number of values of the noise-related power parameter (mostly corrected net thrust values), a set of noise event levels at a number of slant distances. Several similar aircraft may be assigned the same NPD data set.

The noise event levels are given for various single event noise metrics, including at least L_{Amax} and SEL, at ten slant distances: 200, 400, 630, 1000, 2000, 4000, 6300, 10000, 16000, and 25000 feet.

The power settings span normal operating values, both for approach and departures, in order to avoid the need for large modelling extrapolations. NPD data are distinguished by operating mode (approach or departure) as, due to airframe effects, noise depends on flight configuration as well as power setting.

Each table entry (row) contains the following (each parameter representing a column):

- NPD_ID
- Noise Metric: maximum or exposure-based metric
- Operating Mode : 'A' or 'D'
- Noise-related power parameter value
- L_n noise levels at distances d_n for n = 1 to 10

G4.2 Reference conditions for NPD data

NPD data are normalized for the following conditions:

- Atmospheric pressure: 101.325 kPa (1013.25 mb)
- Atmospheric absorption: attenuation rates listed in **Table D-1** of **Appendix D**
- Precipitation: none
- Windspeed: less than 8 m/s (15 kt)
- Reference Speed (for exposure-based metrics): 160 knots

G4.3 Spectral classes table

For each of a number of specified spectral classes, this provides a set of reference sound spectra: these represent average noise spectra for groups of aircraft that have similar spectral characteristics.

The spectral classes represent average spectral shapes at the time of maximum sound level, at a reference distance of 1000 ft, and for the same reference conditions of air temperature and humidity as the NPDs. They are unweighted (unlike NPDs) and, for historical reasons, normalized to 70 dB at 1000 Hz. Sound levels are provided for 24 one-third octave bands, with nominal centre-frequencies from 50 to 10000 Hz.

A detailed description of the method used to develop spectral class data can be found on the website.

The table provides separate spectral shapes for approach and departure conditions. Thus a given aircraft is assigned two spectral classes (through its two spectral class identifiers).

This table contains the following fields (each field representing a column in the table):

- Spectral Class ID
- Operation type: 'A' or 'D'
- Description: general characteristics of the aircraft family that is assigned this spectral shape
- 24 relative one-third octave band sound levels for the centre-frequencies from 50 to 10000 Hz.

G5 SUBSTITUTIONS TABLE

The Substitutions table available on the ANP database website gives a recommended proxy and corresponding decibel and movement adjustments (Δ, N) for a large set of aircraft types,

including multiple engine and MTOW variants. Airframe and engines are designated using the terminology in the aircraft type certificates. In principle, all variants of the same type are assigned the same proxy recommendation, unless the ANP database already includes multiple variants. The variants are therefore provided to refine the decibel and movement adjustments when the MTOW or engine variant of the missing aircraft is known. When the variant to be modelled is unknown, e.g. when only the aircraft ICAO code or airframe is available, modellers wishing to apply decibel or movement adjustments may either select the largest value of Δ or N across all variants (conservative approach) or take the average of the values. Modellers who cannot find a proxy recommendation for certain of their missing aircraft types in the Substitutions table are encouraged to contact the ANP database managers via the ANP website so that the table can be updated in a next release.

The Substitution table contains the following fields (each field representing a column):

- ICAO Code
- Aircraft Manufacturer
- Airframe Type: Aircraft type designation as in the aircraft type certificate
- Engine Manufacturer
- Engine Type: Engine type designation as in the aircraft type certificate
- Other Information: may include - for instance - propeller type designation as in the aircraft type certificate in the case of turboprop aircraft
- Number of engines
- MTOW (kg): Maximum Takeoff Weight
- MLW (kg): Maximum Landing Weight
- Noise Chapter: Noise certification category according to the ICAO Annex 16 Volume 1
- Lateral Level (EPNdB): Certified noise level on the lateral certification point
- Flyover Level (EPNdB): Certified noise level on the flyover certification point
- Approach Level (EPNdB): Certified noise level on the approach certification point
- Overflight Level (dBA): Certified noise level under overflight conditions for Chapter 6 aircraft
- Takeoff Level (dBA): Certified noise level under takeoff conditions for Chapter 10 aircraft
- ANP proxy: ANP proxy aircraft (i.e. ACFT_ID in the ANP Aircraft table)
- Δdep (dB): Noise adjustment to be applied to the departure NPD data of the ANP proxy aircraft
- Δarr (dB): Noise adjustment to be applied to the approach NPD data of the ANP proxy aircraft
- Ndep: Movement adjustment factor to be applied to departure operations of the aircraft to be substituted
- Narr: Movement adjustment factor to be applied to arrival operations of the aircraft to be substituted

G6 HOW TO DOWNLOAD THE DATA

Registered users may download the following aircraft noise and performance data from the website:

- the whole database
- noise and performance tables related to one or several specific aircraft types

- a specific table

The downloaded data are provided in CSV files, with one file per table.

Additionally, registered users are automatically informed (by e-mail) of any update to the database (e.g. new entries).

G7 EXAMPLE DATA

Table G-1: Example aircraft table

ACFT_ID	Description	Source of data	Engine Type	Number of Engines	Weight Class	Owner Category	Max Gross Takeoff Weight (lb)	Max Gross Landing Weight (lb)
737300	Boeing B737-300/CFM56-3B-1 Engines	Manufacturer	Jet	2	Large	Commercial	135000	114000
A320-232	Airbus A320-232 / V2527-A5 Engines	Manufacturer	Jet	2	Large	Commercial	169756	145505
SF340	Saab SF340B/CT7-9B Engines	Manufacturer	Turbo Prop	2	Large	Commercial	27300	26500

Table G-1 (continued)

ACFT_ID	Max Landing Distance (ft)	Maximum Sea Level Static Thrust (lb)	Noise Chapter	NPD Identifier	Power Parameter	App Spectral Class Identifier	Dep Spectral Class Identifier	Lateral Directivity Identifier
737300	4580	20000	3	CFM563	CNT (lb)	202	102	Wing
A32023	4704	26500	3	V2527A	CNT (lb)	205	103	Wing
SF340	3470	4067	3	CT75	CNT (% of Max Static Thrust)	211	110	Prop

Table G-1 (continued)

ACFT_ID	Lateral Level (EPNdB)	Flyover Level (EPNdB)	Approach Level (EPNdB)	Overflight Level (dBA)	Takeoff Level (dBA)	Noise Certification Data Source
737300	90.2	86.5	99.9	-	-	EASA TCDSN Jets Issue 23 (A4142)
A320-232	91.3	84.6	94.4	-	-	EASA TCDSN Jets Issue 23 (A604)
SF340	85.5	77.6	93.0	-	-	EASA TCDSN Heavy Props Issue 21 (B18)

Table G-2: Example jet engine coefficients table

ACFT_ID	Thrust Rating	E (lb)	F (lb/kt)	Ga (lb/ft)	Gb (lb/ft^2)	H (lb/ °C)	K1 (lb/EPR)	K2 (lb/EPR^2)	K3 ($lb/(N1/\sqrt{\theta})$)	K4 ($lb/(N1/\sqrt{\theta})^2$)
737300	MaxClimb	17383.1	-15.61	0.148043	-1.0E-06	-24.2000				
737300	MaxTakeoff	19347.0	-25.87	0.456499	-1.12E-05	-14.7800				
737300	General	11106.0	-10.09000	-4.09000e-02	0.00000e+00	0.000e+00			-3.69800e+02	+4.83500e+00
A320-232	IdleApproach	1138.9	-6.53000	0.166700	-9.2579E-06					
A320-232	MaxClimb	15539.2	-4.09000	0.438331	-1.439E-05	0.000e+00				
A320-232	MaxTakeoff	24746.2	-25.25000	0.304165	9.2451E-06	0.000e+00				
A320-232	General	-65083.3	-7.25000	-1.91800e-02	2.57500e-08	0.000e+00	8.78176e+04	-1.86931e+04		

Table G-3: Example propeller engine coefficients table

ACFT_ID	Thrust Rating	Propeller Efficiency	Installed Net Propulsive Power (hp)
SF340	MaxClimb	0.90	1587.0
SF340	MaxTakeoff	0.90	1763.0

Table G-4: Example aerodynamic coefficients table

ACFT_ID	Op Type	Flap Identifier	B (ft/lb)	C/D (kt/√lb)	R
737300	A	D-15	-	0.463900	0.110300
737300	A	D-30	-	0.434000	0.124700
737300	A	D-40	-	0.421500	0.147100
737300	D	1	0.012600	0.495800	0.076100
737300	D	15	0.011100	0.457200	0.087200
737300	D	5	0.012000	0.477200	0.079100
737300	D	ZERO	-	-	0.062000
A32023	D	1	-	-	0.061500
A32023	D	1+F	0.007858	0.398300	0.072500
A32023	D	ZERO	0.000000	0.000000	0.053900

Table G-5: Example default weights table

ACFT_ID	Stage Length	Weight (lb)
737300	1	96000
737300	2	102000
737300	3	108000
737300	4	119000
A32023	1	135700
A32023	2	141600
A32023	3	147700
A32023	4	158600
A32023	5	162000

Table G-6: Example default departure procedural steps table

ACFT_ID	Profile ID	Stage Length	STEP_NUM	STEP_TYPE	FLAP_ID	THR_RATING	End Point Altitude (ft)	Rate of Climb (ft/min)	End Point CAS (kt)
A32023	ICAO_A	1	1	TakeOff	1+F	MaxTakeoff			
A32023	ICAO_A	1	2	Climb	1+F	MaxTakeoff	300.0		
A32023	ICAO_A	1	3	Climb	1+F	MaxTakeoff	1500.0		
A32023	ICAO_A	1	4	Climb	1+F	MaxClimb	3000.0		
A32023	ICAO_A	1	5	Accelerate	1+F	MaxClimb		751.0	187.3
A32023	ICAO_A	1	6	Accelerate	1	MaxClimb		890.0	201.6
A32023	ICAO_A	1	7	Accelerate	ZERO	MaxClimb		1041.0	226.9
A32023	ICAO_A	1	8	Accelerate	ZERO	MaxClimb		1191.0	250.0
A32023	ICAO_A	1	9	Climb	ZERO	MaxClimb	5500.0		
A32023	ICAO_A	1	10	Climb	ZERO	MaxClimb	7500.0		
A32023	ICAO_A	1	11	Climb	ZERO	MaxClimb	10000.0		
737300	STANDARD	4	1	TakeOff	5	MaxTakeoff			
737300	STANDARD	4	2	Climb	5	MaxTakeoff	1000.0		
737300	STANDARD	4	3	Accelerate	5	MaxTakeoff		1544.0	185.0
737300	STANDARD	4	4	Accelerate	1	MaxTakeoff		1544.0	190.0
737300	STANDARD	4	5	Accelerate	ZERO	MaxClimb		1000.0	220.0
737300	STANDARD	4	6	Climb	ZERO	MaxClimb	3000.0		
737300	STANDARD	4	7	Accelerate	ZERO	MaxClimb		1000.0	250.0
737300	STANDARD	4	8	Climb	ZERO	MaxClimb	5500.0		
737300	STANDARD	4	9	Climb	ZERO	MaxClimb	7500.0		
737300	STANDARD	4	10	Climb	ZERO	MaxClimb	10000.0		

Table G-7: Example default approach procedural steps table

ACFT_ID	Profile_ID	Step Number	Step Type	Flap_ID	Start Altitude(ft)	Start CAS (kt)	Descent Angle (deg)	Touchdown Roll (ft)	Distance (ft)	Start Thrust (% Max thrust)
A320-232	DEFAULT	1	Descend-Idle		6000.0	250.0	2.8			
A320-232	DEFAULT	2	Level-Idle		3000.0	250.0			20003.3	
A320-232	DEFAULT	3	Level-Idle		3000.0	198.7			4629.3	
A320-232	DEFAULT	4	Descend-Idle		3000.0	183.5	3.0			
A320-232	DEFAULT	5	Descend-Idle		2613.0	172.8	3.0			
A320-232	DEFAULT	6	Descend-Idle		2033.0	142.2	3.0			
A320-232	DEFAULT	7	Descend	FULL_D	1819.0	133.8	3.0			
A320-232	DEFAULT	8	Descend	FULL_D	50.0	133.8	3.0			
A320-232	DEFAULT	9	Land	FULL_D				311.0		
A320-232	DEFAULT	10	Decelerate			130.8			2799.4	40.0
A320-232	DEFAULT	11	Decelerate			30.0			0	10.0

Table G-8: Example default fixed-points profiles table

ACFT_ID	Op Type	Profile ID	Stage Length	Point Number	Distance (ft)	Altitude (ft)	TAS (kt)	Corrected Net Thrust (lb)
A32023	A	STANDARD	1	1	-162381.0	6000.0	272.3	1091.30
A32023	A	STANDARD	1	2	-112299.0	4009.0	264.7	912.70
A32023	A	STANDARD	1	3	-87765.0	3000.0	260.9	802.70
A32023	A	STANDARD	1	4	-61823.0	3000.0	204.6	456.50
A32023	A	STANDARD	1	5	-57240.0	3000.0	190.7	362.50
A32023	A	STANDARD	1	6	-54773.0	2871.0	189.8	358.20
A32023	A	STANDARD	1	7	-51725.0	2711.0	187.5	351.20
A32023	A	STANDARD	1	8	-47460.0	2487.0	177.7	391.40
A32023	A	STANDARD	1	9	-36430.0	1909.0	144.6	654.20
A32023	A	STANDARD	1	10	-35298.0	1850.0	139.6	708.10
A32023	A	STANDARD	1	11	-33710.0	1767.0	130.9	817.50
A32023	A	STANDARD	1	12	-33503.0	1756.0	130.9	4888.50
A32023	A	STANDARD	1	13	-19077.0	1000.0	129.5	4753.10
A32023	A	STANDARD	1	14	-1794.0	94.0	127.8	4598.30
A32023	A	STANDARD	1	15	-954.0	50.0	127.7	4570.80
A32023	A	STANDARD	1	16	0.0	0.0	126.7	4570.80
A32023	A	STANDARD	1	17	470.0	0.0	119.7	15900.00
A32023	A	STANDARD	1	18	4704.0	0.0	30.0	2650.00

Table G-9: Example NPD table

NPD Identifier	Noise Descriptor	Op Mode	Power Setting	L _200ft	L_400ft	L_630ft	L_1000ft	L_2000ft	L_4000ft	L_6300ft	L_10000ft	L_16000ft	L_25000ft
V2527A	SEL	A	2000.00	93.1	89.1	86.1	82.9	77.7	71.7	67.1	61.9	55.8	49.2
V2527A	SEL	A	2700.00	93.3	89.2	86.2	83.0	77.7	71.8	67.2	62.0	55.8	49.3
V2527A	SEL	A	6000.00	94.7	90.5	87.4	83.9	78.5	72.3	67.7	62.5	56.3	49.7
V2527A	SEL	D	10000.00	95.4	90.7	87.3	83.5	77.7	71.1	66.3	60.9	54.6	47.4
V2527A	SEL	D	14000.00	100.4	96.1	93.0	89.4	83.5	77.0	72.2	66.7	60.1	53.0
V2527A	SEL	D	18000.00	103.2	99.1	96.2	92.9	87.4	81.1	76.5	71.1	64.9	57.9
V2527A	SEL	D	22500.00	105.1	101.2	98.5	95.4	90.3	84.3	79.9	74.8	68.7	62.0
V2527A	LAmax	A	2000.00	89.3	82.8	78.2	73.4	65.8	57.4	51.2	44.4	36.7	28.6
V2527A	LAmax	A	2700.00	89.5	83.0	78.3	73.5	65.8	57.4	51.3	44.4	36.7	28.6
V2527A	LAmax	A	6000.00	91.6	84.7	79.5	74.2	66.5	58.0	51.9	45.0	37.2	29.1
V2527A	LAmax	D	10000.00	94.5	86.7	81.1	75.1	66.1	56.9	50.3	43.1	35.0	26.5
V2527A	LAmax	D	14000.00	98.0	90.4	85.3	80.1	72.0	63.1	56.6	49.2	40.9	32.0
V2527A	LAmax	D	18000.00	101.9	94.7	89.7	84.3	76.1	67.2	60.7	53.4	45.3	36.7
V2527A	LAmax	D	22500.00	104.1	97.1	92.4	87.4	79.4	70.6	64.4	57.5	49.5	40.5
V2527A	EPNL	A	2000.00	96.9	92.3	88.5	84.6	78.6	71.5	66.3	59.8	51.5	40.7
V2527A	EPNL	A	2700.00	97.0	92.4	88.6	84.7	78.6	71.5	66.3	59.9	51.5	40.8
V2527A	EPNL	A	6000.00	99.0	94.3	90.4	86.2	79.7	72.3	67.0	60.4	52.2	41.6
V2527A	EPNL	D	10000.00	100.7	96.0	92.1	87.6	80.5	72.8	66.0	59.1	49.7	36.8
V2527A	EPNL	D	14000.00	106.1	101.4	97.8	93.4	86.2	78.1	72.2	66.0	57.7	46.9
V2527A	EPNL	D	18000.00	107.7	103.3	99.9	96.1	89.6	82.5	77.2	71.2	63.6	53.8
V2527A	EPNL	D	22500.00	109.8	105.5	102.5	98.9	93.0	86.4	81.2	75.5	68.3	59.3
V2527A	PNLTmax	A	2000.00	103.3	96.5	91.3	85.5	76.9	67.6	60.9	53.0	43.6	32.3
V2527A	PNLTmax	A	2700.00	103.8	96.7	91.1	85.3	76.9	67.7	60.9	53.0	43.6	32.1
V2527A	PNLTmax	A	6000.00	106.3	99.2	93.4	87.0	78.8	68.3	61.4	53.5	44.0	32.6
V2527A	PNLTmax	D	10000.00	112.7	105.0	99.3	92.6	80.9	71.0	59.9	52.0	41.0	27.0
V2527A	PNLTmax	D	14000.00	114.9	107.1	101.4	94.8	84.1	74.0	66.4	58.4	48.6	37.1
V2527A	PNLTmax	D	18000.00	116.6	109.5	104.3	98.5	88.5	78.7	71.2	63.3	54.3	43.5
V2527A	PNLTmax	D	22500.00	118.6	111.4	106.3	100.3	91.5	82.7	76.0	68.4	59.3	48.5

Table G-10: Example spectral class table

Spectral Class Identifier	Operation Type	Description	L_50Hz	L_63Hz	L_80Hz	L_100Hz	L_125Hz	L_160Hz	L_200Hz	L_250Hz	L_315Hz	L_400Hz	L_500Hz
103	Departure	Two engine high bypass ratio turbofan	56.7	66.1	70.1	72.8	76.6	73.0	74.5	77.0	75.3	72.2	72.2

Table G-10: Example spectral class table (continued)

L_630Hz	L_800Hz	L_1000Hz	L_1250Hz	L_1600Hz	L_2000Hz	L_2500Hz	L_3150Hz	L_4000Hz	L_5000Hz	L_6300Hz	L_8000Hz	L_10000Hz
71.2	70.2	70.0	69.6	71.1	70.6	67.1	63.4	63.5	58.2	51.5	42.3	37.7

Table G-11: Example Substitutions Table

ICAO Code	Aircraft Manufacturer	Airframe Type	Engine Manufacturer	Engine Type	Other Information	Number of engines	MTOW (kg)	MLW (kg)	Noise Chapter	Lateral Level (EPNdB)	Flyover Level (EPNdB)	Approach Level (EPNdB)
A318	Airbus	A318-121	Pratt & Whitney	PW6122A	-	2	68000	57500	4	93.0	86.5	92.4
AT43	ATR-GIE Avions de Transport Regional	ATR 42-320	Pratt & Whitney Canada	PW121	-	2	17000	16850	4	84.9	76.7	96.7
B736	Boeing Company	737-600	CFM	CFM56-7B18	-	2	65998	55111	4	89.0	86.1	95.6

Table G-11: Example Substitutions Table (continued)

ICAO Code	Overflight Level (dBA)	Takeoff Level (dBA)	ANP proxy	∆dep (dB)	∆arr (dB)	Ndep	Narr
A318	-	-	A319-131	2.5	-1.9	1.76	0.65
AT43	-	-	DHC8	-2.2	2.0	0.61	1.58
B736	-	-	737700	-1.8	-0.2	0.67	0.95

APPENDIX H: SUMMARY OF DIFFERENCES FROM DOC 29, 3RD EDITION (2007)

The purpose for publishing this Fourth Edition is three-fold: to improve the description of specific steps of the modelling methodology to add clarity on the way to implement those steps in a computerized system; to improve aspects of the noise calculations; and to update the guidance to reflect the most up-to-date science at the time of publication.

The following sections summarise the main differences in this Fourth Edition compared with the previous Third Edition of Doc 29. **Table H-1** then provides a chapter-by-chapter comparison of the two editions.

Improved descriptions of modelling methodology

Greater clarity was given over the method for constructing flight path segments, including: reordering the sections to reflect the intended order of the calculation; specifying a minimum source height; describing more explicitly how the Olmstead heights should be used in sub-segmentation and giving guidance on the extrapolation of profiles and ground tracks.

Generalised equations for thrust and velocity for non-zero start-speeds have been added; previously they were only included for the specific case of zero start-speed. Clarifications have also been made to aspects of the engine installation correction, lateral attenuation and finite segment correction, particularly on the circumstances under which some of these corrections should apply.

Improved noise calculations

Some improvements have been made feasible as a result of advancements made in computer processing speed, such as reducing the recommended minimum angle between segments along a curved ground track. The introduction of sub-segmentation of final approach segments also increases the number of calculations needed to run a whole airport noise contour, but any increases in run time are offset by the improvements in the accuracy of the results.

A new section on acoustic impedance adjustment has also been added. A proportionate approach has again been taken with regards to achieving the appropriate level of accuracy without placing excessive processing loads on computer systems.

Up-to-date science

Eminent technical organisations have recently published reports/guidance in two noise modelling areas: start-of-roll (SOR) directivity [ref. 13] and atmospheric absorption [refs. 15 and 17]. Based on extensive measurement data and analysis, these update the previous understanding held by the noise modelling community on these subjects. The algorithms presented for modelling these have been brought into this Fourth Edition of Doc 29, replacing the previous algorithms.

TABLE H-1: CHAPTER-BY-CHAPTER COMPARISON OF THE PRESENT AND PREVIOUS EDITIONS OF DOC 29

Volume 2 Chapter	**Volume 2 Section**		**Comment/Changes from Doc 29 - 2007**
Foreword			Reflects revised contents
Terms & Symbols			Updated as necessary to reflect revised content of document
1 Introduction	1.1 Aim and scope of document		Updated as necessary, and includes a new paragraph on noise from aircraft engine testing
	1.2 Outline of document		Updated as necessary, and introduces new methodology to calculate atmospheric absorption
2 Summary and applicability of the method	2.1 The concept of segmentation		Materially unchanged
	2.2 Flight paths: tracks and profiles		Materially unchanged
	2.3 Aircraft noise and performance		Materially unchanged
	2.4 Airport and aircraft operations		Materially unchanged
	2.5 Reference conditions		Materially unchanged
3 Description of the flight path	3.1 Relationships between flight path and flight configuration		Materially unchanged
	3.2 Sources of flight path data	3.2.1 Radar data	Materially unchanged
		3.2.2 Procedural steps	Materially unchanged
	3.3 Co-ordinate systems	3.3.1 The local co-ordinate system	Materially unchanged
		3.3.2 The ground track co-ordinate system	Materially unchanged
		3.3.3 The aircraft co-ordinate system	Materially unchanged
		3.3.4 Accounting for topography	Materially unchanged
	3.4 Ground tracks	3.4.1 Backbone tracks	Materially unchanged
		3.4.2 Lateral track dispersion	Changed subtitle
	3.5 Flight profiles		Added clarification of minimum source height
	3.6 Construction of flight path segments, introductory text	3.6.1 Flight profile	Previously Ground track, materially unchanged
		3.6.2 Takeoff ground roll	Title revised, sub-segmentation criteria specified, new

Volume 2 Chapter	Volume 2 Section		Comment/Changes from Doc 29 - 2007
	revised with the new order of material		generalised equations
		3.6.3 Landing ground roll	Clarification in text and Figure 3-6, reference to generalised equations.
		3.6.4 Segmentation of the initial climb and final approach segments	Comprehensive explanation of use of Olmstead heights, and new sub-segmentation of final approach segments.
		3.6.5 Segmentation of airborne segments	Reference to generalised equations and quantification of significant speed change.
		3.6.6 Ground track	Revision of minimum sub-arc angle, clarification of extrapolation of ground track and profile
		3.6.7 Segmentation adjustments of airborne segments	Section extracted from previous section on Segmentation of airborne segments to reflect where this stage should occur in the calculation process
4 Calculation of single event level	4.1 Single event metrics		Materially unchanged
	4.2 Determination of event levels from NPD data	4.2.1 Impedance adjustment of standard NPD data	New section
	4.3 General expressions	4.3.1 Segment event level	Clarifications over when to apply correction terms
		4.3.2 Event level of aircraft movement	Materially unchanged
	4.4 Flight path segment parameters	4.4.1 Geometric parameters	Materially unchanged
		4.4.2 Segment power P	Materially unchanged
	4.5 Segment event level correction terms	4.5.1 Duration correction Δ_V	Updated for greater clarity
		4.5.2 Sound propagation geometry	Materially unchanged
		4.5.3 Engine installation correction Δ_I	Constants presented at appropriate precision, clarifications made to description of methodology
		4.5.4 Lateral attenuation $\Lambda(\beta,\ell)$ (infinite flight path)	Text edits including correction of lateral attenuation constant for $\beta<0$
		4.5.5 Finite segment lateral attenuation	Improvements to text, relating to extended level flight

Volume 2 Chapter	Volume 2 Section		Comment/Changes from Doc 29 - 2007
			path
		4.5.6 Finite segment correction Δ_F	V_{ref} and lower limit for noise fraction defined, new particular forms of noise fraction for departure and arrival operations presented
		4.5.7 Start-of-roll directivity correction Δ_{SOR}	New directivity function presented with supporting text updated accordingly
5 Cumulative level	5.1 Weighted equivalent sound levels		Materially unchanged
	5.2 Weighted number of operations		Materially unchanged
	5.3 Estimation of cumulative maximum level metrics		Materially unchanged
	5.4 Use of level distribution for maximum level metrics		Materially unchanged
6 Calculation of noise contours	6.1 Standard grid calculation and refinement		Materially unchanged
	6.2 Use of rotated grids		
	6.3 Tracing of contours		
	6.4 Post-processing		
References			Reference 5, 6, 11, 12 and 14 updated, new references 13 and 17.
Appendix A: Data requirements	General airport data		Materially unchanged
	Airport designation		
	Runway description		
	Flight track description		
	Air traffic description		
Appendix B: Flight performance calculations	Terms and symbols		Materially unchanged
	B1 Introduction		
	B2 Engine thrust		
	B3 Vertical profiles of air temperature, pressure & density, and		

Volume 2 Chapter	Volume 2 Section	Comment/Changes from Doc 29 - 2007
	windspeed	
	B4 The effects of turns	
	B5 Takeoff ground roll	
	B6 Climb at constant speed	
	B7 Power cutback (transition segment)	
	B8 Accelerating climb and flap retraction	
	B9 Additional climb and acceleration segments after flap retraction	
	B10 Descent and deceleration	
	B11 Landing approach	
	B12 Worked examples	
Appendix C: Modelling of lateral flight track spreading		Materially unchanged
Appendix D: Recalculation of NPD-data for non-reference conditions		Updated to include new methodology for recalculating NPD data for non-reference atmospheric conditions
Appendix E: The finite segment correction	E1 Geometry	Materially unchanged
	E 2 Estimation of the energy fraction	
	E 3 Consistency of maximum and time integrated metrics - the scaled distance	
Appendix F: Maximum level of noise events		Materially unchanged
Appendix G: The international aircraft noise and performance (ANP) database	G1 Introduction	Section G5 added on aircraft substitution, with additional table in Section G7. Text modified throughout to reflect the ANP database.
	G2 Aircraft table	
	G3 Aircraft performance tables	
	G4 Aircraft noise tables	

Volume 2 Chapter	Volume 2 Section	Comment/Changes from Doc 29 - 2007
	G5 Substitutions table	
	G6 How to download the data	
	G7 Example data	
Appendix I: Conversion of units		Materially unchanged

APPENDIX I: CONVERSION OF UNITS

In general the units used in this document adhere to the *International System of Units* (SI), using metres and kilograms. The SI system was adopted by the 11th General Conference on Weights and Measures (1960) and it is described in the standard ISO 31 'Quantities and Units' (1992). However, flight parameters are mostly defined in units of feet, knots and pounds. The conversion factors are:

Symbol	**Name**	**Conversion**
ft	foot, feet	1 ft = 0.3048000 m
nm	nautical mile	1 nm = 1.852000 km
kt	knot (= nm/h)	1 kt = 1.852 km/h = 0.5144 m/s
lb	pound	1 lb = 0.4535924 kg
°F	Degree Fahrenheit	°F = °C *9/5 + 32

- END -